Interaction of the brain-specific Arf-GAP protein p42^{IP4} (centaurin α1, ADAP1) with the metalloendopeptidase nardilysin and modulation by tubulin

Dissertation

Zur Erlangung des akademischen Grades

doctor rerum naturalium
(Dr. rer. nat.)

genehmigt durch die Fakultät für Naturwissenschaften

der Otto-von-Guericke-Universität Magdeburg

von   Dipl. Neurowiss., Claudia Borrmann

geb. am   09.04.1980   in   Hoyerswerda

Gutachter: Prof. Dr. Georg Reiser

                      Prof. Dr. Rolf Heumann

eingereicht am: 25.10. 2011

verteidigt am: 28.03. 2012

In ewiger Erinnerung an Anna Heymann

Danksagung

Mein Dank gilt meinem Doktorvater Prof. Dr. G. Reiser für das interessante Thema meiner Doktorarbeit, sowie für die sehr gute Betreuung und seine immerwährende Diskussionsbereitschaft und Unterstützung neuer Ideen während dieser Zeit.

Des Weiteren möchte ich mich recht herzlich bei Dr. Rolf Stricker für die vielen hilfreichen Ratschläge zu allen proteinbiochemischen Fragen bedanken.

Mein Dank gilt außerdem Dr. Theodor Hanck für die Diskussion aller molekularbiologischen Fragen und aller Fragen die darüber hinausgingen. Weiterhin bin ich ihm sehr dankbar dafür, dass er mit seiner „jungen Kollegin" für viele Jahre die 4 m Laborplatz friedlich geteilt hat und dabei gern obige Fragen diskutiert hat.

Frau Dr. Schneider möchte ich für die Erste Hilfe am Konfokalmikroskop und bei der Immuncytochemie danken, sowie für den täglichen Gang zum Gourmettempel.

Markus Aswendt gilt mein Dank für die Hilfe bei den Klonierungen und den Anfangsexperimenten zur Enzymkinetik.

Big thanks, to everyone[*] who literally lived in the international „seminar-room" over the years for discussion, help, and the great team spirit and to everyone else, who came there for a visit at least once a week.

Mein Dank gilt auch meinen Eltern, meinen Lieblingsgeschwistern und meinen Freunden für all die Unterstützung während dieser Jahre.

---

[*] Dr. Elena Sokolova, Dr. Stepan Aleshin, Dr. Yingfei Wang, Dr. Weibo Luo, Dr. Rongyu Li, Dr. Anastasia Galvita, Daniel Förster, Zhihui Zhu, the Russian Guest scientists, especially Dr. Dmitry Grachev

Table of Figures

1   Introduction

1.1   *The brain-specific protein p42^{IP4}*

1.1.1   Structure (Gene, Protein)

The 42 kDa protein p42^{IP4} , also named centaurin α1 (Venkateswarlu et al., 1999) and PIP$_3$BP (Tanaka et al., 1997) belongs to the family of ADAPs, a subfamily of human ArfGAPs and has been recently renamed as ADAP1 for a consensus nomenclature (Kahn et al., 2008). It has been cloned from rat, bovine, pig and human brain (Hammonds-Odie et al., 1996; Sedehizade et al., 2002; Stricker et al., 1997; Tanaka et al., 1999; Venkateswarlu and Cullen, 1999).

The only other member of this subfamily is centaurin α2, a protein that is 58% identical and 75% homologous to p42^{IP4} (Hanck et al., 2004). Members of this protein family contain an <u>A</u>DP <u>r</u>ibosylation <u>f</u>actor-<u>G</u>TPase <u>a</u>ctivating protein (Arf-GAP) domain, responsible for facilitating the hydrolysis of bound GTP in small GTPases and two pleckstrin homology (PH) domains.

p42^{IP4} is located on chromosome 7p22.3 and contains 11 exons. Although the p42^{IP4}-homologue centaurin α2 is located on chromosome 17q11.2 close to the NF1 locus, the number of exons of both proteins is identical (Hanck et al., 2004).

p42^{IP4} has two PH-domains, one N-terminal Arf-GAP domain, which includes a Zn^{2+}-finger and ankyrin repeats, similar to the human leucocyte ankyrin (Hammonds-Odie et al., 1996; Stricker et al., 1999).

Furthermore, p42^{IP4} can bind phosphatidylinositol (3,4,5)-trisphosphate (PIP$_3$), phosphatidylinositol (3,4)-bisphosphate PtdIns(3,4)P$_2$ (PIP$_2$) and inositoltetrakisphosphate (IP$_4$).
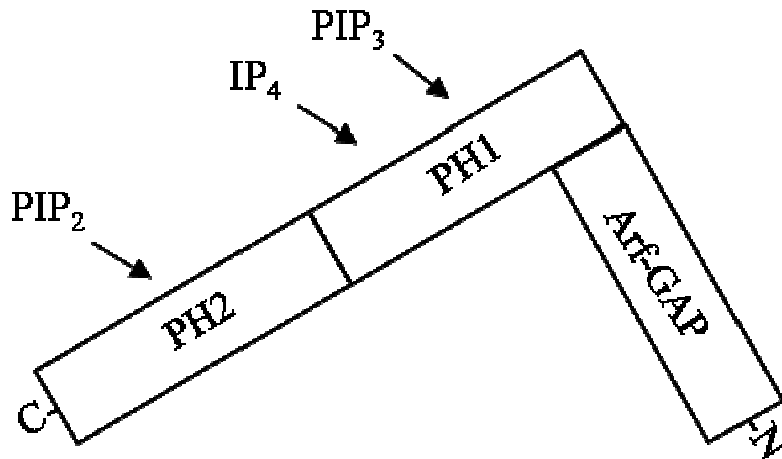
Fig. 1.1 Domain structure of p42^{IP4}.

The domain structure of the L-shaped protein p42^{IP4} is shown including the preferentially binding sites for the p42^{IP4} ligands PIP$_2$, PIP$_3$ and IP$_4$.

Recently the crystal structure of free and IP$_4$-bound p42^{IP4} was solved (Tong et al., 2010). p42^{IP4} is an L-shaped protein with three domains, which are linked by two short helices. Furthermore both PH-domains build a β-barrel with one end blocked by a C-terminal α-helix and the other site open for binding of phosphoinositides (Tong et al., 2010). Additionally, it was shown there that the N-terminal PH domain binds PIP$_3$ and IP$_4$, whereas the PH-domain close to the C-terminus is able to bind PIP$_3$ as well as PIP$_2$ and IP$_4$, although the latter with slightly decreased affinity (see Fig. 1.1).

1.1.2 Localization within the cell

The phosphatidylinositol 3-kinase (PI3K) catalyzes the production of the second messengers PIP$_2$ and PIP$_3$, which are ligands of p42^{IP4} and bind to the PH-domains of p42^{IP4} as described in 1.1.1.. The PI3K can be activated by different growth signals, for instance growth factors (Rodgers and Theibert, 2002).

Binding of PIP$_3$ to p42^{IP4} *in vitro* results in localization on the plasma membrane, whereas binding of the water soluble ligand IP$_4$ is accompanied with a dissociation of p42^{IP4} from the membrane into the cytosol (Stricker et al., 1999; Stricker et al., 2003). Moreover, using deletion mutants it was shown that the Zn^{2+}-finger contains a nuclear localization signal which targets the protein to the nucleus (Sedehizade et al., 2002).

In vivo investigations on the release of p42^{IP4} from membranes under the influence of IP$_4$ confirmed the previously observed dissociation of p42^{IP4} from membranes *in vitro*.

Moreover, both PH-domains, as well as the Zn^{2+}-finger are mandatory for the membrane localization of $p42^{IP4}$ (Sedehizade et al., 2005).

Recent investigations showed that $p42^{IP4}$ is also localized in mitochondria and thereby participates in regulation of mitochondrial Ca^{2+} (Galvita et al., 2009).

1.1.3 Distribution in tissues

$p42^{IP4}$ is mainly expressed in neuronal tissue, and widely distributed in the human brain (Sedehizade et al., 2002). Interestingly, a strong signal for $p42^{IP4}$ not only in brain and spinal chord, but also in peripheral blood and a weak signal in kidney was obtained in Northern Blots (Hanck et al., 2004).

In the human cortex, $p42^{IP4}$ is expressed in pyramidal neurons in the ganglion cell layer. The subcellular distribution of $p42^{IP4}$ in cortical neurons and in Purkinje cells of the cerebellum is comparable; $p42^{IP4}$ is located inside the nucleus and in the cytoplasm (Sedehizade et al., 2002). A similar expression pattern has been found in rat brain (Kreutz et al., 1997a). $p42^{IP4}$ was also detected in retinal neurons of different mammals and the expression was attenuated after optic nerve crush (Kreutz et al., 1997b).

Moreover, $p42^{IP4}$ seems to be developmentally regulated in rat brain (Aggensteiner and Reiser, 2003) and to be expressed in Alzheimer's disease (AD) brains, where it colocalizes with plaques (Reiser and Bernstein, 2002; Reiser and Bernstein, 2004).

Investigations on invertebrates suggest a role for $p42^{IP4}$ in tissue repair and regeneration. The highly conserved protein homologue of $p42^{IP4}$ in the sea cucumber (*Holothuria glaberrima)* has been shown to be upregulated after injury and the subsequent regeneration process. This animal was used as a model to further characterize the molecular events during intestinal regeneration after injury (Rojas-Cartagena et al., 2007).

Additionally, it was shown that the $p42^{IP4}$ homologue MjCent from the shrimp (*Marsupeneaus japonicus)*, was upregulated during white spot syndrome virus (WSSV) infection, but notably decreased in virus-resistant shrimps. The upregulation of the $p42^{IP4}$ homologue was suggested to demonstrate a close relationship between MjCent and WSSV invasion and host defense of the shrimp, *M. japonicus* (Wang et al., 2009).

1.1.4 Interaction partners and substrates

Although the physiological role of $p42^{IP4}$ is not yet clear, the interaction with other proteins indicates a role as a scaffold protein for various cellular processes. Among the

proteins, which interact with $p42^{IP4}$ are all the members of the casein kinase I family (Dubois et al., 2001) (Dubois et al., 2002). Also nucleolin, which contributes to the regulation of the mRNA of the amyloid-precursor-proteins (Dubois et al., 2003), isoforms of the protein kinase C (PKC) (Dubois et al., 2002; Zemlickova et al., 2003), the kinesin motor protein KIF13B (Venkateswarlu et al., 2005), the protein RanBPM (Haase et al., 2008) and the metalloendopeptidase nardilysin (Stricker et al., 2006) interact with $p42^{IP4}$.

It was shown that $p42^{IP4}$ associates with a highly conserved part of casein kinase Iα and it was discussed that $p42^{IP4}$ thereby anchors the kinase on the plasma membrane, because the kinase itself lacks a lipid binding domain (Dubois et al., 2001) . The casein kinase Iα is ubiquitously expressed in many eukaryotes similar to other members of this family of serine/threonine kinases. Casein kinase isoforms phosphorylate some of their target proteins dependent on previous phosphorylation by other kinases few residues C-terminal to the casein kinase phosphorylation site (reviewed in (Gross and Anderson, 1998)). $p42^{IP4}$ is not phosphorylated by casein kinase Iα, but a missing pre-phosphorylation by another kinase could not be excluded. Moreover, $p42^{IP4}$ binds to the kinase domain but does not influence the activity of the kinase (Dubois et al., 2001). Additionally, a functional relationship between $p42^{IP4}$ and casein kinase Iα was discussed as the casein kinase Iα diminishes the effects of a Gcs1 mutant, which is a yeast homologue of $p42^{IP4}$ (Dubois et al., 2001).

Gcs1 is an Arf GAP in yeast (*S. Cerevisiae)* with the highest homology to $p42^{IP4}$. Gcs1 is responsible for the organization of the actin cytoskeleton, by stimulating the polymerization of actin. Yeast, which contain mutants of Gcs1 have problems in distributing the actin to the daughter-cells during cytokinesis (Blader et al., 1999). Moreover, $p42^{IP4}$ was demonstrated to complement the yeast Gcs1-mutant and therefore proposed to have a functional correlation with Gcs1 (Venkateswarlu et al., 1999).

Another interaction partner of $p42^{IP4}$ is nucleolin. Interaction of nucleolin with $p42^{IP4}$ takes place exclusively in the presence of RNA. Both proteins build a complex with RNA, and treatment with RNase prevents the interaction (Dubois et al., 2003). Moreover, nucleolin takes part in the regulation of the mRNA of the amyloid-precursor-protein (APP) (Zaidi and Malter, 1995). The interaction with nucleolin is quite interesting for neurodegenerative diseases as it has been shown that $p42^{IP4}$ is highly expressed in human Alzheimer's disease (AD) brains (Reiser and Bernstein, 2002).

Furthermore, $p42^{IP4}$ interacts with the protein kinase C (PKC) (Zemlickova et al., 2003). PKCs are involved in the regulation of the cytoskeleton and they are important for cell

proliferation, differentiation and apoptosis. Lipid second messengers like PIP_3 can regulate members of the PKC-family. $p42^{IP4}$ binds to the cysteine rich domain C1 of PKC, which is abundant in all members of the PKC-family. Moreover, $p42^{IP4}$ is phosphorylated by the PKC at the PH-domain close to the C-terminus and within the zinc-finger in the region of the putative Arf-GAP-region (Zemlickova et al., 2003). Interestingly, PKCs can activate α-secretase indirectly through the MAP kinases ERK1/2 (Diaz-Rodriguez et al., 2002) but can also directly activate α-secretases TACE and ADAM10 (Skovronsky et al., 2000).

As mentioned before, $p42^{IP4}$ contains an Arf-GAP domain close to the N-terminus. Moreover, experiments could prove that $p42^{IP4}$ can complement the mutant GCS1-KO yeast strain. An *in vivo* evidence for intrinsic Arf-GAP-activity of $p42^{IP4}$ was given for the interaction with Arf6 (Venkateswarlu et al., 2004). Moreover, it was discovered that $p42^{IP4}$ can also interact with Arf1, Arf5 *in vitro* and colocalizes with Arf5 and Arf6 *in vivo*, but only little colocalization with Arf1 was observed *in vivo* (Thacker et al., 2004).

Arf6, as a small GTPase, can be found in two states of activity within the cell: activated ($Arf6_{GTP}$), when bound to GTP, or inactive ($Arf6_{GDP}$), when bound to GDP. $Arf6_{GDP}$ is present in endosomes, whereas, $Arf6_{GTP}$ localizes at the plasma membrane (Donaldson, 2003). To change the activation status, guanine-nucleotide exchange factors (GEFs) and GTPase-activating proteins (GAPs) are necessary. For activation, the GEFs catalyze the exchange of the bound GDP with GTP. For inactivation, GAPs are necessary, which activate the intrinsic GTPase-function of Arfs, which then leads to hydrolysis of the bound GTP to GDP and inorganic phosphate.

It was reported that KIF13B negatively regulates the GAP activity of $p42^{IP4}$ for Arf6 *in vivo* (Venkateswarlu et al., 2005). $p42^{IP4}$ interacts through its GAP domain with the stalk domain of the kinesin motor protein KIF13B, which was discussed to explain the inhibition of the Arf-GAP activity of $p42^{IP4}$ (Kanamarlapudi, 2005).

Arf6 plays a role in migration processes of epithelial cells. Polarized epithelial cells are tightly connected through adherens junctions. To allow cell migration a disassembly of the adherens junctions is necessary. Activation of Arf6 supports the destruction of the adherens junctions.

Moreover, Arf6 has been implicated in G-protein-coupled receptor (GPCR) trafficking, including internalization of the GPCR (Hunzicker-Dunn et al., 2002). It was demonstrated that $p42^{IP4}$ participates in the Arf6 modulated GPCR trafficking of the beta adrenergic receptor, by inhibition of its internalization (Lawrence et al., 2005).

Interestingly, $p42^{IP4}$ does not require its Arf-GAP activity to regulate the actin cytoskeleton (Thacker et al., 2004). Nevertheless, an catalytically inactive Arf-GAP mutant of $p42^{IP4}$ has been shown to diminish dendritic differentiation (Moore et al., 2007).

Furthermore, using large scale genome functional profiling it was shown that $p42^{IP4}$ is a putative modulator of the AP-1 promoter (Chanda et al., 2003). It was discussed there that $p42^{IP4}$ might modulate an oncogene transformation of cells via the AP-1 signaling pathway which also includes changes in cell adhesion (Chanda et al., 2003).

In another large scale screening for activators of the MAP kinase pathways, overexpressed $p42^{IP4}$ was found to be an activator for the ERK-MAP kinase pathway (Harada et al., 2003). Further investigations revealed that after stimulation with EGF and activation of the PI3K, $p42^{IP4}$ is recruited to the plasma membrane, where it subsequently activates Ras (Hayashi et al., 2006). It was discussed there that $p42^{IP4}$ may therefore act as an adaptor protein, linking the PI3K signaling pathway with the MAP-Kinase-pathway.

To get further insight into the function of $p42^{IP4}$, our laboratory performed a yeast two-hybrid screen with a human cDNA library from brain. Among several potential protein interaction partners, a new interaction between $p42^{IP4}$ and RanBPM was found. RanBPM is a protein, which is involved in various different processes in the cell. Further investigations demonstrated that the $p42^{IP4}$-ligand IP_4 is a concentration-dependent and stereoselective inhibitor of the interaction between RanBPM and $p42^{IP4}$ (Haase et al., 2008). Interestingly, investigations on RanBPM showed that it can interact with the low density lipoprotein receptor-related protein (LRP) and the amyloid precursor protein (APP) in the brain (Lakshmana et al., 2009). Additionally, overexpression of RanBPM results in an increased Aß-production via interaction with LRP and BACE1 (Lakshmana et al., 2009).

Recent investigations from our laboratory could demonstrate that $p42^{IP4}$ interacts with the 2',3'-Cyclic-nucleotide 3'-phosphodiesterase (CNP) and α-tubulin. $p42^{IP4}$ also influences the opening of the mitochondrial permeability transition pore (PTP), and thereby participates in the mitochondrial Ca^{2+} metabolism (Galvita et al., 2009).

Although all interactions mentioned above give an idea about the manifold processes in which $p42^{IP4}$ might be involved, a clear physiological function of $p42^{IP4}$ has yet to be established.

1.2 The metalloendopeptidase nardilysin (NRD)

1.2.1 Structure (Gene, Protein)

Nardilysin (NRD) is a 140 kDa metalloendopeptidase, which cleaves their substrates preferentially at the N-terminus of arginine doublets (therefore the acronym NRDc) but it can also cleave on dibasic amino acids (Chesneau et al., 1994) and on monobasic sites (Chow et al., 2003). The NRD gene is located on chromosome 1p32.3 and contains 31 exons.

There are two alternatively spliced variants of NRD (NRD1 and NRD2) which exhibit similar biochemical and enzymatic properties but differ in their expression in tissues (Hospital et al., 2000) (Hospital et al., 1997).

NRD has an inverted consensus-binding site for Zn^{2+}, where the common motif HEXXH, which is present in most metallopeptidases (Hooper, 1994), is replaced by HXXEH. Enzymes like NRD, containing this inverted motif belong to the Inverzinkin/M16-family of metalloendopeptidases. The difference to other members of the M16- family is that NRD contains an insertion of acidic amino acids –glutamate and aspartate- N-terminal to its catalytic domain. This insertion was therefore named „Acidic Domain (AD)[†] or DAC.

Depending on the species, the DAC differs in the number of amino acid residues. The DAC from rat (*Rattus norvegicus*) has 71 amino acids, while the human DAC is shorter and has only 53 amino acids. Comparison of the amino acid sequence from mouse *(Mus Musculus)* with the rat sequence shows almost identical amino acids (Csuhai et al., 1998; Pierotti et al., 1994).

It was demonstrated that NRD can be inhibited by polyamines like putrescine, spermidine, and spermine (Csuhai et al., 1998). Further characterization of the binding of spermine to NRD revealed that it binds to the DAC, which is not part of the active site of the enzyme (Csuhai et al., 1999a). Studies with the DAC from rat, mouse and human alone, suggest that the DAC can work as a functional binding domain (Ma et al., 2001).

A report using trypsin and protease V8 to study the effects of limited proteolysis on NRD, suggest that although the N-terminal region of NRD is not important for enzymatic activity, together with the C-terminal region it may be important for proper folding of the metalloendopeptidase (Ma et al., 2002).

It was shown that the DAC is not necessary for the catalytic activity of NRD and that this domain is considered to be an appendix to the global structure of the enzyme, which is

---

[†] To avoid confusion with AD, the abbreviation commonly used for Alzheimer's disease, the Acidic Domain is named DAC in this thesis, although it is common in published reports of NRD to use AD to describe the Acidic Domain.

able to influence the activity of the enzyme (Hospital et al., 2002). Moreover, it was demonstrated in the same work that removal of this domain results in a three fold decreased activity of the enzyme. It was discussed that the DAC may act as a regulator for activity and stability of NRD. The DAC it is the part of NRD that takes part in binding of HB-EGF, Ca^{2+} and polyamines, the latter cooperatively.

1.2.2 Distribution in tissues

Using Northern Blot it was shown that NRD is abundant in all examined tissues, especially in skeletal muscle, in heart and testis (Fumagalli et al., 1998), where the highest expression can be found in testis. Furthermore, the expression of NRD seems to be developmentally regulated. In early development of mouse (E 10.5) NRD is highly expressed in neuronal tissue, like the CNS and in cephalic and spinal ganglia (Fumagalli et al., 1998). After that time point, it is possible to detect NRD also in other tissues.

Comparison between the expression levels of NRD in different tissues showed that it is highly expressed in the urogenital system, especially during spermatogenesis (Chesneau et al., 1996) but also during maturation of oocytes (Ma et al., 2005).

Recent investigations could reveal that NRD is widely but unevenly expressed in the human brain (Bernstein et al., 2007). Moreover, it was shown in that work that NRD is differently expressed at certain developmental stages. In early development NRD is expressed in both neuronal and glial cells, whereas at later time points the expression remains exclusively in neurons.

Most recent reports could show that a considerable amount of neurons co-express NRD together with the α-secretases ADAM10 and ADAM17 (Bernstein et al., 2009). Additionally, co-expression of NRD, ADAM10 and ADAM17 is reduced in AD or Down Syndrome brains.

1.2.3 Localization within the cell

Besides the mainly cytosolic localization, NRD resides in many cells and cell lines on the cell surface and seems not to enter the secretory pathway (Hospital et al., 2000). It can be released from the cell membrane, but how NRD is anchored and released from the cell membrane is still not known. It was speculated that these processes occur in interaction with a protein partner because NRD has neither a peptide signal for export nor a domain for anchoring at the membrane. Furthermore, it was discussed that NRD could be myristoylated

but this was not shown until now (Hospital et al., 2000). Moreover, it was reported that NRD is able to shuttle between the nucleus and the cytosol (Ma et al., 2004).

1.2.4 Substrates and protein interaction partners of NRD

Only a few *in vitro* substrates were known for NRD. NRD cleaves somatostatin-28, dynorphin A, α-neoendorphine and miniglucagon *in vitro* (Csuhai et al., 1995), (Chesneau et al., 1994), (Fontes et al., 2005) (Chow et al., 2000). Moreover, the protein neuregulin 1 (NRG1) is a substrate for NRD. Most recent studies showed for the first time physiologically relevant substrates of NRD (Kessler et al., 2011). NRD is able to complement the proteasome activity, where it contributes to both the C-terminal and N-terminal generation of Cytotoxic T lymphocytes epitopes of the Epstein-Barr virus protein EBNA3C and an epitope from the melanoma protein MART-1 (Kessler et al., 2011).

NRD has different protein interaction partners. These are HB-EGF, the tyrosyl-tRNA-ligase, $p42^{IP4}$, ADAM10 and ADAM17.

HB-EGF was originally identified in the culture medium of cultivated macrophages. It is synthesized as a type I transmembrane protein and can be shed enzymatically. This leads to a release of a 14 – 20 kDa growth factor, which can act then as an chemoattractant for cell-proliferation and migration for many cell types (reviewed in (Nishi and Klagsbrun, 2004)).

Furthermore, NRD supports the building of a complex between the mitochondrial malate dehydrogenase and the citrate synthase (Chow et al., 2005).

Investigations of the ectodomain-shedding of HB-EGF via activation of the TNF-α-converting enzyme (TACE, also known as a disintegrin and metalloprotease 17 (ADAM17)) have shown that NRD is able to enhance the shedding of HB-EGF (Nishi et al., 2006). Interestingly, NRD itself does not cleave HB-EGF (Nishi et al., 2001). Downregulation of NRD expression by siRNA technique diminishes the HB-EGF-shedding. Therefore, it was discussed that NRD might have an important function in ectodomain-shedding of HB-EGF.

Extracellular shedding of proteins is a posttranslational modification, which releases the extracellular domain of membrane-bound proteins through proteolysis. This happens to a variety of membrane proteins and is rapidly induced by activation of cells from their resting state. How this induction happens is still unclear.

Moreover, NRD enhances the α-secretase activity of ADAM10 and ADAM17, which results in lowered Aß-levels, increased sAPPα levels and thereby promotes the non-amyloidogenic pathway (Hiraoka et al., 2007). It was also demonstrated that NRD can enhance the ectodomain shedding of TNF-α via the activation of ADAMs (Hiraoka et al., 2008)

A report on the regulation of a voltage-gated potassium channel in smooth muscle cells demonstrated that NRD is expressed in human myometrium. There NRD regulates the expression of the maxi-K channel isoform mK44 on the plasma membrane and the expression of mK44 in response to changes in intracellular Ca^{2+}. Moreover, NRD colocalizes with mK44, and the expression of NRD decreases in late gestation, whereas an increase can be observed during labor (Korovkina et al., 2009).

1.2.5 Functionality

Besides recent reports on NRD to complement the proteasome activity, the function of NRD is not yet clear (Kessler et al., 2011). Homozygous knock out mice for NRD have impaired axonal maturation and hypomyelination (Ohno et al., 2009). Additionally, these mice have impaired motor activity and display cognitive deficits.

It is known that through binding of HB-EGF the activity of NRD can be modulated and might therefore have a role in migration processes or in processes of wound healing. It was shown that NRD enhances the cell migration via HB-EGF and the EGF-receptor (Nishi et al., 2001). The fact that NRD, as a receptor for HB-EGF is expressed in brain in neuroproliferative zones like the subventricular zone (SVZ) but less expressed in the granular layer of the hippocampus further supports the idea that NRD participates in migrational processes (Nishi et al., 2001).

Additionally, as described in 1.2.4, NRD seems to play an important role not only in shedding of transmembrane proteins like HB-EGF, but also in shedding of neuregulin (NRG1) (Ohno et al., 2009). NRG1 is a major regulator of myelination, which can be shed via β-secretase (BACE1) (Willem et al., 2006) and also TACE (Montero et al., 2000).

A special feature of some members of the M16-family of metalloendopeptidases is their ability to act bifunctionally, that is as a protease and through a non-enzymatic behavior. One example is the mitochondrial processing peptidase (MPP), which is also a member of the M16 family. MPP acts as peptidase on proteins which are encoded in the nucleus and removes their mitochondrial targeting sequences (Ito, 1999). On the other hand, MPP as a subunit of the cytochrom-c-oxidase is part of the respiratory chain in some organisms and has no enzymatic function.

1.3 Role of proteases in Alzheimer's disease

Alzheimer's disease (AD) is a neurodegenerative disease characterized by extracellular neuritic plaques and intracellular neurofibrillary tangles (Alzheimer et al., 1995).

Neuronal plaques are caused by the abnormal cleavage of the amyloid precursor protein (APP) through the β-secretase (BACE1), whereas the "tangles" are composed of hyperphosphorylated tau – a microtubule-associated protein (reviewed in (Mattson, 2004)).

APP is a type 1 transmembrane glycoprotein with a single-membrane spanning domain, a large extracellular N-terminal domain and a short C-terminal domain, located inside the cytosol (Kang et al., 1987).
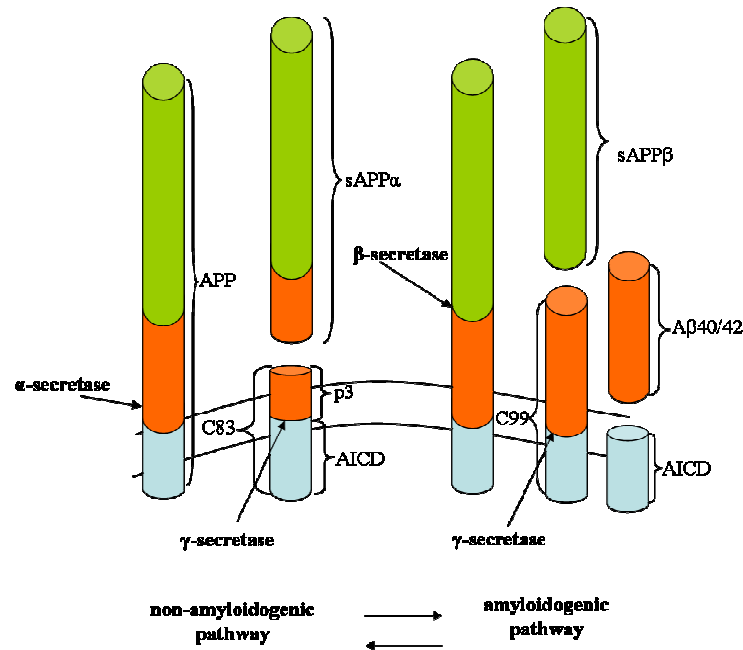
Fig. 1.2 Schematic representation of the proteolytic shedding of the amyloid precursor protein (APP) (modified from (Mattson, 2004))

APP is transmembrane protein with a large extracellular N-terminal domain (green, N-terminal parts of the orange tube) and a short C-terminal domain (indicated in light blue), which is located inside the cytosol. APP is shed by secretases and the emerging products lead to either the non-amyloidogenic (illustrated on the left site) or the amyloidogenic (right site) pathway. The arrows indicate different cleavage sites in APP for the secretases. It is believed that an equilibrium between both pathways exists (arrows in the lower part). Shedding by α-secretase releases sAPPα and leaves an 83 aa C-terminal fragment of APP (C83) in the membrane, which will be processed by γ-secretase to p3 and AICD (APP intracellular domain). Shedding by β-secretase leads to the release of sAPPβ and the 99 aa C-terminal fragment of APP (C99) remains in the membrane. Subsequent cleavage by γ-secretase produces the neurotoxic Aβ40/42 and the AICD. AICD, produced by the γ-secretase can translocate to the nucleus and influence transcription.

APP can be processed at different cleavage sites (Fig. 1.2) by different secretases resulting in the neurotoxic Aβ40/42, through cleavage of BACE1 and subsequent γ-secretase (Haass, 2004), or in the neuroprotective sAPPα, produced by α-secretase (Selkoe and Schenk, 2003).

Although the identity of the α-secretase is not yet clear, several ADAMs (9, 10, 17) were shown to cleave APP at the α-secretase site (Asai et al., 2003). After α-secretase cleavage the remaining 83 amino acid C-teminal fragment of APP is further processed by the γ-secretase and leads to the release of p3 peptides.

Cleavage by BACE1 leads to the amyloidogenic pathway as it results in production of sAPPβ and subsequent cleavage by the γ-secretase releases the neurotoxic Aß-peptides which are parts of the neuronal plaques. It is believed that under non-pathological conditions an equilibrium between α- and β- secretase cleavage of APP exists. As mentioned before, the shedding of APP by α-secretases releases the neuroprotective sAPPα. Increased release of sAPPα also reduces the Aß-levels and is therefore called the non-amyloidogenic pathway (amyloid hypothesis reviewed in (Hardy and Selkoe, 2002)).

The accumulation of Aß in the brain was proposed to be the primary influence in AD, followed by hyperphosphorylation of tau (reviewed in (Hardy and Selkoe, 2002)). Nevertheless, it is also discussed that the tau-pathology might be more important for the neurodegenerative development, because other dementias, like frontotemporal dementia are also linked to tau pathology (Spillantini et al., 1998), but lack amyloid plaques.

1.4 Retinoic Acid

Retinoic acid (RA) is a derivative of retinol (vitamin A), which has an important role not only in pattern formation during embryonal development but also in the adult brain (Niederreither and Dolle, 2008). Moreover, in neurodegenerative diseases like AD, the supply of RA is diminished in patients suffering from AD (Goodman, 2006; Goodman and Pardee, 2003). Moreover, it was shown that an age-related decline of RA results in reduction of hippocampal function in memory processes (Mingaud et al., 2008).

The precursor retinol enters the cell and is converted to retinal and finally to RA. RA binds to retinoic acid receptors (RAR and RXR) which then translocate to the nucleus and activate the transcription of target genes. RA receptors are ligand-activated nuclear transcription factors, which can bind to RA-responsive elements (RARE).

RA regulates the expression of various target genes, which are involved in AD like BACE1, ADAM10, PS1 or APP. Most recent reports showed that all secretases involved in APP shedding are regulated by RA on gene and protein level (Koryakina et al., 2009).

RA is often used to differentiate neuroblastoma cells (Pahlman et al., 1984). It was shown that NRD is upregulated in SK-N-BE cells after stimulation with RA (Draoui et al., 1997). Furthermore, it was proposed in that paper that the NRD gene might contain RARE elements. Studies on the promoter of NRD revealed that the 5´upstream region lacks this proposed RARE sequence (Winter and Pierotti, 2000).

1.5 SH-SY5Y neuroblastoma cells

SH-SY5Y cells are a catecholaminergic neuroblastoma cell line, which was derived as a third generation subclone of the cell line SK-N-SH (Biedler et al., 1973) (Biedler et al., 1978).

Like many other neuroblastoma cell lines, SH-SY5Y can be differentiated into a neuronal-like cell type when exposed to low concentrations of RA and used as an *in vitro* model to study the properties of neurons (Pahlman et al., 1984).

This cell line was shown to consist of two phenotypes with a majority of neuroblast-like cells. Additionally, upon stimulation with RA 25% of the cells grow extensions longer than 50 µm and the non-neuronal phenotype will increase dramatically at the same time (Preis et al., 1988). The ratio of actin expression to total protein expression was significantly increased in cells differentiated with RA (Asada et al., 1994). Moreover, it was demonstrated that treatment of SH-SY5Y cells with RA upregulates the gene expression of APP (Beckman and Iverfeldt, 1997).

Investigations on SH-SY5Y cells on cell renewal and commitment using electrophysiological and immunocytochemical approaches revealed that the parental SH-SY5Y clone contains a pool of cells (S_0 cells) which are able to renew and to differentiate to both smooth muscle (S_1 and finally S_2 cells) and neuronal cells (N_S) (Biagiotti et al., 2006). Furthermore, the parental cells contain highly clonogenic cells (N_N cells). Differentiation into the smooth muscle cells occurs with prolonged culture of the SH-SY5Y cells but only a simultaneous removal of the N type enables the final differentiation and leads also to the exhaustion of the culture (Biagiotti et al., 2006).

1.6 Aims for the thesis project

The interaction between $p42^{IP4}$ and NRD was discovered using a NRD -affinity-matrix (Chow et al., 2005). In this study, $p42^{IP4}$ was identified via mass spectrometry as one of the proteins which were eluted from the NRD-affinity matrix (Chow et al., 2005). Investigations in our laboratory demonstrated that the DAC of NRD is sufficient for the interaction with $p42^{IP4}$, can be regulated by ligands of both proteins (Stricker et al., 2006).

1.6.1 Cloning of human NRD and purification of the active enzyme for *in vitro* experiments

The first aim of this study is to clone the whole sequence of human NRD and to express it as an active enzyme. The purified, active enzyme should then be used to study functional aspects of the interaction with $p42^{IP4}$, to clarify, whether $p42^{IP4}$ can serve as a substrate for NRD. Further investigations should clarify whether the binding of $p42^{IP4}$ to NRD has an impact on the activity of the enzyme.

1.6.2 *In vitro* and *in vivo* experiments to investigate the interaction of $p42^{IP4}$ and NRD

It is known from the literature that $p42^{IP4}$ and NRD are regulated during development, but it is unknown whether there is a connection between both proteins. Therefore, the expression of $p42^{IP4}$ and NRD under developmental aspects should be studied in a suitable cell model system using RT-PCR and Western Blotting and confocal microscopy.

Moreover, besides colocalization demonstrated by confocal microscopy, the interaction of $p42^{IP4}$ and NRD has to be confirmed with biochemical methods. This helps to elucidate the relevance of their colocalization. For this purpose, pull down experiments and Far Western blots should be performed using recombinant $p42^{IP4}$, recombinant NRD, and NRD-mutants.

It has been published that NRD is able to enhance the α-secretase cleavage of APP and thereby provides evidence to be an anti-AD protein. $p42^{IP4}$ is localized in AD plaques and interacts with RanBPM, a protein recently shown to enhance the cleavage of APP by BACE. Therefore, it has to be investigated, whether $p42^{IP4}$ has an impact on the shedding of APP.

2 Materials and methods

2.1 Materials

2.1.1 Chemicals

Gentamycin	Invitrogen
Tetracycline	
Bluo-Gal	
Isopropylthio-β-galactoside	
Blasticidin S HCl	
Trypsin	
Ampicillin	Biochrom, Berlin, Germany
Dulbecco's Modified Eagle's Medium (DMEM)	
DMEM + HAM'S F12 (1:1)	
Fetal calf serum (FCS)	
HBSS (w/o Ca^{2+} and Mg^{2+})	
Kanamycin sulphate	
Trypsin/EDTA	
Penicillin and Streptomycin	
Aprotinin	Biomol
Leupeptin	
Pepstatin A	
Pefablock	
Bacto Agar	BD Bioscience (Clontech), Heidelberg, Germany
Bacto Tryptone	
Bacto Yeast extract	
Bio-Rad protein assay dye reagent concentrate	Bio-Rad Laboratories, München, Germany
KCl	Roth, Karlsruhe, Germany
Ethanol	
Guanidine-HCl	
Isopropanol	
$MgCl_2$	
$Na_2HPO_4*2H_2O$	
NaCl	
$NaHCO_3$	
RNase	
Non-fat dry milk	
Rotiblock ®	
Complete Protease Inhibitor Cocktail	Roche Diagnostic, Mannheim, Germany
FuGENE™ 6 transfection reagent	

G418 Sulphate	Calbiochem, La Jolla, CA, USA
ImmersolTM 518N (Immersion oil for microscopy)	Carl Zeiss, Oberkochen, Germany
KH$_2$PO$_4$	Merck, Darmstadt, Germany
MATra solution	IBA, Göttingen, Germany
PFA (paraformaldehyde)	Fluka Chemika, Sigma, Germany
Protein A/G Agarose	Santa Cruz, Heidelberg, Germany
Protein A-Sepharose	GE Healthcare
Tween 20	SIGMA, Deisenhofen, Germany
all-trans-Retinoic Acid	
Benzamidine	
β-mercaptoethanol	
DMSO	
TEMED	
Ponceau S	

2.1.2 Antibodies

2.1.2.1 Primary Antibodies

Beta-amyloid 6E10, Protein G-Purified,	Innovative Diagnostik-Systeme, Hamburg
Nardilysin N20 (polyclonal goat, affinity purified),	Santa Cruz Biotechnology
β-tubulin mouse monoclonal anti-β-tubulin I antibody	Sigma
GAPDH mouse monoclonal anti GAPDH antibody	Millipore
Synaptotagmin mouse monoclonal	Synaptic Systems
Synapsin1, mouse monoclonal	Synaptic Systems
GFP rabbit polyclonal anti-GFP antibody	Cell signaling technology
Mab-117-2 mouse monoclonal antibody, U- Kunzelmann, Dissertation Tübingen, 1994	
Rai-1 rabbit polyclonal antibody ; (Reiser et al., 1995)	
Rai-2 rabbit polyclonal antibody ; (Reiser et al., 1995)	
GM130 mouse monoclonal anti-GM130	BD Transduction Laboratories
EEA1 mouse monoclonal anti-EEA1	BD Transduction Laboratories
Anti-Xpress^{TM}-mouse monoclonal antibody	Invitrogen
His-Antibody mouse monoclonal	Qiagen

2.1.2.2 Secondary Antibodies

goat anti-mouse-HRP IgG+M	Dianova, Hamburg, Germany
goat anti-rabbit-HRP IgG	Dianova, Hamburg, Germany
mouse anti-goat-HRP IgG	Dianova, Hamburg, Germany
Alexa Fluor 488 donkey anti-goat IgG	Molecular Probes
Alexa Fluor 555 donkey anti-goat IgG	Molecular Probes
Alexa Fluor 546 goat anti-rabbit IgG	Molecular Probes
Alexa Fluor 555 goat anti-rabbit IgG	Molecular Probes
Alexa Fluor 568 goat anti-rabbit IgG	Molecular Probes

2.1.3 Oligonucleotides

Unless otherwise indicated, all primers were purchased from MWG, Ebersberg, Germany

primer	Sequence 5´-> 3´
CBhNRDHXXAHup	TGG CAC ACT TTT TG G**C**G CAC ATG GTA TTC AT
CBhNRDHXXAHlo	AT GAA TAC CAT GTG C**GC** CA AAA AGT GTG CCA
CBhNRDC948Aup	GCA CAT GGA AGAA CCT G**C**T TTT GAC TTC CTT CGA
CBhNRDC948Alo	TCG AAG GAA GTC AAA A**GC** AGG TTCT TCC ATG TGC
CBhNRDnoDAC1up	ACA GGA AAT ACA ACC G**G**T GAT GAA GAA GAA GA
CBhNRDnoDAC1lo	TC TTC TTC TTC ATC A**CC** GGT TGT ATT TCC TGT
CBhNRDnoDAC2up	TTG GAA GAA TTA **ACC G**GT AGA GCA GAA GCT
CBhNRDnoDAC2lo	AGC TTC TGC TCT **ACC GGT** TAA TTC TTC CAA
CBhNRDcor1054up	CTT TTT GGA GCA CAT GGT ATT CAT GGG TAG TTT G
CBhNRDcor1054lo	C AAA CTA CCC ATG AAT ACC ATG TGC TCC AAA AAG
hNRD2c1up	TAA GTC AAC TTA TTC **A**AA AAT GTC TTC AAC
hNRD2c1lo	GTT GAA GAC ATT TT**T** GAA TAA GTT GAC TTA
hNRD2c2up	CTG CTG GTC GAG ACA **AG**A AAT CTT TAT GGG GT
hNRD2c2lo	AC CCC ATA AAG ATT T**CT** TGT CTC GAC CAG CAG
CBHsNRDFW	GAT CGC GGC CGC CCC GGG ATG CTG AGG AGA GTC ACT GTT G
CBHsNRDstopRV	GAT CCT CGA GTT ATT TGA CTA TTT TAT GGT AG
CBHsNRDnonstopRV	GAT CCT CGA GAA GCT TTG CTT TGA CTA TTT TAT GGT AGG GG
CBRnNRDFW	GTG GAG GGT AAA ACA GGA AAT GCA
CBRnNRDRV	AGG CAT CAA ATC CAT TCT CAT CTG
CBNOFW	CCT GGG AAG CGG GAT GTC
CBN1FW	TGA ATC TGA GGA AGA GGG AC
CBN3FW	AAA ATG TCT TCA ACC CTG C
CBN4FW	GAA TAA TAT TGA TAC ACA TGC
CBN5FW	GTT ATG AAC ATT TTT ATG AGG
CBN6FW	GGT TGC CTG TGG TAT AAG
CBN7FW	GGA ATG TCA CAA GCA CAG
CBN8FW	CTG GAA TGA AGT GGT TAC ACA CAG C
CBN2RV	GCT GGG AGA CTT GAC GAT C
CBN3RV	CCA TCC TGC CAA ATG CTG AAC
CBN4RV	GCA TGT GTA TCA ATA TTA TTC
CBN5RV	GCA ACC TCA TAA AAA TGT TCA TAA C
CBN6RV	CTT ATA CCA CAG GCA ACC
CBN7RV	GAT TCT GTG CTT GTG ACA TTC C
CBN8RV	GCT GTG TAA CCA CTT CAT TCC AG
CBN9RV	TTC AGG CCA ACG TGA CTG CAG
M13fw (Invitrogen)	GTA AAA CGA CGC CCA G
M13rv (Invitrogen)	CAG GAA ACA GCT ATG AC

2.1.4 Plasmid Vectors

pcDNA6/HisB (Version B)	Invitrogen, Karlsruhe, Germany
pFastBacHT_C (Version C)	Invitrogen, Karlsruhe, Germany
pBluescriptII KS	Fermentas Life sciences
pEGFP-C1	BD Biosciences Clontech

2.1.5 Enzymes and buffers

Shrimp Alkaline Phosphatase	Boehringer, Mannheim, Germany
T4 DNA Ligase	Invitrogen
T4 DNA Polymerase	Invitrogen
Not I, XhoI, EcoRI, HindIII, BamHI, PvuI&II, NsbI Y/Tango (10X), R(red), G(green)	Fermentas Life sciences
AgeI, NEB1	New England Biolabs, Beverly, MA, USA

2.1.6 Kits

QuickChange Site-directed Mutagenesis kit	Stratagene, LaJolla,CA,USA
Accu Prime	Invitrogen, Karlsruhe, Germany
Bac-to-Bac®HT Vector Kit	Invitrogen, Karlsruhe, Germany
Max Efficiency®DH10Bac^{TM} Competent E.coli Reagents	Invitrogen, Karlsruhe, Germany
Cellfectin® Transfection Reagent	Invitrogen, Karlsruhe, Germany
HiSpeed Plasmid Midi kit	Qiagen, Hilden, Germany
MinElute Gel extraction kit	Qiagen, Hilden, Germany
QIAquick PCR purification kit	Qiagen, Hilden, Germany
Taq Master Mix kit	Qiagen, Hilden, Germany
Omniscript Reverse Transcription kit	Qiagen, Hilden, Germany
RNase-Free DNase Set	Qiagen, Hilden, Germany
RNeasy Mini kit	Qiagen, Hilden, Germany
hAmyloid β40 ELISA (HS)	the GENETICS company, Schlieren, Switzerland)
Supersignal West Pico kit	Pierce, Rockford, IL, USA

2.1.7 Cells and cell culture reagents

2.1.7.1 Mammalian cell lines

2.1.7.1.1 HEK 293 cells

Human embryonal kidney cells were cultured in DMEM/Ham's F-12 (1:1) supplemented with heat-inactivated 10% FCS, 100 U/ml penicillin, 100 µg/ml streptomycin (Biochrom, Berlin, Germany) in a humified, 5% CO_2, 37°C incubator.

2.1.7.1.2 SH-SY5Y cells

SH-SY5Y cells were cultured in DMEM supplemented with heat-inactivated 15% FCS and antibiotics mixture (penicillin, 100 U/ml and streptomycin, 0.1 mg/ml; Sigma) in a humified, 5% CO_2, 37°C incubator.

2.1.7.2 Insect cells

2.1.7.2.1 Sf9 (Spodoptera frugiperda) – cells

Sf9 cells were cultured with IPL-41 insect medium with L-amino acids (Gibco), supplemented with 10% heat-inactivated FCS (Biochrom), 2% (v/v) yeast extract (Sigma), 1% (v/v) lipid medium supplements (Sigma), 100 µg/ml gentamycin sulfate (Cell Concepts), and 2.5 µg/ml amphotericine B (Cell Concepts) in at 27°C.

2.1.7.3 Bacterial strains

	Strain	Genotype	Reference
	DH10Bac^{TM}	F´*mcr*A□(*mrr-hsd*RMS-*mcr*BC) □80*lac*Z□M15 □lacX74 *rec*A1 *end*A1 *ara*D139 □(*ara,leu*)7697 *gal*U *gal*K □-*rps*L *nup*G/bMON14272/pMON7124	(Luckow, 1993)
	DH5α	F´*end*A1, *hsd*R17 *(rk-mk+),* *gln*V44, *thi-1,* *rec*A1, gyrA (Nalr)*, rel*A1, D*(lac*lZYA*arg*F*)* U169, *deo*R, (f80*dlac*D(*lac*Z)M15*)*	
	XL1-Blue	*sup*E44, *hsd*R17, *rec*A1, *end*A1, *gyr*A46, *thi, rel*A1, *lac,* [F' *pro*AB, *lac*Iq, Z_M15, *Tn*10(*tet*r)	

2.1.8 Technical equipment

Sorvall RC5CPlus	Dupont Instruments, Hamburg, Germany
BIOFUGE pico (Lab centrifuge)	Heraeus, Hamburg, Germany
AHT35 Centrifuge (midi)	Hettich Zentrifugen
T3 thermocycler	Biometra, Göttingen, Germany
Thermomixer comfort	Eppendorf ,Wesseling-Berzdorf, Germany
LABINCO LD-79 (Rotating wheel)	LABINCO b.v., Breda (NL)
Agitateur Top-Mix 1118 (vortex)	Bioblock Scientific
Ultraturrax , IKA T25	IKA, Staufen, Germany
LSM510 laser scanning confocal microscope	Carl Zeiss, Jena, Germany
Microplate reader	Molecular devices
BioRad GelDoc XR (Gel documentation system) Gel electrophoresis system Semi-dry Transfer Cell Electrophoresis power supply GS-800 Calibrated Densitometer	Bio-Rad Laboratories, München, Germany
UV/visible Spectrophotometer	Pharmacia Biotech
Ultrasonic homogenizer	Bandelin electronic, Berlin, Germany
Mighty Small II (for western blotting electrophoresis)	Amersham Pharmacia Biotech, Buckinghamshire, UK
Magnet plate	IBA, Göttingen, Germany
Gel-blotting-papers	Schleicher & Schuell, Dassel, Germany
Hybond^{TM}-C Extra, Nitrocellulose, 45 Micron	GE-Healthcare
PD10 column	GE-Healthcare
X Ray films	FUJI Super RX
GENiosPlus (Microplate Reader)	Tecan, Crailsheim Germany
HB2448 LaminAir (bench)	Heraeus, Hamburg, Germany
Biofuge A, 13 R, 3.2 RS (centrifuge)	Heraeus, Hamburg, Germany

2.2 Methods

2.2.1 Methods in molecular biology

2.2.1.1 Isolation of nucleic acids

2.2.1.1.1 Isolation of RNA from animal cells

Isolation of RNA was done using the Qiagen RNeasy Mini kit.

1. Add 350 µl buffer RLT to cell pellet (freshly harvested or frozen pellet, thawed on ice beforehand)

2. add 350 µl 70% EtOH to lysate, mix by pipetting and apply solution to a RNeasy mini spin column
3. centrifuge for 15 min at 10000 rpm
4. add 350 µl buffer RW1 to column
5. centrifuge for 15 min at 13000 rpm to wash column
6. add 10 µl DNase and 70 µl buffer RDD onto column membrane, incubate for 15 min at RT
7. add 350 µl buffer RW1 to column
8. centrifuge for 1 min at 10000 rpm
9. add 500 µl buffer RPE to column, centrifuge for 15 min at 10000 rpm
10. add 500 µl buffer RPE to column, centrifuge for 2 min at 10000 rpm, to wash column
11. to dry the silica membrane centrifuge empty column
12. put column into fresh tube, add 25 µl RNase-free H_2O directly onto the membrane and incubate for 10 min at RT
13. centrifuge for 1 min at 10000 rpm to elute RNA, put on ice
14. store RNA at – 80 °C

2.2.1.1.2 Isolation of plasmid DNA from bacteria (Mini-Preparation)

Mini I-solution	50 mM Glucose
	25 mM Tris-HCl (pH 8.0)
	10 mM EDTA (pH 8.0)
	100 µg/ml RNase
Mini II-solution	0.2 M NaOH
	1% SDS
Mini III-solution	60 ml 5 M potassium acetate solution
	11.5 ml acetic acid
	28.8 ml H_2O
TE-buffer	10 mM Tris/HCl, pH 7.4
	1 mM EDTA, pH 8.0

Isolation of plasmid DNA from bacteria:

1. centrifuge overnight-culture for 5 min at 13000 g
2. discard supernatant
3. add 100 µl Mini I to resuspend the bacterial pellet
4. add 200 µl Mini II, incubate for 10 min (alkaline lyses of bacterial cell wall)
5. add 150 µl Mini III, incubate for 15 min on ice (denaturing proteins)
6. centrifuge for 15 min at 13000 g
7. transfer supernatant into a fresh Eppi
8. add 300 µl isopropanol, invert tube and centrifuge for 5 min at 13000 g
9. discard supernatant
10. add 70% EtOH to precipitate DNA
11. centrifuge at max speed for 10 min
12. discard supernatant, dry pellet at 37°C
13. dissolve pellet in 30 µl TE-buffer (optional: instead of TE add 30 µl TE-buffer containing RNase solution, incubate for 1 h at 37°C, to destroy any RNA (if present))

2.2.1.1.3 Isolation of plasmid DNA from bacteria (Midi-preparation)

Isolation of plasmid DNA in medium amount was done with the Qiagen HighSpeed Plasmid Midi Kit in steps as follows:

1. inoculate culture, grow ON
2. prechill buffer P3 on ice before starting
3. centrifuge ON-culture at 6000 g for 5 min, discard supernatant
4. add 6 ml buffer P1 (incl RNase), vortex to resuspend pellet
5. add 6 ml buffer P2, mix and incubate for 5 min at RT
6. add prechilled buffer P3, mix and put on QIAfilter Cartridge
7. incubate for 10 min at RT
8. during incubation time equilibrate the HiSpeed Midi Tip with 4 ml buffer QBT
9. apply lysate to HiSpeed Midi Tip
10. wash with 20 ml buffer QC
11. eluate DNA with 5 ml buffer QF
12. add 3.5 ml isopropanol to precipitate DNA, incubate for 5 min at RT and transfer precipitate onto a QIAprecipitator
13. wash precipitator with with 2 ml 70% EtOH and dry precipitator by pressing air through
14. elute DNA from precipitator by adding 1 ml buffer TE
15. store DNA at -20°C

2.2.1.1.4 Transforming DH10Bac^{TM} E.coli

Production of LB-plates for pFastBac-Transformations, containing Tetracycline, Kanamycin, Gentamycin, Bluo-Gal and IPTG (TetKaGeBlIP-plates)

for 500 ml:

> 5 g Tryptone
> 2.5 g Yeast extract
> 5 g NaCl

adjust to pH 7.0 and add 7.5 g agar before autoclaving.

After autoclaving cool liquid to ~ 55°C and add antibiotics, Bluo-Gal and IPTG using the following scheme:

	Final concentration	Stock solution	for 500 ml
Kanamycin	50 µg/ml	10 mg/ml	2.5 ml
Gentamycin	7 µg/ml	10 mg/ml	0.350 ml
Tetracyclin	10 µg/ml	10 mg/ml	0.5 ml
Bluo-Gal	100 µg/ml	20 mg/ml	2.5 ml
IPTG	40 µg/ml	200 mg/ml	0,1 ml

(Dissolve 0.2 g Bluo-Gal in 10 ml DMSO)

Pour LB-agar into 10cm plates, let them harden, invert them and store at 4°C, without exposure to light (Bluo-Gal and Tetracycline are light sensitive).

SOC media (250 ml):

Bacto tryptone	5 g	
Yeast extract	1.25 g	
NaCl	0.15 g	
KCl	0.125 g	
1M Glucose	5 ml (final 20 mM)	
1M $MgCl_2$	2.5 ml (final 10 mM)	
1M $MgSO_4$	2.5 ml (final 10 mM)	

Transformation procedure:
1. thaw competent MAX Effiency® DH10Bac^{TM} cells on ice
2. add 100 µl cells for each transformation into a 2ml Eppi
3. add 1 ng (5 µl) cloned pFastBacHT-C-NRD-construct, mix gently
4. incubate cells on ice for 30 min
5. heat-shock: 45 sec at 42°C
6. transfer tubes for chilling on ice for 2min
7. add 900 µl SOC medium (RT)
8. shake pFastBac-Transformations: 4 h, 225 rpm, at 37 °C
9. pFastBac- Transformations: make 10 – fold dilutions (1:10, 1:100, 1:1000) with SOC – Media
10. plate 100 µl of each dilution on a TetGeKaBlIP-LB-plate
11. incubate for 48 h at 37°C
12. pick 10 white colonies from each plate an replate them on a fresh TetGeKaBlIP-LB-plate
13. incubate plates overnight at 37°C
14. pick white colonies and inoculate them in LB, containing TetGeKa (10 / 7 / 50 µg/ml)
15. incubate overnight in a shaking incubator at 37°C

2.2.1.1.5 Isolation of recombinant bacmid DNA from DH10Bac^{TM} E.coli

Isolation of bacmid DNA differs not much from isolation of plasmid DNA. All steps have to be done with more care, especially pipetting steps, as shearing forces may destroy the desired large sized recombinant bacmid DNA.

Solution I (15 mM Tris-HCl, pH 8.0, 10 mM, 100 µg/ml RNaseA)
Solution II (0.2 M NaOH, 1% SDS)
3 M potassium acetate, pH 5.5
1. Transfer 1.5 ml of cultures into an Eppi and centrifuge at 14000 g for 1 min
2. Remove supernatant and gently resuspend pellet in 300 µl Solution I by careful pipetting up and down
3. Add 300 µl Solution II, mix gently and incubate for 5 min at RT
4. Slowly add 300 µl of 3 M potassium acetate, mix gently and place on ice for 10 min
5. centrifuge for 10 min at 14000 g
6. take fresh Eppi, add 800 µl isopropanol and transfer supernatant (step 5.) into Eppi
7. invert tube several times, put on ice for 10 min
8. centrifuge for 15 min at 14000 g (RT)
9. remove supernatant, add 500 µl EtOH (70%) to wash pellet
10. centrifuge for 5 min at 14000 g, RT, repeat 9. and 10
11. remove supernatant, dry pellet and dissolve DNA pellet in 40 µl 1X TE-buffer
12. store DNA at 4°C
13. analyse recombinant bacmid DNA

2.2.1.1.6 Analysis of recombinant bacmid DNA

Due to the larger size of recombinant bacmid DNA, PCR was performed using M13 Forward and M13 reverse Primers or Primers specific for NRD (CBRnNRDFW, CBRnNRDRV), Taq-Polymerase Master Mix and a standard PCR protocol with annealing temperature of 62°C and 30 cycles.

2.2.1.1.7 Isolation of DNA- fragments from agarose gels

To elute DNA-fragments from agarose gels the MinElute Gel extraction kit (Qiagen) was used. The protocol was done as follows:

1. Weight 2 ml Eppi
2. cut DNA from gel (BioRad GelDoc XR, preparation mode) and put gel into the 2 ml Eppi
3. weight again, calculate agarose weight
4. add 3 fold gel-weight of buffer QG
5. place Eppi on shaker for 10 min at 50 °C until the gel is dissolved
6. add 1 gel volume isopropanol, invert Eppi and transfer mixture on a MinElute column
7. centrifuge for 1 min at 13000 rpm
8. add 500 µl buffer QG, centrifuge again for 1 min
9. to wash column add 750 buffer PE, centrifuge for 1 min
10. to dry column, centrifuge again and place column into fresh Eppi
11. add 15 µl buffer EB (10 mM TrisHCl, pH 8.5) and incubate for 10 min at RT
12. centrifuge for 2 min at 13000 rpm to elute DNA
13. store DNA at -20°C

2.2.1.2 Quantification of nucleic acids

To quantify isolated DNA or RNA, dilute nucleic acids 1: 10 with water and measure the absorption in a quartz cuvette (5.00 mm thickness) by the UV absorption ratio 260 nm /280 nm using an Ultrospec 2000 UV/visible spectrophotometer (Pharmacia Biotech, Freiburg, Germany). Measurement at 260 nm shows the absorption of nucleic acid, at 280 nm the protein absorption. The ratio 260 nm /280 nm was used to determine the quality of the nucleic acid, as this ratio shows the contamination with proteins. A ratio of > 1.7 was considered to be acceptable. Additionally the quality of the nucleic acid was checked on a agarose / TBE gel, prestained with ethidium bromide (1.5 µl of stock solution 10 mg/ml).

2.2.1.3 Precipitation of DNA for sequencing

1. Take 20 µl DNA
2. Add 2 µl Na-Acetate and 55 µl EtOH abs.
3. Centrifuge 13000 rpm for 15 min
4. Discard supernatant
5. Wash with 250 µl 70% EtOH
6. Centrifuge again for 15 min at 13000 rpm
7. Remove supernatant, dry pellet
8. Dissolve in 20 µl 10 mM TrisHCl and quantify the amount of precipitated DNA

Sequencing was done by Seqlab GmbH, Göttingen, Germany

2.2.1.4 Production of cDNA

cDNA was done with the Omniscript Reverse Transcription kit (Qiagen). For each RNA-sample the following Kit-components were added into a cDNA-Eppi:

2 µl buffer
2 µl dNTPs
2 µl OligodT
1 µl Reverse Transcriptase
x µl RNA (x corresponds to the volume of 1 µg RNA)
H_2O ad 20 µl

Synthesis was done using a T3 Thermocycler (Biometra®) and the following program:

Lid temperature110°C
37°C for 1h
99°C for 5 min
4°C until removal of samples

2.2.1.5 Polymerase Chain Reaction (PCR)

Amplification of DNA with PCR was done with the Taq-Polymerase Kit (Qiagen).

The PCR reaction (25 µl) was set up in the following scheme:

Add 1 µl specific cDNA, 2 µl specific Primer fw, 2 µl specific Primer rv, 12.5 µl Taq-Polymerase-Mastermix and 7.5 µl H_2O. PCR was performed in a T3 Thermocycler (Biometra®) using the following program:

Standard PCR NRD:
1. 94°C 3 min
2. 94°C 30 sec
3. 62°C 30 sec
4. 72°C 1 min, 4.->2. 30 cycles
5. 72°C 10 min
6. 4.0°C, pause

Standard PCR p42[IP4]:
1. 96°C 2 min
2. 95°C 30 sec
3. 58°C 45 sec
4. 72°C 3 min, 4.->2. 34 cycles
5. 72°C 10 min
6. 4.0°C, pause

2.2.1.5.1 Non-quantitative PCR

For first detection of expressed genes from different tissues or cell lines, PCR was performed using the cDNA and suitable primers for the gene. The PCR product was run on an agarose-gel and captured with a gel documentation system (BioRad GelDoc XR, Bio-Rad Laboratories).

2.2.1.5.2 PCR for molecular cloning

Primers for cloning of the full coding sequence of NRD were designed according to sequences available in the Genbank (PubMed NM_002525.1) and included suitable restriction sites for subsequent cloning into the multiple cloning site (MCS) of pcDNA6/HisB and pFastBacHT_C. Moreover, primers with similar annealing temperature were used. The cloning PCR was done using the AccuPrime kit (Invitrogen).

Cloning hNRD from HEK 293 cells
       5 µl cDNA
       5 µl Accu Prime Reaction mixture
       1 µl AccuPrime Polymerase
       2 µl CBHsNRDFW
       2 µl CBHsNRDstopRV
       35 µl H_2O (ad 50 µl)

PCR program for cloning NRD
1. 95°C 2 min
2. 95°C 15 sec
3. 50°C 30 sec
4. 68°C 3 min 36 sec, 4.->2. 40 cycles
5. 68°C 10 min
6. 4.0°C, pause

Afterwards the complete volume of the reaction was loaded on a 2%-TBE-agarose gel and the fragment with the correct size was excised and purified using the MinElute Gel extraction kit (Qiagen). Then the fragment was digested with the same restriction enzymes used to cut the DNA-vector. The digested fragment was purified with the QIAquick PCR purification kit (Qiagen) to remove the buffer. The concentration was measured to set up the ligation reaction of the digested PCR-product and target vector.

2.2.1.5.3 Mutagenesis PCR

To perform site directed mutagenesis the QuickChange kit (Stratagene) was used to make point mutations in plasmid DNA. 100 ng of plasmid DNA were used as template. Primers containing the mutated codon were designed that 15 bp were flanking the codon both up- and downstream and the primer pairs are complementary to opposite strands of the vector.

To setup the mutagenesis reaction, add 5 µl 10x reaction buffer, 100 ng plasmid DNA, 12.5 pmol primer fw, 12.5 pmol primer rv, 1 µl dNTP-Mix and 1 µl PfU Turbo DNA Polymerase (high fidelity).
Reaction was performed in a T3 Thermocycler (Biometra), using this program:

1. Initial denaturation at 98 °C for 30 sec
2. Denaturation at 95°C for 30 sec
3. Annealing at 55 °C for 1 min,
4. Extension for 12 min at 68°C, 4.->2. 15 cycles
5. 4°C until removal of samples

Directly after the program was finished, samples were put on ice for 2 min. Then 1 µl of DpnI was added and samples were incubated for 1 h at 37°C. Products were directly transformed into E.coli using the KCM method.

2.2.1.6 Agarose gel electrophoresis

10 X TBE (3000 ml):

890 mM Tris base	323.4 g
890 mM Boric acid	323.4 g
100 mM EDTA (pH 8.0)	111.7 g
autoclave for 20 min	

The quality of the DNA (RNA, recombinant plasmid DNA, PCR product) or DNA restriction analysis was visualized with a 1.5% TBE agarose gel. The gel was prestained with ethidium bromide (10 mg/ml). DNA samples were prepared in 6x loading buffer (containing bromophenol blue dye, MBI Fermentas). Gel was run in 1x TBE for about 30 min at 80 V. A standard marker (GeneRuler 100 bp DNA Ladder (1 kb) or GeneRuler DNA Ladder Mix (10 kb)) depending on the expected size of the band/fragment was used. DNA bands were visualized using the BioRad gel documentation system
.

2.2.1.7 Digestion of DNA with restriction endonucleases

Digestion of DNA with restriction endonucleases was done using the appropriate digestion buffer and incubation temperature. DNA was digested either with one restriction enzyme, to verify the success of a ligation reaction, or DNA was double / triple digested using two restriction enzymes at one time.

Enzyme(s)	NotI XhoI	HindIII	HindIII XhoI	AgeI	BamHI	NotI XhoI PvuI	PvuII	HindIII EcoRI NsbI	EcoRI HindIII
buffer	Y-Tango (2X)	R(red)	R(red)	NEB1	G(green)	Y-Tango (2X)	G(green)	Y-Tango (2X)	Y-Tango (2X)

Enzymes were purchased at New England Biolabs (AgeI, including buffer) or Fermentas Life Science (all other enzymes & buffers).

2.2.1.8 Purification of DNA

To purify DNA fragments after PCR or after restriction digestion the QIAquick PCR purification kit (Qiagen) was used.

Add 5 fold sample volume buffer BP to the sample and pipet everything on a column
Centrifuge for 1 min at 13000 rpm, discard supernatant
Wash bound DNA with 750 µl buffer PE, centrifuge at 13000 rpm for 1 min, repeat last step to get rid of remnants of buffer PE
To elute DNA, add 30 µl buffer EB, incubate for 10 min, place column in fresh Eppi and centrifuge for 1 min at 13000 rpm. Discard column and store purifed DNA at -20°C.

2.2.1.9 Dephosphorylation of digested plasmid DNA

To avoid self-ligation of the linearized plasmid during subsequent ligation, it was subjected to dephosphorylation using the Shrimp Alkaline Phosphatase (Boehringer). For dephosphorylation add:

> 1-2 µl digested DNA
> 2 µl Shrimp Alkaline Phosphatase (1 U/µl)
> 10% (v/v) dephosphorylation buffer (10 X)
> H_2O variable

and incubate for 1 h at 37°C. To denature the phosphatase, incubate the reaction for 20 min at 65°C. To remove the dephosphorylation buffer, the dephosphorylated DNA was purified again.

2.2.1.10 Ligation of DNA insert and plasmid vector

Ligation of DNA-fragments was done using T4-Ligase (Invitrogen). Digested vector and gene of interest were ligated using the following scheme:

	Reaction 1	Reaction 2	Reaction 3
Vector (in fmol)	3	15	30
Insert (in fmol)	15	75	150
H_2O	Ad 15 µl	Ad 15 µl	Ad 15 µl

4 µl 5X ligase buffer (Invitrogen) and 1 µl T4-Ligase was added to each reaction
The ligation was done in a T3 Thermocycler (Biometra®) using the following program:

Lid temperature: 110°C
8 h at 16°C, 4 h at 22°C, 2 h at 37°C and 4°C until removal of samples.

2.2.1.11 Transformation of plasmid DNA into bacteria

2.2.1.11.1   Production of KCM competent cells

To produce KCM competent cells, inoculate a single colony of XL1-Blue or DH5αF
E.coli strain in 5 ml LB media (without antibiotic) and incubate overnight at 37°C, shaking at 250 rpm.

1. Transfer 1 ml of overnight culture into 150 ml of fresh LB media
2. Let the bacteria grow until they reach an OD_{600} of 0.6
3. Centrifuge cell suspension for 10 min at 500 rpm at RT
4. Discard supernatant
5. Resuspend pellet in 15 ml (1/10 volume) buffer TSB
6. Incubate for 10 min on ice
7. Aliquot suspension (500 µl each) into Eppendorf safelock tubes
8. Freeze Eppis in liquid nitrogen and store in -80°C

2.2.1.11.2   Transformation of KCM competent cells

For transformation of plasmid DNA (ligation mix or plasmid DNA from Mini-preparation) KCM competent cells were used. The transformation was done as follows:

1. Pre-warm appropriate volume of SOC media at 37°C (1 ml for 1 transformation)
2. Add 20 µl of ligation mix or 10-20 ng of super-coiled plasmid DNA to 20 µl KCM buffer
3. Mix and put on ice
4. Take KCM competent cells from -80°C and thaw them on ice
5. Add 100 µl competent cells to DNA-KCM buffer mix
6. Incubate on ice for 10 min (for re-transformation) or 50 min (ligation mixture)
7. Add 1 ml pre-warmed SOC media
8. Incubate for 1 h at 37°C with shaking at 300 rpm
9. Pellet transformation mixture and plate on LB agar, containing appropriate antibiotic
10. Incubate plates upsite down overnight at 37°C
11. For retransformation and subsequent Midi preparation, inoculate 50 ml LB (including antibiotic) directly with transformation mixture

2.2.1.12 Generation and production of recombinant baculovirus

To generate recombinant baculovirus the purified recombinant Bacmid-DNA has to be transfected into insect cells. For that split Sf9-cells to a densitiy of ~ 3x 10^6 cells (~ 0.25 ml of a confluent 25ml bottle). Add 4.75 ml Sf9-Media (27°C) (Media for transfection w/o FCS and antibiotics) and control the cells for attachment after 1 h incubation.
To transfect the Sf9 cells, prepare 2 Eppis using the following table:

1	3 µg (30 µl)	Bacmid-DNA
	100 µl	IPL41 w/o serum and antibiotics (Insect.Media)
2	18 µl	Cellfectin®
	100 µl	IPL41 w/o serum and antibiotics (Insect Media)

Mix reaction 1 & 2 and incubate for 30 min at RT
Remove media from Sf9-cells and add 5 ml IPL41 (w/o antibiotics and FCS)
Add the mix (1&2) to the cells and incubate ON and change the cell media the following day.
Let transfected cells grow for 6 days, to amplify virus. Centrifuge cells, discard the Sf9-cell pellet but store the supernatant (Baculo virus supernatant, BVSN).
Take 200 µl BVSN and infect Sf9-cells (2 bottles with Sf9 cells) and grow cells for 4 days to amplify virus. Harvest cells, centrifuge, freeze cell pellet and store supernatant at 4°C (stock virus 1, SV1)
Take 200 µl SV1 and infect 2 bottles with fresh Sf9-cells and grow them for 4 days. Harvest cells, centrifuge, freeze cell pellet and store supernatant at 4°C (stock virus 2, SV2)
Prepare 6 bottles with Sf9-cells. Infect 5 bottles with 200 µl SV2 (A) and one bottle with 500 µl SV2 (P). Grow cells, harvest bottle P after 60 –72 h, lyse cell pellet. Purify protein using Ni-beads and verify protein expression (Coomassie-Gel). Harvest bottles A after 5-6 days, centrifuge and store supernatant at 4°C (working virus, wv) and pellet at –80°C.
Infect Sf9-cells with 500 µl wv and optimize culturing time for optimal protein expression.

2.2.2 Methods in cell biology

2.2.2.1 Cell culture

Cryopreservation

For long time storage cells were frozen in DMSO and stored in liquid nitrogen. Briefly, medium was removed; cells were washed with PBS and trypsinized (2 ml trypsin per 10cm dish). Trypsinized cells were transferred into a 15 ml tube, containing 8 ml cell media and centrifuged for 3 min at 200 rpm. Supernatant was removed, 1.8 ml media was added, cells carefully resuspended and aliquoted into 2 cryo-tubes, each containing 100 µl DMSO. Cryo-tubes were kept in –20°C for 2 h, transferred to –80°C for 5 h and finally stored in liquid nitrogen.

Thawing of cryo-preserved cells: suitable cell media was directly poured into a bottle for culturing cells (10 ml media) and placed in a incubator; 9 ml cold media was added into a 15ml tube. Cryo-tubes were taken out of the liquid nitrogen and thawed in a 37°C-waterbath (shaking by hand) until the ice has the size of a pea. Cell suspension was transferred into the 15ml tube (with cold media) and centrifuged for 3 min at 200-300 g. Supernatant was removed, cells carefully resuspended in fresh media and transferred into the cell culture bottle (with pre-warmed media, in incubator).

2.2.2.2 Lipotransfection

Transfection of mammalian cells was done using Fugene6 (Roche Diagnostics). Briefly, Fugene6 was added to 180 µl serum-free medium and incubated for 5 min. Then 500 ng DNA was added, mixed and incubated for 30 min. For transient transfection, medium of cells was changed to serum free media. The Fugene6-DNA complex was added to the cells, incubated overnight and serum free medium was changed to complete medium. For stable transfection the medium was not changed to serum free media. The Fugene6-DNA complex was directly added to the cells and incubated overnight. Then the medium changed to fresh complete medium.

2.2.2.3 Transfection with magnetic beads

SH-SY5Y cells were split in 60mm dishes and grown until a confluence of 60-80% was reached. 6.6 µg DNA was mixed with media (w/o FCS and supplements) and 6.6 µl MATra-solution and incubated for 20-30 min at room temperature.
After incubation media was changed, 4 ml fresh media (w/o FCS and supplements) and the DNA/MATra-Mix was added and incubated for 15 min on a magnetic plate at 37°C.
Afterwards media was changed and fresh media (complete with FCS and supplements) was added. 24-48 h post transfection, cells were inspected for transfection and antibiotic was added for selection of stably expressed DNA in these cells.

2.2.3 Methods in protein chemistry

2.2.3.1 Production whole cell lysate

4x Lysis buffer:

> 200 mM Tris / HCl, pH 7.5
> 4 mM EDTA
> 4 mM β-mercaptoethanol
> 600 mM NaCl
> 4% Igepal

According to the size of the cell culture dish 1X lysis buffer is added to the frozen cell pellet (1 ml (10cm dish), 0.5 ml (6cm dish) or 250 µl (3.5cm dish)) and resuspended. The lysate was incubated at 4°C, 15 min on a rotating wheel. The samples are then centrifuged at 14000 g, 15 min, 4°C (Beckmann Avanti), the supernatant is transferred into a new tube.

2.2.3.2 Protein quantification (Bradford)

Protein quantification of whole cell lysate was done using the BioRad Protein assay. A dilution series of a standard ([BSA] = 1 mg/ml) was prepared as follows:

Standard No	Final concentration (µg/ml)	BSA-solution (µl)	H_2O (ml)
1	0	-	1
2	1	1	0.999
3	2	2	0.998
4	5	5	0.995
5	10	10	0.990
6	15	15	0.985
7	20	20	0.980
8	25	25	0.975

For each sample, 2 different dilutions are prepared in an amount suitable for triple measurement.

50 µl BioRad-Reagent are added to each well of a ELISA-microtiter-plate (NUNC-IMMUNO™MODULE 160 BAG or 80 BAG) and 200 µl sample resp. standard are added and incubated for 10 min. Protein concentration is measured at 595 nm in a ELISA-Reader (Emax precision microplate reader, Molecular Devices) and quantified using the program SOFTmax®PRO.

2.2.3.3 Methanol/acetone precipitation of proteins

To concentrate aqueous protein solutions they are mixed with their 4 fold volume of a methanol/acetone solution, incubated at 37°C for 15 min and centrifuged at 14000 rpm, RT, 15 min; the supernatant removed and the pellet dried at 37°C. The dry pellet is then dissolved in 20 µl 1X sample buffer.

2.2.3.4 TCA precipitation of proteins

100% TCA (w/v):

> 100 g TCA (trichloroacetic acid)
> 45.4 ml H_20

1. Add 1/11 of sample volume 100% TCA to sample (medium, supernatant) (110 µl 100% TCA to 1 ml medium)
2. mix by inverting the tube several times
3. incubate for 10 min at room temperature
4. centrifuge for 15 min, max speed, remove supernatant
5. add 200 µl 10% TCA to pellet
6. mix by vortexing, centrifuge for 15 min, max speed, remove supernatant
7. add 200 µl 10% TCA to pellet
8. mix by vortexing, centrifuge for 15 min, max speed, remove supernatant
9. add 200 µl ice cold acetone
10. mix by vortexing, centrifuge for 15 min, max speed, remove supernatant
11. dry pellet at room temperature and dissolve in sample buffer (containing β-Mercaptoethanol)

2.2.3.5 SDS PAGE

2.2.3.5.1 Preparation of polyacrylamide gels

Buffer and solutions

30% Acrylamid / BIS (Roth)

Separating gel buffer:
> 750 mM TRIS / HCl (18.2 g / 200 ml) adjust with 5 M HCl to pH 8.8

Stacking gel buffer:
> 250 mM TRIS / HCl (6.1 g / 200 ml) adjust with 5 M HCl to pH 6.8

SDS-Solution:
> 10% (w/v) SDS in H_2O (1 g / 10 ml)

PER- Solution:
> 10% (w/v) Ammonium peroxydisulfate in H_2O (1 g / 10 ml)

TEMED:
> N,N,N´,N´-Tetramethylethylendiamin (Roth)

5x gel running buffer:
> 125 mM TRIS (15.31 g / l) / 960 mM Glycine (72.1 g / l)

4x Sample buffer:

> 500 mM TRIS / HCL (6.05 g / 100 ml), pH 6.8
> 8% (w/v) SDS (8 g / 100 ml)
> 40% Glycerol (40 g / 100 ml)
> 0.005% (w/v) Bromphenolblue (1 ml Bromphenolblue in H_2O)
> add H_2O to a total volume of 80 ml and adjust to pH 6.8 with HCl
> 20% mercaptoethanol (add prior to use)

The proteins were separated using the method of Laemmli (Laemmli, 1970). The gels were done using the following scheme (for 2 gels each)

	Resolving gel				Stacking gel	
	5%	7%	10%	12.5%	3%	4%
30% Acrylamide / BIS	2 ml	2,8 ml	4 ml	5 ml	0.5 ml	0.67 ml
Resolving gel buffer	6 ml	6 ml	6 ml	6 ml	-	-
Stacking gel buffer	-	-	-	-	2.5 ml	2.5 ml
H_2O	3.8 ml	3.0 ml	1.8 ml	0.8 ml	1.9 ml	1.73 ml
10% SDS-solution	0.12 ml	0.12 ml	0.12 ml	0.12 ml	0.05 ml	0.05 ml
PER-solution	0.06 ml	0.06 ml	0.06 ml	0.06 ml	0.04 ml	0.04 ml
TEMED	24 µl	24 µl	24 µl	24 µl	10 µl	10 µl
Bromphenolblue	-	-	-	-	15 µl	15 µl

The glass and metal plates were cleaned with 70% EtOH and prepared for the gel caster system. 4.6 ml of the desired resolving gel solution was poured into the gel caster and immediately overlaid with isopropanol to get a smooth resolving gel surface. After polymerization the isopropanol is carefully removed with H_2O. Remaining H_2O is soaked out with a small stripe of Whatman paper. A suitable gel comb is inserted and the stacking gel solution is added.

2.2.3.5.2 *Preparation of protein samples for SDS PAGE*

The protein samples are either precipitated (in case of lower protein concentration) with methanol / acetone precipitation and dissolved in 1 X sample buffer or the protein samples (in case of higher protein concentration) are directly dissolved in 2 X sample buffer. To quantify the molecular weight of the samples 5 µl of molecular standards were diluted in 15 µl 1 X sample buffer.

The following **markers** were used:

Low Molecular Weight (LMW, GE-Healthcare):
Contains a mixture of these proteins:

> Phosphorylase b M_w = 97 kDa
> Albumin M_w = 66 kDa
> Ovalbumin M_w = 45 kDa
> Carboanhydrase M_w = 30 kDa
> Trypsininhibitor M_w = 20.1 kDa
> α-Lactalbumin M_w = 14.4 kDa

Precision Prestained Plus (BioRad):

Contains 10 prestained recombinant proteins in the following sizes:
10 kDa, 15kDa, 20 kDa, 25 kDa, 37 kDa, 50 kDa, 75 kDa, 100 kDa, 150 kDa, 250 kDa.

Prepared samples and marker are boiled for 5 min and spun down shortly. The prepared gels are placed into the gel chamber, fastened and the upper and lower chamber is filled with running buffer. After removal of the gel comb the sample wells are washed using a syringe (Hamilton) and samples are applied.

The gel chamber is connected to the power supply and the samples are electrophoretic separated at 80 V until they reach the separation gel. Then the voltage is increased to 120 V until the (coloured) running front of the samples has reached the bottom of the gel.

After finishing the electrophoresis the glass plates are removed from the gel, the stacking gel is cut off and discarded. The remaining gel can be stained with Coomassie Dye or transferred onto a nitrocellulose membrane for Western Blotting.

2.2.3.5.3 Coomassie-staining of SDS-gels

Staining solution:

0.25% (w/v) Coomassie Brilliant Blue R250 (2.5 g/l)
10% (v/v) pure acetic acid
45% (v/v) methanol
in H_2O

Destaining solution:

10% (v/v) pure acetic acid
30% (v/v) methanol
in H_2O

For staining of polyarcylamide gels the gels are placed into staining solution on a rocker for at least 30 min. To destain the background, gels are transferred into destaining solution, covered with a small piece of foamed material, and rocked until sufficient destaining. Afterwards the gels are dried overnight using a gel drying frame.

2.2.3.5.4 Blotting and immunostaining (Western Blot)

5 X Transfer buffer:

125 mM TRIS (15.1 g / l) / 960 mM Glycin (72.1 g / l)

1 X Transfer buffer:

20% (v/v) methanol, 20% (v/v) 5 X Transfer buffer, 60% (v/v) H_2O

Ponceau-S-solution:

0.2% (w/v) Ponceau S (Boehringer, Mannheim) in 3% acidic acid

Washing buffer:

PBS / Tween 0.05%:
100 ml 10 X PBS
900 ml H_2O
0.5 ml Tween[®]20

The polyacrylamide gel is equilibrated for blotting in the transfer buffer for a few minutes, placed onto a gel-sized nitrocellulose membrane (Hybond[TM]-C Extra, Nitrocellulose, 45 Micron).

Similarly, two blotting papers (Gel-Blotting Paper GB 003, Schleicher & Schuell) are equilibrated in transfer buffer, placed directly into the semidry-blot cell (Trans-Blot SD; BIO-RAD, München), and covered with two equilibrated blotting papers.

The blotting is done at 15 V, 200 mA (for 1 gel) or at 15 V, 400 mA (high voltage; for more than 1 gel). The transfer of proteins is controlled with Ponceau-S-solution; markers as they are not prestained – are marked and the membrane is destained in H_2O.

To block unspecific binding the membrane is blocked with Rotiblock[®] (1:10 in H_2O) or non-fat-dry milk (3.5 or 5% w/v) for at least 1 h.

After blocking, the membrane was incubated with the antibody directed against the specific protein. The duration for the incubation with the primary antibody was adjusted to the target protein and the antibody. Usually, the incubation was done for 1 h or ON.

After the incubation with the primary antibody the membrane was washed three times (15, 10 and 5 min) with PBS-Tween 0.1% and incubated with the secondary antibody (HRP conjugated) for 1 h. Then the membrane was washed as done with the primary antibody, incubated with the ECL reagent (Supersignal West Pico kit) for 5 min, and exposed to X-Ray films. Films were scanned with a GS-800 Calibrated Densitometer and quantified using the Biorad Quantitiy One Program and if desired, statistical analysis was done using SIGMA Plot 8.0.

2.2.3.5.5 Stripping of membranes for reprobing

For reprobing of Western Blot membranes with a different primary antibody, the membranes have to be cleaned from the firstly used primary antibody (stripping).
Stripping buffer for removal of antibodies:

> 62.5 mM TRIS/HCl pH 6.7 (0.757 g / 100 ml)
> 2% (w/v) SDS (2 g / 100 ml)
> 100 mM β-Mercaptoethanol (800 µl / 100 ml)

After detection with first antibody, membranes are washed with (PBS /Tween 0.1%) and incubated for 30 min at 50°C covered in stripping buffer. After incubation, membranes are carefully washed and incubated with blocking buffer.

2.2.3.6 Purification of His-tagged proteins

Purification of His-tagged proteins from Sf9-cells was done using a modified protocol as published in Ma et al 2001.

Lysis buffer (200 ml):

50 mM TrisHCl	(1.21 g)
150 mM KCl	(2.24 g)
pH 8.5	

Washing buffer (200 ml):

50 mM TrisHCl	(1.21 g)
2 M NaCl	(23.38 g)
pH 8.5	

Materials and methods

Elution buffer (200 ml):

50 mM TrisHCl	(1.21 g)
250 mM Imidazole (MW 68.08)	(3.40 g)
pH 8.5	

	His-HsNRD (example)
Number of bottles- harvested for pellet (KF)	6 (example)
Lysis buffer (KF x 3ml= V_L)	18 ml
Protease inhibitors: Leupeptin (V_L x 1 µl/ml) Pepstatin A (V_L x 1 µl/ml) Aprotinin (V_L x 1 µl/ml) Pefablock SC (V_L x 2.5 µl/ml) Benzamidine (V_L x 2 µl/ml)	 18 µl 18 µl 18 µl 45 µl 36 µl
Nickel Agarose Beads (KF x 100 µl = V_B)	600 µl
Washing buffer (KF x 1.5 ml) (Sf9-Lysis buffer without protease inhibitors)	9 ml
Elution buffer (=V_B)	600 µl

Calculate and prepare desired amount of Sf9 lysis buffer, washing buffer, nickel agarose beads using the example shown above. Purify His-tagged protein:

1. add lysis buffer (including protease inhibitors) to cell pellet
2. homogenize cell pellet using a Ultraturrax (IKA T25)
3. centrifuge lysate for 30 min, 4 °C, at 35000 x g (Sorvall centrifuge 20000 rpm, Sorvall SS34 rotor)
4. during centrifugation equilibrate Ni-Agarose-Beads by washing them 3 times with 2V_B (see table) at 2000xg, for 5 min at 4°C
5. after last washing step resolve Ni-Beads in 0.5V_B Lysis buffer
6. take supernatant of centrifuged lysate, take aliquot for SDS-PAGE *[Input I]*
7. add Ni-agarose- beads to supernatant and incubate on a rotating wheel for 1 h at 4 °C
8. centrifuge at 500-1000 xg (1700 rpm), for 10 min at 4°C; take aliquot for analysis *[D]*
9. wash 3 times with V_L (see table) lysis buffer, take aliquots for gel *[L1, L2, L3]* (centrifuge at 500-1000 xg (1700 rpm), 4°C for 10 min each time)
10. add washing buffer, centrifuge at 500-1000 xg (1700 rpm), for 10 min at 4°C, take aliquot for gel: W)
11. to elute protein add elution buffer (V_B see table) and shake on ice for 15 min; centrifuge at 3300 rpm, 4°C for 5 min, take aliquot (E1)
12. add 1 V_B elution buffer, shake on ice for 10 min, centrifuge at 3300 rpm, 4°C for 5 min, take aliquot (E2)

Run SDS PAGE with aliquots of I, D, E1 and E2 an stain with Coomassie to verify efficiency of purification and expression of desired His-tagged protein.

When the protein is expressed in sufficient amounts (verified by Coomassie-staining), total amounts of elution E1 and E2 were pooled and the buffer was exchanged with storage buffer as follows:

Storage buffer:

20 mM KH_2PO_4,

10 % Glycerol,   pH 7.0

For washing add 20 ml storage buffer on the column (PD10 column, GE-Healthcare) and let buffer flow through the column.

Meanwhile adjust the pooled protein to a volume of 2.5 ml using storage buffer and apply it to the column.

Collect fractions and check the protein concentration using 12.5 µl Bradford reagent, 45 µl H_2O and 5 µl of sample. Use the same Bradford assay program but set samples as standard (no BSA standards required). Pool fraction with highest protein concentration (highest peak in Bradford assay) and apply to an equilibrated (washed one time with storage buffer, centrifuged for 5 min at 4000 rpm) concentrator (Centricon-10 (Millipore) concentrator). Concentrate protein approximately to 1ml final volume and quantify final concentration (Standard Bradford protein assay including BSA dilution series). Prepare aliquots of concentrated protein, freeze in liquid nitrogen and store protein at – 80°C.

2.2.3.7 Purification of GST-tagged proteins

Lysis buffer (200 ml):

50 mM TRIS (MW 121.1)	1.21 g
150 mM NaCl (MW 58.44)	1.75 g
10 mM NaF	20 ml 100 mM NaF
1% TRITON X100	2 ml
adjust to pH 7.5 using HCl	

4 M NaCl

NaCl (MW 58.44)	23.4 g
ad 100 ml using H_2O	

1 M NaCl /Lysis buffer (30 ml):

7.5 ml 4x Lysis buffer (modified RIPA-buffer)
6.375 ml 4 M NaCl
16.125 ml H_2O

10X TRIS/NaCl (200 ml)

500 mM TRIS (MW 121.1)	12.11 g
1 M NaCl (MW 58.44)	11.69 g
pH 8.0 with HCl	

storage buffer (200ml):

        50 mM TRIS/HCl pH 8.0
        100 mM NaCl
        20 ml 10xTRIS/NaCl
        1 mM β-mercaptoethanol   16 µl
        20% Glycerol

	GST-p42^{IP4} (example)
Number of bottles- harvested for pellet (KF)	6
Sf9 lysis buffer(Triton) (KF x 3 ml = V_L)	18 ml
Protease inhibitors: Leupeptin (V_L x 1 µl/ml) Pepstatin A (V_L x 1 µl/ml) Aprotinin (V_L x 1 µl/ml) Pefablock SC (V_L x 2.5 µl/ml) Benzamidine (V_L x 2 µl/ml)	 18 µl 18 µl 18 µl 45 µl 36 µl
Glutathion Sepharose Beads (KF x 100 µl=V_B)	600 µl
Washing buffer (KF x 1.5 ml) 1 M NaCl / Lysis buffer (modified RIPA-buffer)	9 ml

Calculate and prepare desired amount of Sf9 lysis buffer, washing buffer, Glutathione sepharose beads using the example shown above. Purify GST-tagged protein:

1. Add Sf9-lysis buffer (Triton) containing Protease inhibitors to cell pellet
2. homogenize cell pellet using a Ultraturrax (IKA T25)
3. centrifuge homogenate for 20 min, 38400 xg (17000 rpm) (Sorvall AH629 Rotor) at 4°C
4. equilibrate GSH-beads: wash 1 time with V_B and 2 times with $2xV_B$ Sf9-Lysis buffer (Triton) for 5min, 500 xg at 4°C
5. take supernatant from cell homogenate (after centrifugation, step 3) add 100 µl Glutathion Sepharose Beads per bottle (=V_B) and incubate for 1 h at 4°C on a rotating wheel
6. centrifuge at 500-1000 xg (1700 rpm), 4°C for 7 min [after Beads D]
7. wash beads 3 times with Sf9-lysis buffer (Triton) [aliquots L1, L2, L3]
8. resuspend beads in 1 M NaCl / lysis buffer (modified. RIPA-buffer), shake on ice for 15 min, centrifuge [aliquot W]
9. adjust beads to a final concentration of 50% slurry (use ½ V_B) Sf9- storage buffer
10. run SDS-PAGE [input, D, GST-beads, L1/2/3, W] to verify quality of purification

2.2.3.8 Pull-down recombinant His tagged proteins with GST-tagged proteins

Adjust His - tagged protein to a final concentration of 50 µg/ml using lysis buffer/BSA Prepare six samples using the following table:

Reaction (µg His - tagged protein)	µl lysis buffer/BSA	X µl of His-tagged protein (50 µg/ ml)	µl Beads
1 (0)	90 µl	0	20 µl GST
2 (1)	70 µl	20 µl	20 µl GST
3 (0)	90 µl	0	20 µl GST-tagged protein
4 (0,1)	88 µl	2 µl	20 µl GST-tagged protein
5 (0,5)	80 µl	10 µl	20 µl GST-tagged protein
6 (1)	70 µl	20 µl	20 µl GST-tagged protein

1. Incubate for 2 h at 4°C on a shaker
2. Centrifuge samples for 5 min at 1000xg
3. wash 2 times with 200 µl lysis buffer/BSA at 1000xg, 4°C for 5 min
4. wash 2 times with 200 µl lysis buffer without BSA at 1000xg, 4°C for 5 min
5. incubate with 100 µl lysis buffer containing 1 M NaCl for 15 min at 4°C
6. to elute bound proteins; centrifuge at 13000xg, 4°C for 5 min
7. precipitate eluted proteins using methanol/acetone precipitation

2.2.3.9 Immunprecipitation

Take 500 µg lysate, add anti-GFP (5-10 µl), incubate for 4 h at 4 °C on rotating wheel
Add Sepharose-A or –G-beads, incubate overnight at 4°C on rotating wheel
Wash 3 times with 1X lysis buffer (1 ml/ tube) (with or without P_i), centrifuge at 500g for 5 min (Beckmann 2500 rpm, 4°C)
Leave 10-20 µl supernatant, add 2X (or 4X) sample buffer, mix
Boil samples for 5 min, centrifuge (max speed), take supernatant for analysis on SDS-PAGE

2.2.3.10 Far Western Blot

Far Western Blots, including the buffers used, were done according to a modified protocol published previously (Wu et al., 2007). To allow tubulin polymerization, the amount of glycerol was increased to 4 M in the protein binding buffer, as it was published before (Shelanski et al., 1973). For experiments, using nonpolymerized tubulin, the protocol was performed as described before, except that after adding of protein binding buffer, blots were kept on a shaker at 4°C for 1.5 h, followed by addition of hsNRD1 and tubulin in 4°C, without prior exposure to heated buffer.
Milk-solution:
3g milk powder in 14.7 ml ddH$_2$O
Buffer AC:
14.7 ml milk solution
3 ml NaCl (5 M)
3 ml Tris (1 M), pH 7.5
0.3 ml EDTA 0.5 M
1.5 ml Tween-20 (10%)
15 ml Glycerol
150 µl DTT (1 M)

buffer 6:

       18.75 ml Guanidine-HCl (8 M)

       6.275 ml buffer AC

buffer 3:

       9.3 ml Guanidine-HCl (8 M)

       10.37 ml H_2O

       6.275 ml buffer AC

buffer 1:

       3.13 ml Guanidine-HCl (8 M)

       15.62 ml H_2O

       6.275 ml buffer AC

buffer 0.1:

       310 µl Guanidine-HCl (8 M)

       18.44 ml H_2O

       6.275 ml buffer AC

buffer 0:

       18.75 ml H_2O

       6.275 ml buffer AC

buffer 6: 30 min, RT; buffer 3: 30 min, RT; buffer 1: 30 min, RT; buffer 0.1: 30 min, 4°C; buffer 0: overnight, 4°C

blocking:

cut membranes and block in Rotiblock® during tubulin polymerization (5 h); remove Rotiblock ® and add 1050 µl protein binding buffer, incubate box 1 and box 2 for 1.5 h at RT (shaker), incubate box 3-8 for 1.5 h at 4°C (=during incubation of tubulin with NRD)

protein binding buffer:

Milk-solution:

       0.2 g milk powder in 6.47 ml ddH_2O

Buffer AC:

       6.47 ml milk solution

       200 µl NaCl (5 M)

       200 µl Tris (1 M), pH 7.5

       20 µl EDTA 0.5 M

       100 µl Tween-20 (10%)

       3 ml Glycerol (30% ~ 4 M for tubulin polymerisation without GTP)

       10 µl DTT (1M)

- incubate for box 2 tubulin+buffer (ad 200 µl) for 5 h at 37°C in a 1.5 ml Eppi
- add hsNRD1 [210 µg/µl] (reaction: 1, 2) and incubate for 1.5 h at 20°C

	1	2	3	4	5	6	7	8
NRD	10 µg	10 µg						
	hsNRD1	hsNRD1						
tubulin	0	10						
NRD (µl)	48	48						
tubulin (µl)	0	5						
buffer AC (ad 200 µl)	152	147						
adjust to 1.25 ml (µl AC)	1050	unpolymerized tubulin						

add hsNRD1+tubulin */ NRD + nonpolymerized tubulin (reaction: 3-8)* mixture to blocked membrane

- incubate overnight (4°C, shaker)
- wash blots 8 times, each 15 min with PBS Tween 0.1%
- incubate with NRD antibody (N20 1:2000) for 2h at RT, wash 3 times (15, 10, 5 min)
- incubate with mouse anti goat-HRP 1:20000 for 1h at RT, wash 3 times (15, 10, 5 min), detection see chapter 2.2.3.5.4
- strip membranes, block in Rotiblock®
- incubate with p42^{IP4}-antibodies: 117-2 1:5000; goat anti mouse-HRP 1:20000, detection see description above and chapter 2.2.3.5.4

2.2.3.11 Fluorescence measurements

The quenched substrate (abz =Abz-Gly-Gly-Phe-Leu-Arg-Arg-Val-Gly-Gln-EDDnp) derived from bovine adrenal medulla peptide ((Csuhai et al., 1999b); custom synthesis BACHEM, Switzerland) was used to monitor the cleavage activity of the purified NRD at 34°C, in 20 mM potassium phosphate, pH 7 in a 200 µl reaction using a TECAN-fluorescence reader with excitation wavelength 320 nm and emission wavelength 420 nm.

2.2.3.12 Cleavage assay p42^{IP4}

To test, whether p42^{IP4} can serve as a substrate for NRD, equimolar amounts (80 nM) of both proteins were incubated for 1, 4, 7 and 10 hours at 37°C in potassium phosphate-buffer, pH 7 (Csuhai et al., 1999b). The reaction was stopped by adding 4X sample buffer, containing β-mercaptoethanol, 5 min boiling and immediate storage at –20°C. Afterwards samples were boiled and loaded onto a 12.5% SDS-PAGE. Western Blot was done using the following p42^{IP4} specific antibodies 117-2, Rai-1 and Rai-2. Secondary antibodies: goat anti mouse and goat anti rabbit.

2.2.4 Confocal microscopy

Cells were fixed with 4% paraformaldehyde solution (PFA)(4% sucrose, 120 mM Na-phosphate buffer, pH 7.4) for 30 min at RT, after removal of PFA, fetal serum blocking buffer (FSBB; 6% FCS, 20 mM Na-phosphate buffer, 0.45 M NaCl, 0.1% Triton-X100, pH 7.4) was added for 20 min to block unspecific binding. Coverglasses were washed three times in low salt (0.15 mM NaCl and 10 mM phosphate), three times in high salt (0.5 mM NaCl and 20 mM phosphate) buffer.

For SH-SY5Y cells primary antibodies were used according to the experimental setup: for detection of NRD and p42^{IP4} (goat anti-NRD N20 1:100, rabbit polyclonal anti-p42^{IP4} antibody 1:200, diluted in FSBB), for detection of NRD and tubulin (goat anti-NRD N20, 1:100 and mouse anti β-tubulin I antibody 1:500) were added ON.

GFP- transfected SH-SY5Y cells were incubated with primary antibodies (goat anti-NRD N20, 1:100 and mouse anti β-tubulin I antibody 1:500, diluted in FSBB) overnight at 4°C.

Cells were washed three times with high salt buffer and incubated with the appropriate (directed against the species of the primary antibody) secondary Alexa-dye conjugated antibody. For example for NRD and tubulin staining: Alexa 555 donkey anti-goat antiserum for 90 min at RT, wash three times with high salt buffer and incubate with Alexa 633 goat anti-mouse antiserum (Molecular Probes) for 90 min at RT.

After incubation with secondary antibodies, cells were washed once with high salt buffer, then with 120 mM Na-phosphate, and once with 5 mM Na-phosphate. After washing with PBS (pH 8.9), cover glasses were drained and mounted onto microscope slides. Fluorescence images were captured sequentially with excitation at 488 nm, 543 nm and 633 nm using a LSM510 laser scanning confocal microscope (Carl Zeiss, Jena, Germany) and analyzed using the program Lsmix (Carl Zeiss, Jena, Germany).

3 Results

3.1 Cloning of human NRD from HEK293 cells

To study the interaction between NRD and p42^{IP4} *in vivo* and *in vitro* it was necessary to clone human NRD from cDNA. In exploratory experiments, different human cell lines were tested for the expression level of NRD with RT-PCR.

Based on the results from these experiments HEK293 cells were chosen for cloning of HsNRD1 via RT-PCR. The obtained fragment transcribed from HEK293 cDNA (see 2.2.1.5.2 for details) was cloned into pBSKII. Blue-white screening for successful cloning revealed 16 positive clones for NRD. Further sequencing confirmed the complete sequence of human NRD. Nevertheless, using BLAST no gene sequence could be found, which was 100% identical to the clones obtained from HEK293. Several hsNRD1/2 sequences, were not only different from our clones but they also differed among themselves.

For production of recombinant NRD protein, later to be used for *in vitro* experiments, human NRD was subcloned into vectors suitable for expression in Sf9-insect cells and mammalian cells.

Position Reference	Nucleotide Reference	Nucleotide clones from HEK293
205	c	g
206	g	c
500	c	t
502	a	g
1054	g	a
1350	c	a
1919	t	a
1597	c	t
2766	t	c
3561	t	c
3606	g	a
3636	a	t
3637	t	a

Table 3.1 Comparison of clones from HEK293 with the reference sequence NM_002525.1

Several clones obtained with from RT-PCR cloning from HEK293 cells were compared with the reference sequence.

For future reference, the sequence NM_002525.1 is used as reference sequence. This sequence comprises the complete human NRD sequence, including the specific insertion for the human NRD2 isoform. Sequencing of the clones revealed 13 differences in the nucleotide sequence compared to the reference sequence, as shown in Table 3.1.

```
Virtual: VIRT27806
ID   VIRT_27806   PRELIMINARY;  PRT;  1151 AA.
AC   VIRT27806;
DE   Translation of nucleotide sequence generated on ExPASy
DE   on 08-May-2006 by proxy1.med.uni-magdeburg.de.
CC   -!- This virtual protein sequence will automatically be deleted
CC       from the server after a few days.
CC   4.88 PI.
DR   SWISS-2DPAGE; VIRT27806; VIRTUAL.
SQ   SEQUENCE  1151 AA;  131715 MW;  5EF2744FA9FAB54E CRC64.
     MLRRVTVAAV CATRRKLCEA GRELAALWGI ETRGRCEDSA AARPFPILAM PGRNKAKSTC
     SCPDLQPNGQ DLGENSRVAR LGADESEEEG RRGSLSNAGD PEIVKSPSDP KQYRYIKLQN
     GLQALLISDL SNMEGKTGNT TDDEEEEEVE EEEEDDDEDS GAEIEDDDEE GFDDEDEFDD
     EHDDDLDTED NELEELEERA EARKKTTEKQ SAAALCVGVG SFADPDDLPG LA HFLEH MIF
     MGSLKYPDEN GFDAFLKKHG GSDNASTDCE RTVFQFDVQR KYFKEALDRW AQFFIHPLMI
     RDAIDREVEA VDSEYQLARP SDANRKEMLF GSLARPGHPM GKFFWGNAET LKHEPRKNNI
     DTHARLREFW MRYYSSHYMT LVVQSKETLD TLEKWVTEIF SQIPNNGLPR PNFGHLTDPF
     DTPAFNKLYR VVPIRKIHAL TITWALPPQQ QHYRVKPLHY ISWLVGHEGK GSILSFLRKK
     CWALALFGGN GETGFEQNST YSVFSISITL TDEGYEHFYE VAYTVFQYLK MLQKLGPEKR
     IFEEIRKIED NEFHYQEQTD PVEYVENMCE NMQLYPLQDI LTGDQLLFEY KPEVIGEALN
     QLVPQKANLV LLSGANEGKC DLKEKWFGTQ YSIEDIENSW AELWNSNFEL NPDLHLPAEN
     KYIATDFTLK AFDCPETEYP VKIVNTPQGC LWYKKDNKFK IPKAYIRFHL ISPLIQKSAA
     NVVLFDIFVN ILTHNLAEPA YEADVAQLEY KLVAGEHGLI IRVKGFNHKL PLLFQLIIDY
     LAEFNSTPAV FTMITEQLKK TYFNILIKPE TLAKDVRLLI LEYARWSMID KYQALMDGLS
     LESLLSFVKE FKSQLFVEGL VQGNVTSTES MDFLKYVVDK LNFKPLEQEM PVQFQVVELP
     SGHHLCKVKA LNKGDANSEV TVYYQSGTRS LREYTLMELL VMHMEEPCFD FLRTKQTLGY
     HVYPTCRNTS GILGFSVTVG TQATKYNSEV VDKKIEEFLS SFEEKIENLT EEAFNTQVTA
     LIKLKECEDT HLGEEVDRNW NEVVTQQYLF DRLAHEIEAL KSFSKSDLVN WFKAHRGPGS
     KMLSVHVVGY GKYELEEDGT PSSEDSNSSC EVMQLTYLPT SPLLADCIIP ITDIRAFTTT
     LNLLPYHKIV K
//
VIRT27806 in FASTA format
```

Fig. 3.1 Translation of the nucleotide sequence of the HEK293 clone into an amino acid sequence.

The sequenced nucleotide sequence (see also Table 3.1) was translated. The highly conserved HFLEH-motif is underlined.

We then used ENSEMBL to translate the nucleotide sequences into amino acid sequences. Comparison of this translated sequence with the amino acid sequence of the translated reference sequence showed a difference only in one amino acid (isoleucine instead of valine) close to the HFLEH-motif (Fig. 3.1 HFLEH M**I**). We were uncertain, whether the Ile is a mutation close to the highly conserved HFLEH-motif. To address this issue we checked the GenBank for other protein sequences of NRD. Nine different human NRD amino acid sequences can be found in GenBank with only one sequence displaying 1218/1219 identities (CAH74099.1) with our sequence. Most importantly, all nine sequences differ in their sequence, but they do not contain an exchange of this valine to isoleucine. Moreover, eight sequences had differences in their sequences ranging from two up to seven amino acids, which as mentioned before, occur at positions different from the position of the valine close to the HFLEH-motif. To confirm further that the isoleucine is indeed a mutation, the genomic sequence was controlled at that position. As expected, also the genomic sequence displayed a valine there.

Unfortunately, sequencing of other clones gave few clones without this mutation but all with mutations at different positions even within the DAC, the HFLEH-motif or they lacked numerous nucleotides. We therefore decided to repair the clone using site directed mutagenesis, thereby exchanging the isoleucine with valine. To exclude any additional changes, not only the nucleotide sequence close to the HFLEH-motif was sequenced but the complete sequence of the clone. This clone (HsNRD1 in pBSKII) was then used for cloning into other vectors for expression in mammalian or insect cells and as basis for the production of NRD mutants.

In the process of cloning human NRD1 we also found one NRD clone, which had the nucleotide insertion that is typical for the NRD2 isoform. Comparison with the reference sequence NM_002525.1 and the NRD1, cloned by us from HEK293 cells, revealed that the NRD2 clone lacked several nucleotides. The missing nucleotides were at different positions, which resulted in two frameshifts, the latter readjusted the reading frame to normal mRNA translation. Due to the weak expression of NRD2 in HEK293 cells (see Fig. 3.2 upper band in the HEK control lane) and the otherwise identical sequence to our HEK293 clones and the reference sequence, together with difficulties to reproduce the cloning of hNRD2, we performed site directed mutagenesis. We inserted the missing nucleotides (hNRD2 primers, see chapter 2.1.3; added nucleotides in bold) into the clone for NRD2. The NRD2 clone is now identical to the NRD1 clone and additionally contains the NRD2 insertion as published in NM_002525.1.
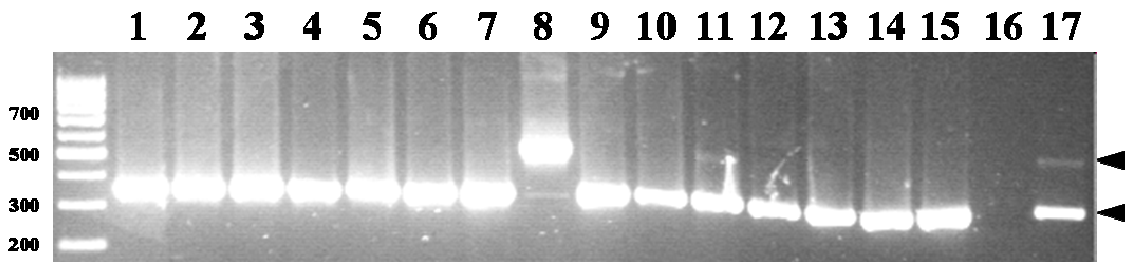
Fig. 3.2 Cloning of human NRD. Agarose Gel with EtBr staining
PCR with positive clones from cloning hNRD from HEK293 was performed according to Fontes et al. 2005. Lanes 1-7 and 9-15 show positive signals for NRD1 (385 bp) as indicated with the lower arrowhead. Lane 8 shows a signal for NRD2 (385bp) as indicated with the upper arrowhead. Lanes 16 (negative control), 17 cDNA from HEK293 with both NRD1 (lower strong band) and NRD2 (upper band, weak staining).

3.1.1 Production of NRD1- mutants

For production of catalytically inactive NRD1 we aligned the sequences as shown in Fig. 3.3. The mutants published before were done in mouse NRD1 but not in the human NRD protein. These NRD mutants have either a point mutation in either the Zn^{2+}-binding motif (HXXEH to HXXAH) or the catalytically important Cys948 (Cys to Ala) or a deletion of the DAC.
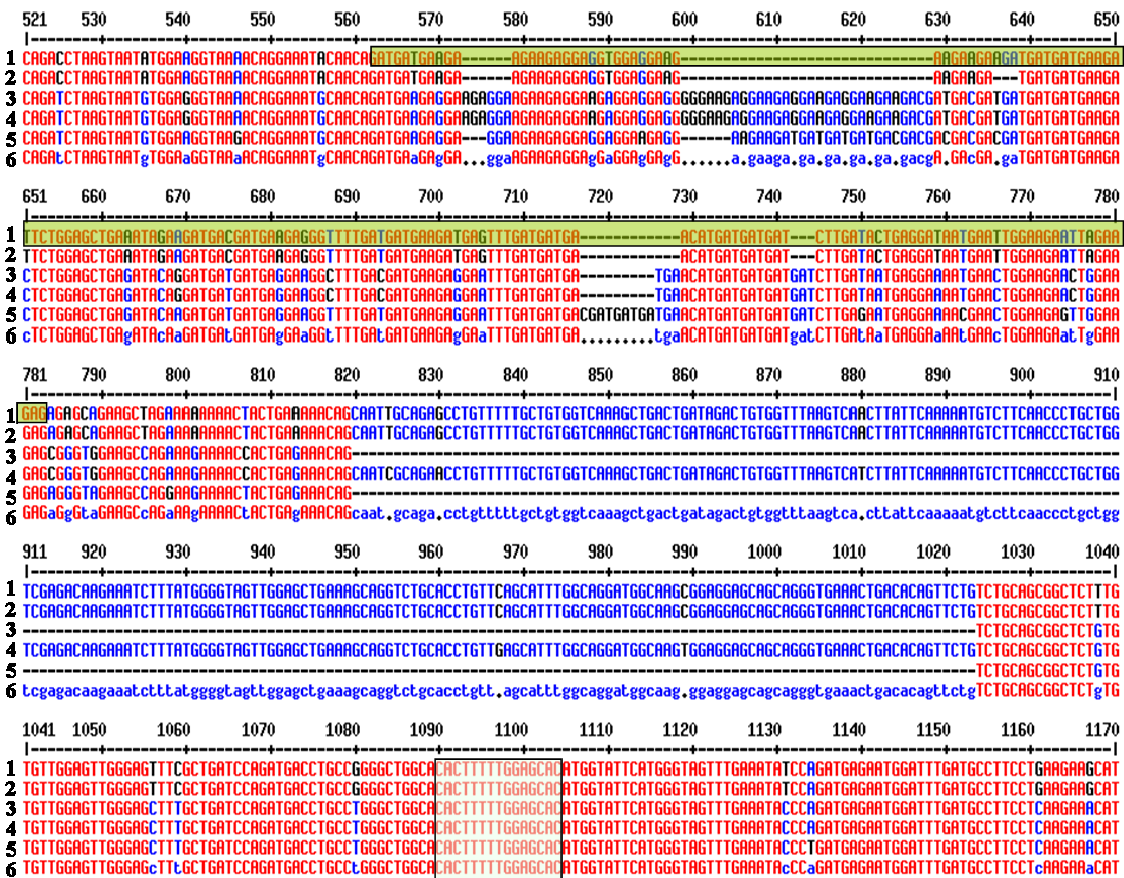
Fig. 3.3 Alignment of NRD sequences of different species

Alignment of (1) the human NRD sequence (Reference Sequence NM_002525.1) with (2) AY3602651 (homo sapiens nardilysin isoform (NRD1) mRNA, complete cds), (3) NM_012993 (Rattus norvegicus nardilysin1 (Nrd1), mRNA), (4) X93208 (Rattus sp. mRNA for NRD2 convertase), (5) NM_146150 (Mus Muculus Nardilysin, N-arginine dibasic convertase, NRD convertase1 (Nrd1), mRNA), line (6) displays the consensus sequence. Due to space limitations, only the region comprising the DAC (marked in green) and the HFLEH-motiv (marked light grey) are shown. Alignment was done using the online multi align tool (Corpet, 1988).

All mutations were carried out here in the previously sequenced HsNRD1-pBSKII. The production of the ΔDAC mutant is illustrated in Fig. 3.4. Following the mutagenesis, the sequenced insert was cloned into pFastBacHtc or pcDNA6His-B, for expression in insect or mammalian cells.

Fig. 3.4 Scheme for the production of the ΔDAC deletion mutant of hsNRD1.

Using site directed mutagenesis, we introduced point mutations into the hsNRD1 sequence to add a restriction site for AgeI. After digestion of the plasmid with AgeI and subsequent religation, the translation of the remaining sequence results in a replacement of the DAC with a single glycine residue, and links the protein sequence N- and C-terminal to the original DAC sequence.
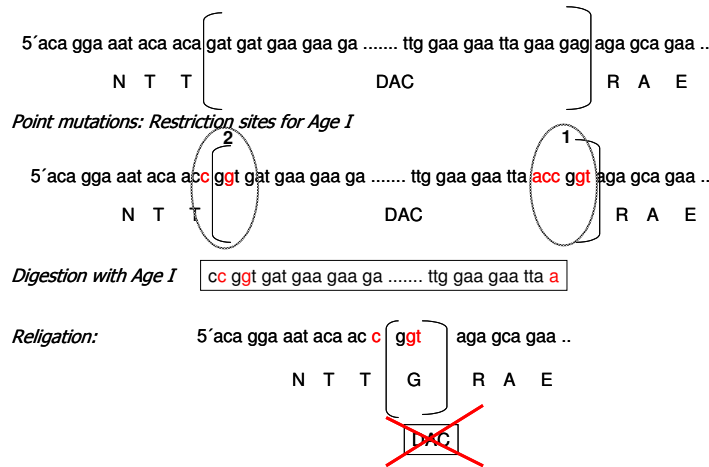
3.1.1.1 Recombination, transfection and protein expression of NRD with purification
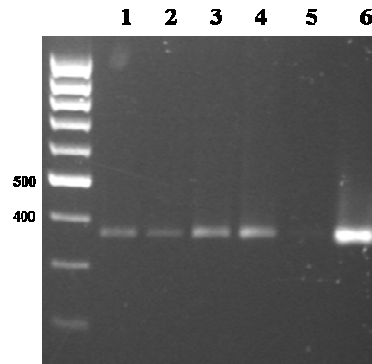
Fig. 3.5 Control of recombination of NRD-Bacmid-DNA

A typical EtBR stained agarose gel with products from standard NRD PCR (see 2.2.15 for details) to control the successful recombination of NRD. The mix from several clones shown here in lane 1-4 was used to transfect Sf9 cells. Lanes 1-4: hNRD1- FB1; -FB2-; FB5; - FB6, lane 5 H_2O; lane 6 control (pBSKhsNRD1); for transfection in Sf9 cells the concentration was estimated from the agarose gel.

The recombination of pFastBac-Htc-NRD (NRD1, NRD1, NRD1-mutants) with MaxEffiecency DH10 Bac^{TM} – cells, expression of NRD in Sf9 cells, followed by protein purification, were optimized for both NRD isoforms as well as for the NRD-mutants and are described in detail in materials and methods (see chapter 2.2.1.1.4 to 2.2.1.16 and 2.2.1.12). Tests on the optimal duration of Sf9-cells, transfected with working virus from any of the above mentioned constructs' revealed that the harvest at 72 hours post transfection is optimal for the expression of the desired protein.

3.2   NRD as possible endopeptidase for p42^{IP4}

We here studied, whether the full-length metalloendopeptidase NRD might cleave p42^{IP4}. Both proteins were incubated for 30 min up to 10 h. Only examples for one to four hours (Fig. 3.6) and 30 min (Fig. 3.7) are presented here. As shown by Western Blot in Fig. 3.6 (A, B, C) there are no fragments of p42^{IP4} detectable albeit after longer incubation it appears that the intensity of the protein band appears weaker. This may result from ongoing precipitation of the protein, but is not critical for the general conclusion because the intensity of the protein bands in the control lanes (lane 5 and lane 10) is comparable in the lanes, which belong to the same incubation time (lanes 1-4 or lanes 6-9).

Moreover, this decrease can be observed in all blots in Fig. 3.6, irrespective of the specific antibody used for detection of p42^{IP4}. Western blots were done using specific antibodies directed against amino acids in the C-terminal, the N-terminal parts and amino acids in the central part of p42^{IP4}. The antibody specificity is as indicated in the scheme above the blots in Fig. 3.6. Incubation of p42^{IP4} with NRD for 7 or 10 h under the same conditions and staining of the Western blots with the same antibodies also revealed no fragments of p42^{IP4} (data not shown).

To exclude fragments, which might not be detectable with our antibodies, we checked the possible cleavage of p42^{IP4} by NRD after incubation on a Coomassie-gel. In addition to the results from Western blotting, Coomassie staining (Fig. 3.7) also revealed no fragments of p42^{IP4} after incubation with NRD.
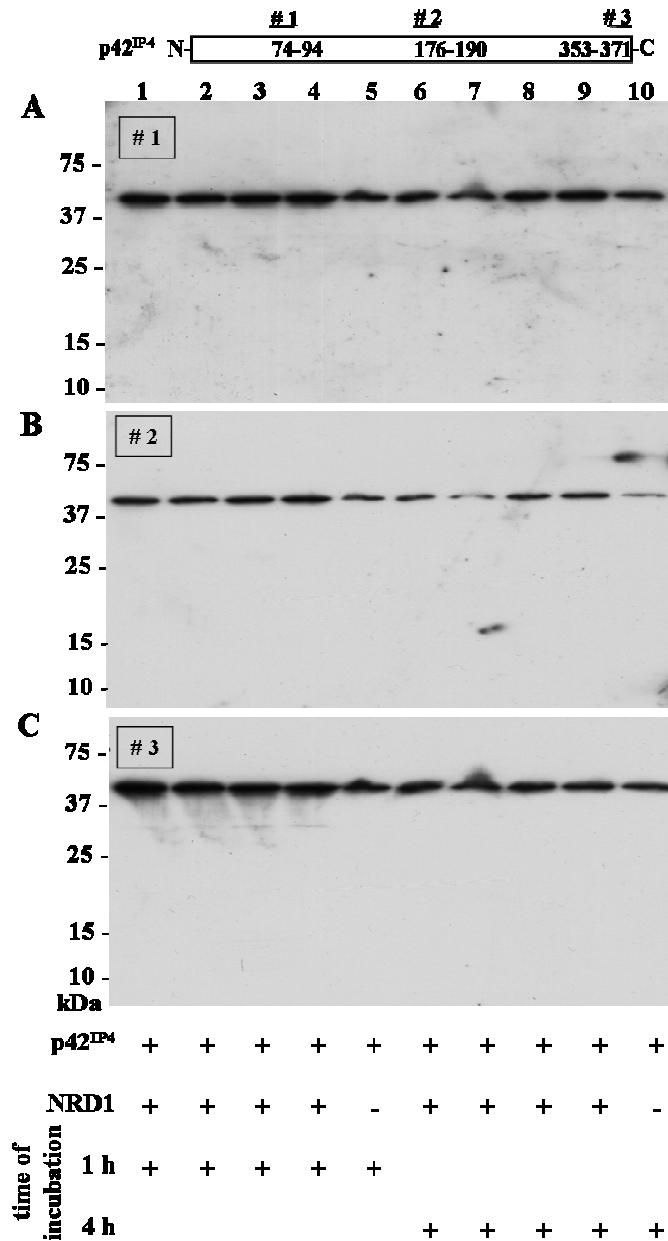
Fig. 3.6 NRD does not cleave p42^{IP4} after 1 or 4 h. Western Blot.

p42^{IP4} (*Sus scrofa*) was tested as a substrate for NRD. Equimolar amounts (80 nM) of both proteins were incubated for 1 or 4 h. The reaction was stopped, samples were loaded onto a 12.5% SDS-PAGE. Western Blot was done using the following p42^{IP4}-specific antibodies: A, # 1 (N-terminal part), and B, # 2 (central part). C, #3 (directed against the C-terminal part). Antibody target amino acid residues are indicated in the p42^{IP4} protein scheme given on top. Lanes 5 and 10: control incubations; buffer was added instead of NRD.
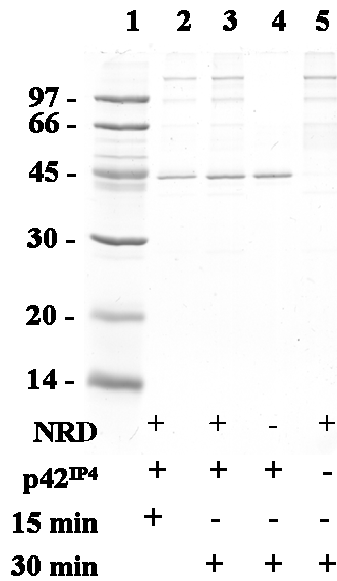
Fig. 3.7 NRD does not cleave p42^{IP4} . Coomassie staining.

p42^{IP4} (Sus scrofa) was tested as a substrate for NRD. 80 nM recombinant p42^{IP4} was incubated with 40 nM NRD for 15 min or 30 min in 20 mM potassium phosphate buffer, pH 7.0 (Csuhai E. et al 1998). The reaction was stopped by incubation at 90°C for 5 min. Samples were precipitated with methanol/acetone, dissolved in sample buffer and run on a 12.5% SDS-PAGE and stained with Coomassie dye.

3.3   Modulation of peptidase-activity of NRD by p42^{IP4}

After we could demonstrate here that NRD does not cleave p42^{IP4}, we were interested to verify whether p42^{IP4} instead influences the enzymatic activity of NRD. We performed a kinetic assay using the substrate Abz-GGGFLRRVGQ-EDDnp. In this substrate, the fluorescence of the N-terminal Abz-group is masked by the quenching effect of the Dnp-group. After cleavage of the peptide bonds, this quenching effect is abrogated and the fluorescence of the Abz-group can be detected.

As shown in Fig. 3.8A, p42^{IP4} positively modulates the enzymatic activity of NRD by shifting the reaction curve to the left side and increasing the slope of the reaction curve. Addition of p42^{IP4} increases the reaction by approximately 12% after 5 min and 25% after 20 min. Experiments using recombinant human NRD, lacking the DAC showed no reaction (data not shown here). Because p42^{IP4} binds to the DAC of NRD, we were interested to see whether this potentiation of enzyme activity depends on the equimolar ratio. As shown in Fig. 3.8, there are no differences for the enzyme kinetics with equimolar, two-fold and 0.5 ratio of p42^{IP4} and NRD. To further confirm that p42^{IP4} is indeed a modulator of NRD and not a substrate, the samples of experiment 3.8. A were analyzed by Western Blot. As shown in Fig. 3.8B, there are no fragments of p42^{IP4} detectable. Moreover, lanes 5-8, which correspond to

the curves in Fig. 3.8A (same symbols in curves and Western Blot) show the increasing amounts of $p42^{IP4}$ (lane 6: 40 nM, lane 7: 80 nM, lane 8: 160 nM). Additionally, comparison of lane 4 and 7 shows identical signal strength. This supports the idea that $p42^{IP4}$ and the peptide substrate Abz-GGGFLRRVGQ-EDDnp do not compete for the active site of NRD.
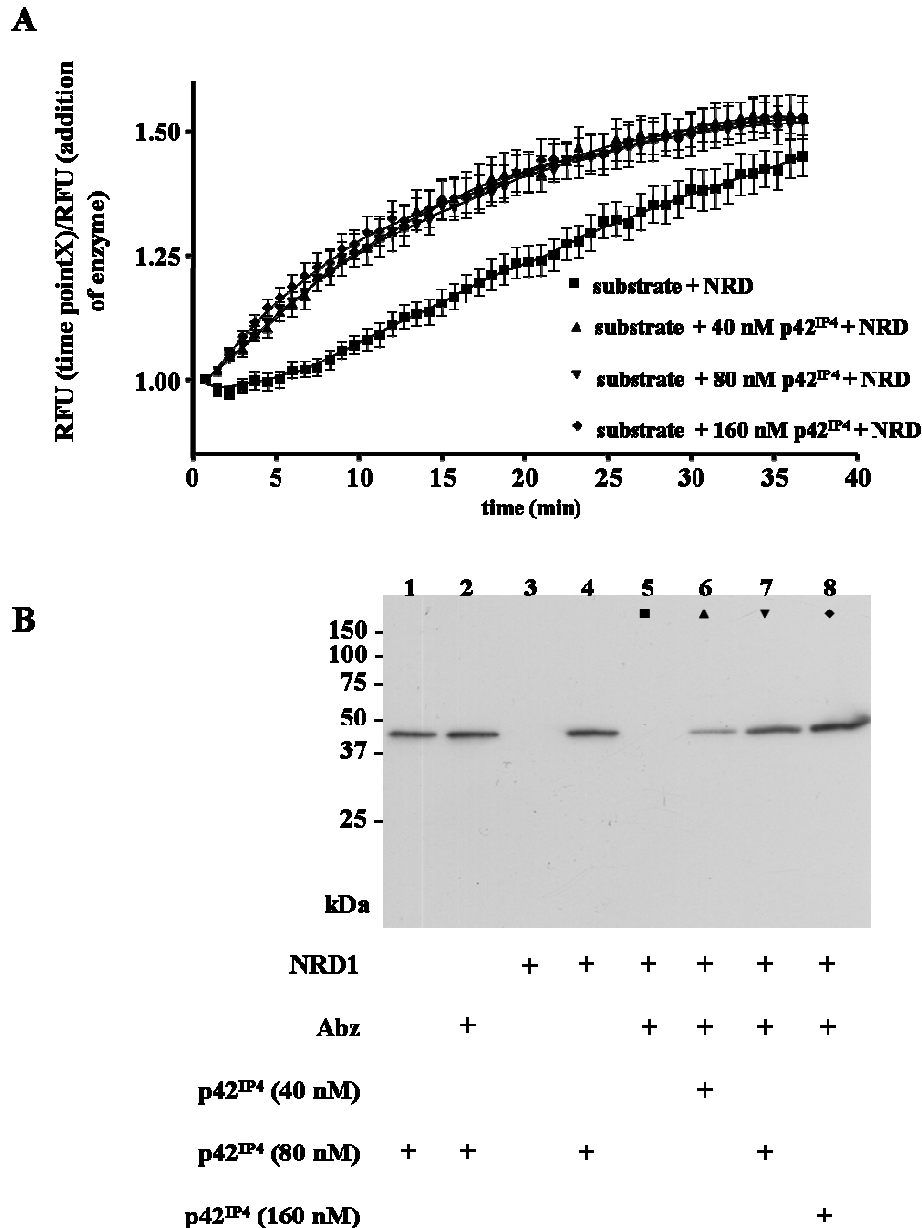
Fig. 3.8 $p42^{IP4}$ enhances the enzymatic activity of NRD.

A. Enzymatic activity of NRD in the presence of $p42^{IP4}$. Fluorescence measurement using 1 µM of the quenched substrate Abz-GGGFLRRVGQ-EDDnp (bovine adrenal medulla peptide; (Csuhai et al., 1999b). Mean values and error bars for SEM; RFU = relative fluorescence units. Medium lowess curve fitting was done using GraphPad Prism. Data are from five experiments, performed in triplicate. B. $p42^{IP4}$ is not a substrate for NRD1 and does not compete with substrate for the active site of the enzyme. B: Western Blot. After fluorescence measurement (time of incubation 30 min; see above) using the peptide substrate Abz-GGGFLRRVGQ-EDDnp, the different samples of the enzyme kinetic experiment (see Fig. A), were run on a 12.5% SDS-gel for Western Blot using the $p42^{IP4}$ antibody 117-2. Lanes 5-8 correspond to measurements shown in Fig. 3.8 A. $p42^{IP4}$ does

not compete with Abz-GGGFLRRVGQ-EDDnp for the active site of the enzyme because the signals in lanes 4 and 7 are equal.

3.4   Expression of NRD and p42^{IP4} in SH-SY5Y cells

To investigate the relevance of the interaction between p42^{IP4} and NRD *in vivo*, we used SH-SY5Y cells. These cells represent a neuroblastoma cell line, which was originally derived from the cell line SK-N-SH (Biedler et al., 1978). Moreover, these cells can be used as a model system for investigations of processes in neurons. SH-SY5Y can be differentiated into a neuronal-like cell type when exposed to low concentrations of RA like many other neuroblastoma cell lines (Pahlman et al., 1984).

It is important to consider that this cell line consists of two phenotypes of cells with a majority of neuroblast-like cells, which display different behavior after treatment with RA (Preis et al., 1988). Upon stimulation with RA, 25% of the cells grow extensions longer than 50 µm but at the same time, the non-neuronal phenotype increases dramatically and overgrows the culture dish. Additionally, many gene products used as control for normalization of gene expression are also subject to changes after RA treatment. For example, the ratio of actin expression to total protein expression was significantly increased in cells differentiated with RA (Asada et al., 1994).

These SH-SHSY5Y cells were used as a model system to investigate the role of the proteins p42^{IP4} and NRD during differentiation. Moreover, we studied the localization of both proteins in the SH-SY5Y cells.

3.5   Expression of p42^{IP4} and NRD in SH-SY5Y cells after RA-treatment

3.5.1   Upregulation of NRD2 on mRNA-level after RA stimulation

Semi-quantitative RT-PCR showed that p42^{IP4} and both isoforms of NRD are expressed in SH-SY5Y cells on mRNA-level (Fig. 3.9, normalized to day 0). After stimulation with 10 µM RA the mRNA level of NRD2 is upregulated after 3 days and stays at this elevated level for 15 days. Interestingly, after several days of RA treatment the mRNA-level of NRD1 appears not to be changed at all. In contrast to that, the p42^{IP4} mRNA level is not upregulated, even more, a down-regulation of approximately 25% by day 6 and by 50% at day 15 could be observed. Interestingly, at day 15 NRD2 is upregulated together with a concomitant reduction of p42^{IP4}, which is significant and becomes noticeable already at day 6 of RA stimulation.
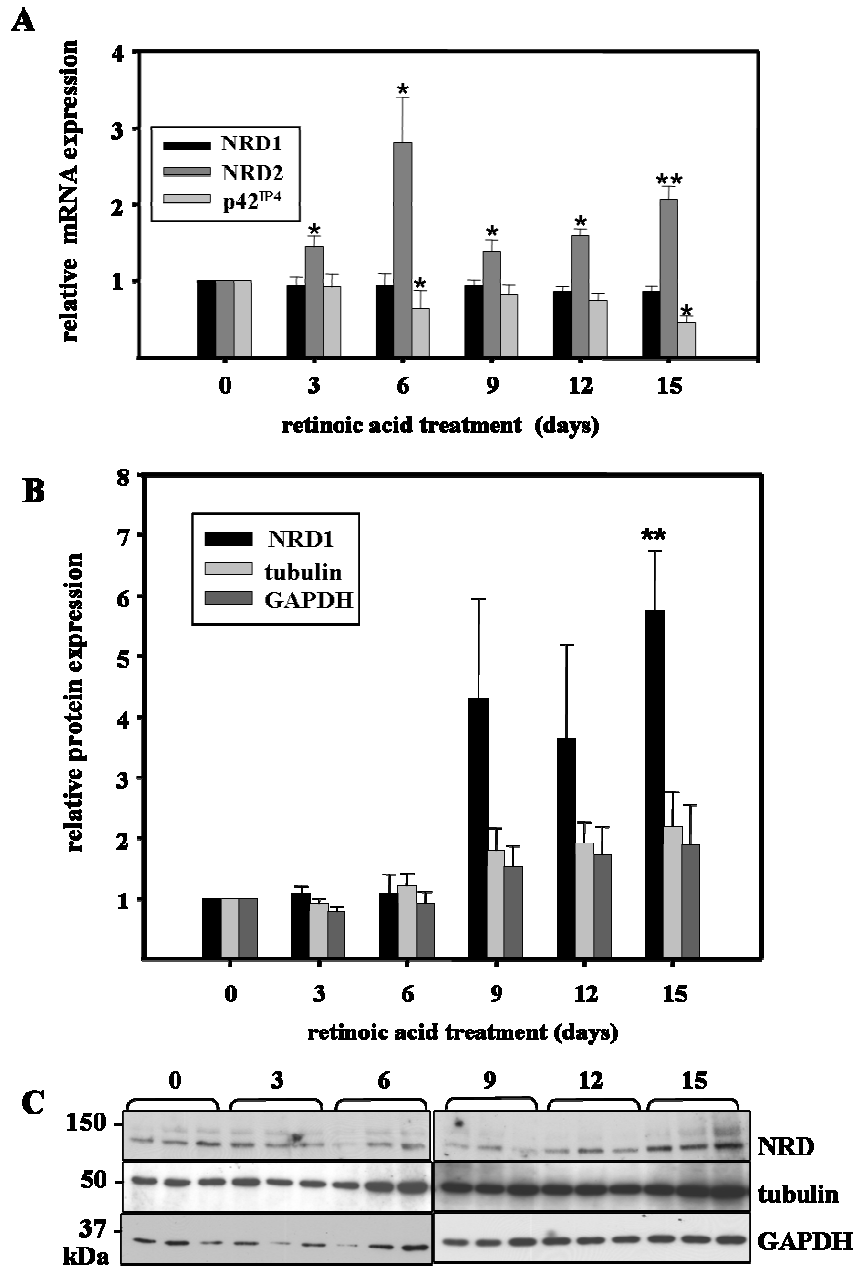
Fig. 3.9 Change in mRNA - and protein expression in SH-SY5Y cells after retinoic acid (RA) treatment.

SH-SY5Y cells were exposed to RA (10 µM) for 3, 6, 9, 12, or 15 days. Medium containing 10 µM RA was changed every 3 days. Then cells were harvested. A. RNA was isolated and RT-PCR was done using specific primers for p42^{IP4}, and primers for NRD. PCR products were quantified (Biorad Quantitiy One). B. Cells were lysed, precipitated with methanol/acetone 1:1 loaded onto a 10% (for p42^{IP4}) or 5% (NRD) SDS-polyacrylamide gel. Blots were scanned and quantified (Biorad Quantitiy One). Blots were stained for NRD using the N20 antibody (polyclonal goat, Santa Cruz Biotechnology). Data are expressed as mean ± SE from 4 – 5 experiments. Statistical analysis, * p<0.05, ** p<0.01 compared to day 0. Error bars indicate Standard Error. C. Typical blots showing NRD, tubulin and GAPDH staining.

3.5.2 Upregulation of NRD on protein level after RA stimulation

As demonstrated above, the mRNA-levels of both NRD1 and NRD2 are not equally expressed after stimulation with RA. Therefore, we were interested to investigate whether the protein expression of both isoforms displays a similar regulation. To improve the resolution of the different protein bands of the two NRD isoforms, which by differ only about ~ 5 kDa, protein samples were loaded on 5% polyacrylamide gels to enhance the electrophoretic separation.

However, contrary to the findings on mRNA level, we were not able to detect any upregulated NRD2 protein (not shown in Fig. 3.9). We can exclude that this is caused by the use of the NRD antibody, because this antibody is able to detect recombinant NRD2 protein, cloned from HEK293 cells. The Western blot for recombinant NRD2 is not shown here.

Nevertheless, we were able to detect a strong upregulation of the NRD1 protein, which was highly significant after 15 days of RA treatment.

Staining with antibodies against p42^{IP4} revealed that p42^{IP4} is not expressed as protein in detectable amounts in SH-SY5Y cells. Treatment of the SH-SY5Y cells with RA did not induce a protein expression of p42^{IP4}.

3.5.3 NRD is expressed in the neurites of stimulated SH-SY5Y cells

Since we could show an upregulation of NRD in SH-SY5Y cells stimulated with 10 µM RA, we were interested in the cellular localization of NRD and p42^{IP4}.

Treatment of SH-SY5Y cells with RA induces morphological changes in these cells. Compared to untreated cells they appear in a lengthened shape and start to develope neurites followed by establishing neural networks in the culture dish. This can be observed from day three onwards in the cell culture (see also Fig. 3.10 panel B). Moreover, the network of the neurites is more prominent over the time course of our experiments. This is visible from day 6 until day 15 (Fig. 3.10 B-F middle panel), but the network is fully developed between day 9 and day 12 (Fig. 3.10 D and E, middle panel).

Using confocal microscopy, we found that NRD is located in the cytosol and in the growing neurites of the stimulated SH-SY5Y cells, as indicated by arrowheads in Fig. 3.10 D-F, right panel. Interestingly, after 6 days RA treatment (Fig. 3.10 C), NRD appears to be located within vesicular structures, which are even more visible after day 9 of RA-treatment (Fig. 3.10 D). As shown before by Western blot, staining with antibodies against p42^{IP4} could not detect an expression of this protein. This finding proves that SH-SY5Y cells are optimal

for analyzing the cellular consequences of p42^{IP4} after stable transfection of GFP-tagged p42^{IP4} into neural cells.
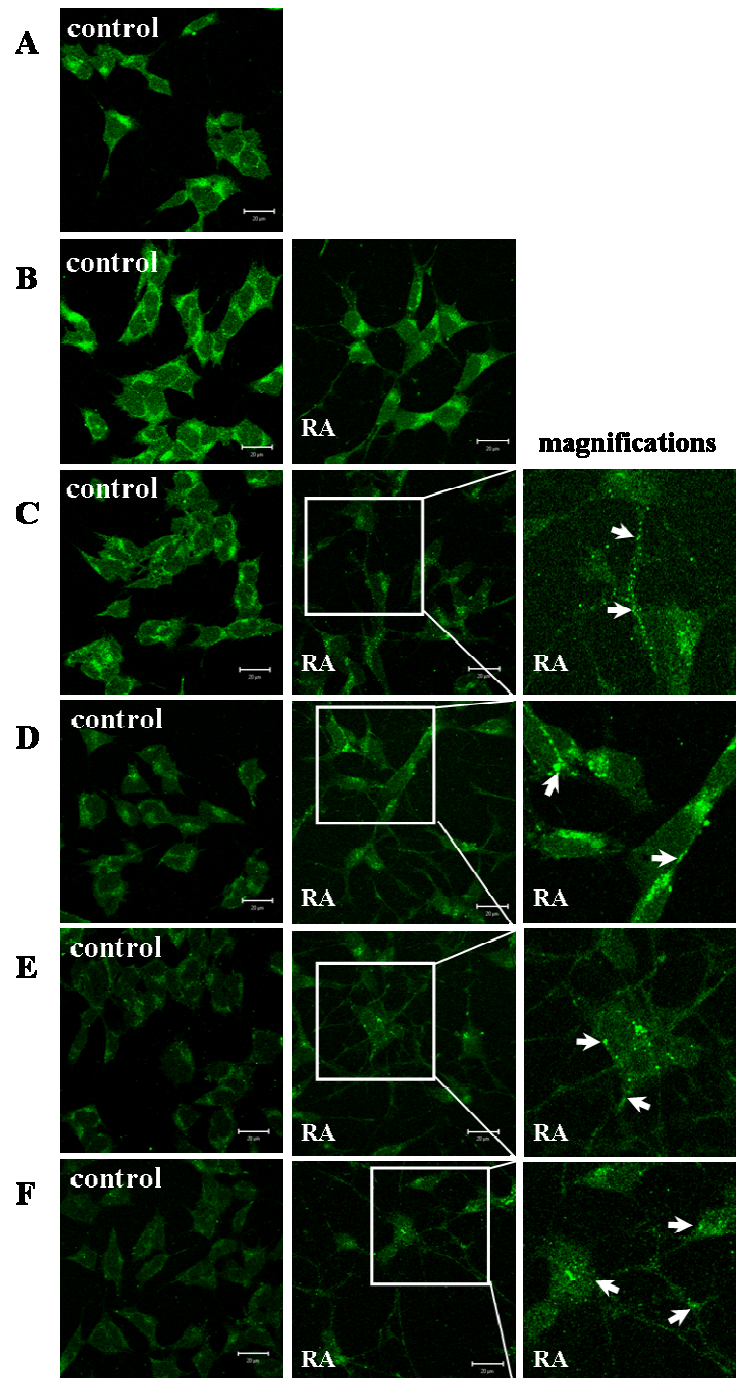
Fig. 3.10 Expression of NRD in SH-SY5Y cells after retinoic acid (RA) stimulation.

NRD is expressed in neurites and vesicular structures (arrowheads). SH-SY5Y cells were exposed to RA (10 µM) for 3 (B), 6 (C), 9 (D), 12 (E), or 15 (F) days. Control SH-SY5Y cells were maintained in DMEM supplemented with 15% FCS. Medium, containing 10 µM RA was changed every 3 days. Cells were fixed at the indicated time points, and immunohistochemistry was done using the antibodies N20 for NRD and Alexa Fluor 488 anti goat for detection. The white bar in the left and middle panels indicates 20 µm.

3.5.4 Influence of stable transfection of GFP-tagged p42^{IP4} on NRD expression

We did not observe an expression of p42^{IP4} on protein level in SH-SY5Y cells and, therefore, we decided to use this cell line to verify, whether p42^{IP4} can influence the RA-induced upregulation of NRD on the protein level.

We stably transfected SH-SY5Y cells with GFP-p42^{IP4} and stimulated the transfected cells with 10 µM RA with the same protocol as before in untransfected SH-SY5Y cells. As shown in Fig. 3.11, NRD is not upregulated after 15 days. Surprisingly, the upregulation, albeit at a lower level, appears at an earlier time point. This indicates a shift of the upregulation from day 15 to day 6 compared to untransfected SH-SY5Y, treated with RA.

Additionally, to exclude any influences of the GFP-tag, SH-SY5Y cells were stably transfected with pEGFP-C1-empty vector and stimulated as described before for SH-SY5Y and SH-SY5Y-p42^{IP4} cells. As demonstrated in Fig. 3.12, NRD is not upregulated after 6 days in SH-SY5Y-GFP cells, which gives evidence for a similar behavior of GFP-transfected cells and untransfected SH-SY5Y cells.

It is important to note that the down regulation of NRD in p42^{IP4}-transfected cells, observed at later time points is not caused by p42^{IP4}. Most probably, the protein expression after day 6 is influenced by the GFP-tag, as the NRD expression at day 9 and progressing until day 15 is comparable to cells transfected with p42^{IP4} or GFP-only (comparison Fig. 3.9, Fig. 3.11, Fig. 3.12).
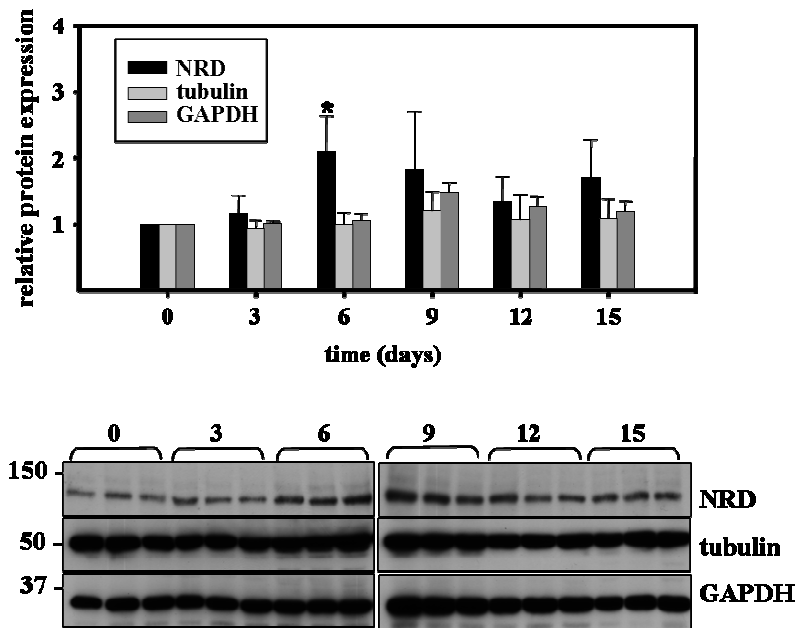
Fig. 3.11 Change in protein expression in SH-SY5Y cells, stably transfected with p42^{IP4} after retinoic acid (RA) treatment.

SH-SY5Y-p42^{IP4} cells, stably transfected with GFP-tagged p42^{IP4} were exposed to RA (10 µM) for 3, 6, 9, 12, or 15 days. Medium containing RA was changed every 3 days. Cells were harvested at the incubation points mentioned and lysates were analyzed by Western Blot for the presence of NRD, as described in Fig. 3.9.
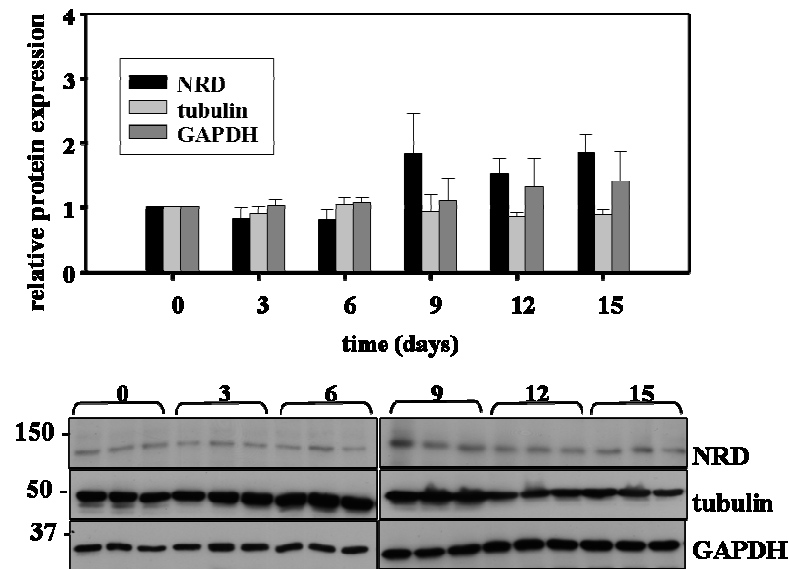
Fig. 3.12 Change in protein expression in SH-SY5Y-GFP-only cells after retinoic acid (RA) treatment.

SH-SY5Y-GFP-only cells, stably transfected with GFP-only were exposed to 10 µM RA for 3, 6, 9, 12, or 15 days. Medium containing RA (10 µM) was changed every 3 days. Cells were harvested and lysates were treated as described in Fig. 3.9. Error bars indicate Standard Error; Data are from four independent experiments with each treatment performed in triplicate.

3.5.5 Localization of p42^{IP4} and NRD in p42^{IP4}-transfected SH-SY5Y cells

We further elucidated the interaction between p42^{IP4}, NRD, and tubulin. For that purpose cells were analyzed by confocal microscopy. For this, SH-SY5Y-p42^{IP4} cells, stably expressing p42^{IP4}-GFP, were seeded on cover glasses, fixed and permeabilized for immuncytochemistry. Confocal imaging revealed the co-localization of p42^{IP4}, NRD, and β-tubulin in the cytosol and at the plasma membrane (light–pink staining) (merged picture in Fig. 3.13a and histogram in Fig. 3.13b). This colocalization is clearly visible in the histograms, where the peaks overlap as seen in the region from 25 µm to 45 µm from start of the arrow. This is seen for all three curves as marked by tick lines on the arrow in the merged picture and in the histogram in Fig. 3.13a and Fig. 3.13b.

Contrary to tubulin and NRD, p42^{IP4} is also localized in the nucleus. The colocalization of NRD alone with β-tubulin was published before (Ma et al., 2005) and we previously found an interaction of p42^{IP4} with α-tubulin (Galvita et al., 2009).

Therefore, we were interested to find out, whether the interaction of both proteins with tubulin might have an impact on the interaction between p42^{IP4} and NRD. For this, we decided to verify whether changes in the tubulin-cytoskeleton would affect the binding of NRD and p42^{IP4}.
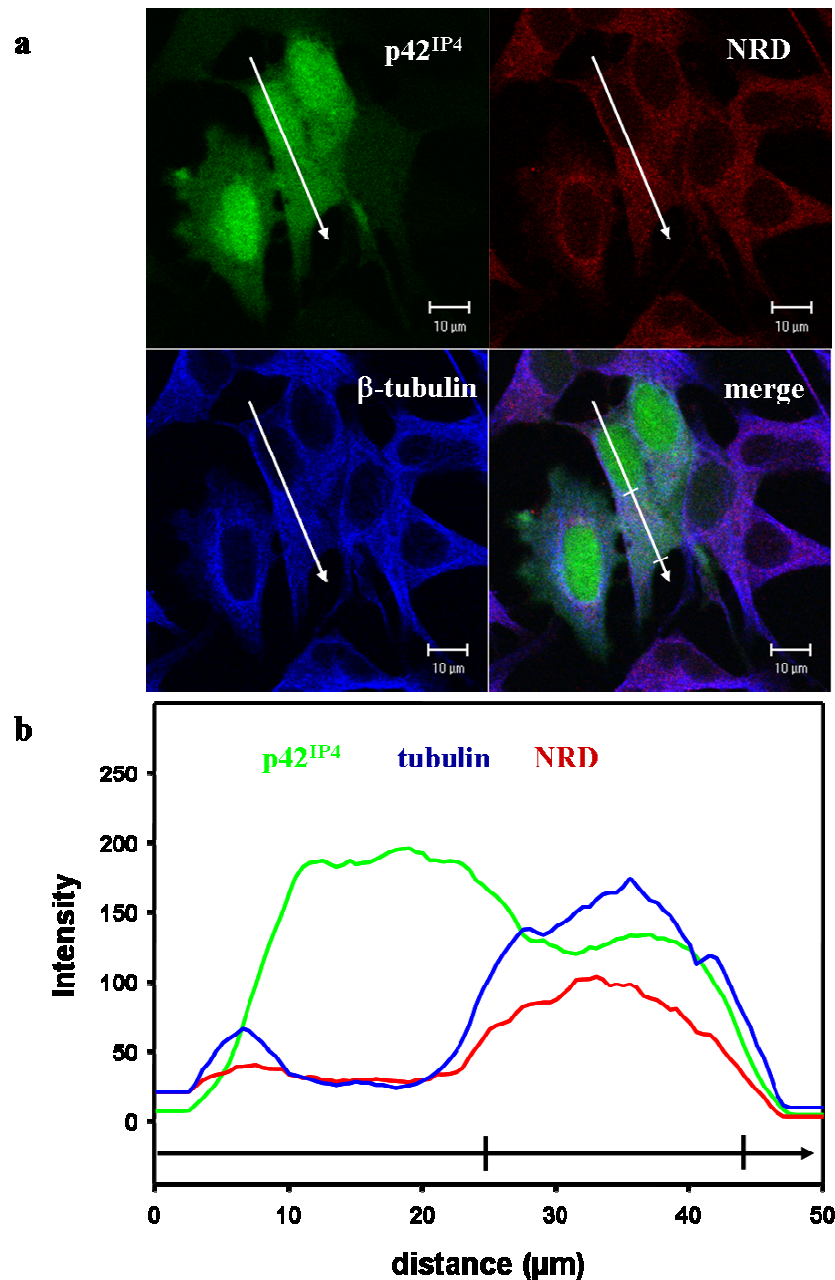
Fig. 3.13 Colocalization of NRD, p42^{IP4} and tubulin in SH-SY5Y-p42^{IP4} cells.

SH-SY5Y cells, stably expressing p42^{IP4}-GFP, were seeded on cover glasses, fixed and permeabilized for immuncytochemistry. Cells were double stained with NRD and β-tubulin antibodies and with Alexa Fluor 555 followed by Alexa Fluor 633 antiserum, as described in Materials and methods (see chapter 2.2.4). (a) Confocal imaging of p42^{IP4}-GFP (green; left upper panel), β-tubulin (blue; in left lower panel) and NRD (red; in right upper panel). The merged picture (right lower panel) illustrates the co-localization of p42^{IP4}, NRD, and β-tubulin in the cytosol and at the plasma membrane (light–pink staining). Pictures shown are representative of at least three independent experiments. (b) Histograms represent the fluorescence intensity distribution determined for a cross-section of the cell, as indicated by the white arrow in (a), which corresponds to the black arrow in (b). Curves show smoothened data, which were calculated from average values of neighboring points. The peaks overlap for all three curves in an area marked by tick lines on the arrow (25 µm to 45 µm from start of the arrow), indicating co-localization of p42^{IP4}, NRD and β-tubulin in SH-SY5Y cells, transfected with p42^{IP4}-GFP.

For this purpose, we used nocodazole, known to be a potent inhibitor of tubulin polymerization, to check if the colocalization of p42^{IP4} and NRD is changed. To increase the protein expression of NRD we stimulated the cells with 10 µM RA for 6 days prior to nocodazole treatment. Preliminary experiments showed that p42-GFP transfected cells, pre-treated with 10 µM RA for 6 days, detached from the cell culture dish when incubated with 5 µM nocodazole for 1.5 –4 h. We therefore treated stably transfected p42^{IP4}-GFP and GFP-only cells with 5 µM nocodazole for only 1 h. Interestingly, the detaching could not be observed in cells transfected with GFP-only.
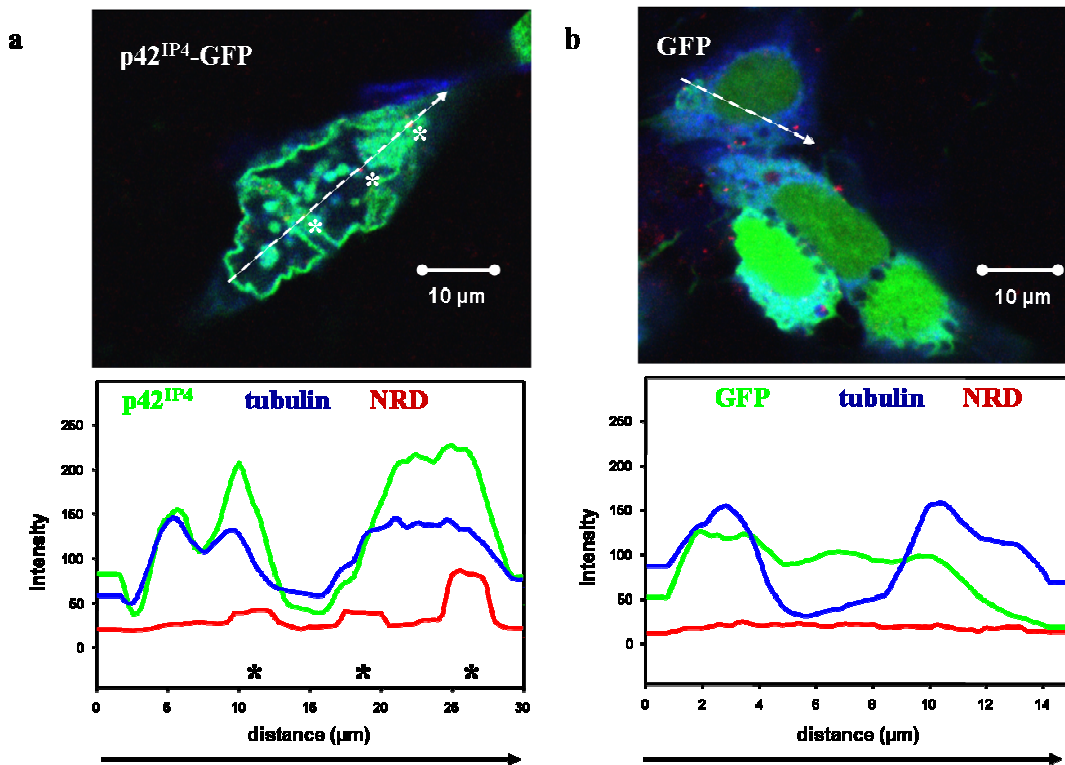
Fig. 3.14 Influence of treatment of SH-SY5Y-p42^{IP4} cells with nocodazole on localization of NRD, p42^{IP4} and tubulin.

SH-SY5Y cells, stably transfected with p42^{IP4}-GFP (or control cells, transfected with empty GFP-vector), were seeded on cover glasses and treated with 10 µM retinoic acid (RA) for 6 days, washed and treated with 5 µM nocodazole for 1 h at 37°C before they were fixed and permeabilized for immuncytochemistry. Cells were double stained with NRD and β-tubulin antibodies and with Alexa Fluor 555, followed by Alexa Fluor 633 antiserum, as described in Materials and Methods. (a) Treatment of p42^{IP4}-GFP transfected cells: Confocal imaging of co-localization of p42^{IP4}-GFP (green), β-tubulin (blue) and NRD (red). The merged picture and the curves for fluorescence intensity distribution demonstrate that treatment with nocodazole caused a co-localization of p42^{IP4} and tubulin (overlapping intensity peaks), whereas a co-localization of all three proteins is visible only at vesicular structures (indicated by asterisks). (b) Treatment of control cells (GFP-transfected SH-SY5Y cells). Confocal imaging of the localization of GFP, β-tubulin (blue), and NRD (red). The merged picture and the curves for fluorescence intensity distribution show that there are no specific overlapping peaks for the distribution of the three proteins: GFP is almost evenly distributed, NRD is weakly expressed, and tubulin has a similar distribution like in cells not treated with nocodazole (see Fig. 3.13). All curves show smoothened data, which were calculated from average values of neighboring points.

As indicated by the overlapping intensity peaks in Fig 3.14a, treatment with nocodazole causes a redistribution of p42^{IP4} and tubulin, but does not alter their colocalization. A colocalization of all three proteins is only visible in vesicular structures, which occur at the peaks at 11, 18 and 26 µm distance. Comparison of the SH-SY5Y-p42^{IP4} with (Fig. 3.14a) or without nocodazole treatment (Fig. 3.13), clearly shows the influence of nocodazole on the distribution of all three proteins in the cells.

Without nocodazole treatment, p42^{IP4} is located in the nucleus, cytosol and at the plasma membrane. Moreover, p42^{IP4} appears to be colocalized with tubulin and NRD in the cytosol and at the plasma membrane in, where it is more evenly expressed (Fig. 3.13 region, indicated by the tick lines on the arrow starting at 25 µm). After treatment, the colocalization of p42^{IP4} and tubulin remains throughout the cytoplasm and at the membrane, albeit the distribution of both proteins resembles a punctuated pattern. This leads to regions with high occurance of both proteins (Fig. 3.14a peaks at 0 µm and at ~5 µm distance) and other regions in the cell, which show a low intensity for both proteins (intensity below 50 at 2.5 µm and 15 µm in Fig. 3.14).

SH-SY5Y-GFP cells, which were used as control did not show such comparable specific peaks in their protein distribution after nocodazole treatment (Fig. 3.14b). Similar to cells, which were not treated with nocodazole, these cells show an almost even distribution of GFP fluorescence and the same distribution of tubulin.

It is important to note that the stimulation of the cells, presented in Fig. 3.13 and 3.14 with RA for 6 days, was done solely to enhance the expression of NRD. It is possible to detect NRD in SH-SY5Y cells without RA treatment (see also Fig. 3.10, left panel), but compared to the expression of tubulin and the overexpression of GFP-p42^{IP4} or GFP alone, the levels of NRD are rather low. This low NRD expression makes it difficult to investigate the colocalization of the three proteins and their changes after nocodazole treatment. Investigations concerning the influence of p42^{IP4} on NRD expression revealed an upregulation of the metalloendopeptidase after 6 days (see Western blots shown in Fig. 3.11). Therefore, the different intensities in NRD expression in SH-SY5Y-p42^{IP4} cells compared to SH-SY5Y-GFP cells, displayed in the graphs in Fig. 3.14 confirm this on cellular level. Compared to p42^{IP4}-expressing cells, NRD is weakly expressed in the GFP-only expressing cells after 6 days of RA treatment, which is in agreement with our findings shown before (see chapter 3.5.4 for reference).

3.5.6 Altered response to nocodazole treatment in p42^{IP4} expressing SH-SY5Y cells

Due to the remarkable differences observed in the p42^{IP4} transfected versus control cells, we estimated the number of cells with such structural changes, which are indicated by arrows in the example of SH-SY5Y-p42^{IP4}-GFP cells shown in the inset picture in Fig. 3.15. For this purpose, within all GFP-only and GFP-p42^{IP4}-transfected cells, we counted the cells, which showed these characteristic differences in their distribution of GFP, like accumulation in vesicles, or uneven distribution in parts of the cell with surrounding cellular areas devoid of any GFP-fluorescence.

Counting of the number of cells (Fig. 3.15) revealed that both p42^{IP4}-GFP as well as GFP control cells, which received a treatment of RA or nocodazole alone, have a basal level of cells with these structural changes. This number of affected cells corresponds to approximately 20% of the total cell number in these cells.

Only treatment of SH-SY5Y-p42^{IP4} cells with RA and subsequent treatment with nocodazole caused a dramatic increase in the number of cells showing signs of structural changes. On the contrary, control cells did not display such increased structural changes after the same treatment. The number of cells with structural changes remained at the same low level, similar to single RA or nocodazole treated control cells.
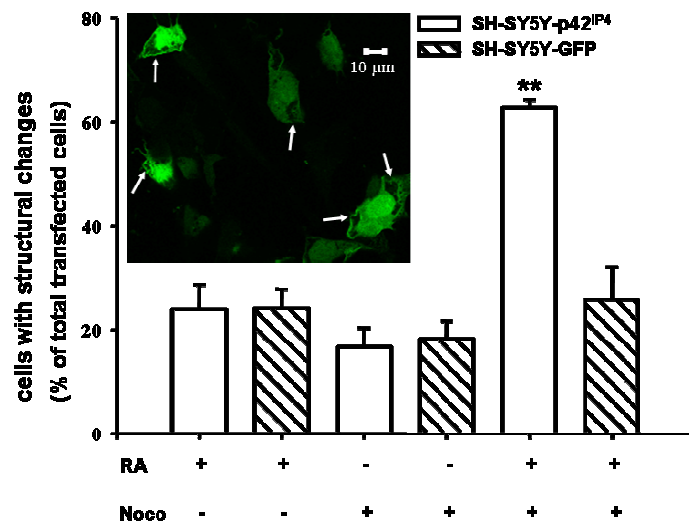
Fig. 3.15 Structural changes in SH-SY5Y-GFP and SH-SY5Y-p42^{IP4} cells treated with nocodazole.

SH-SY5Y cells, stably transfected with p42^{IP4}-GFP (or control cells, transfected with empty GFP-vector), were seeded on cover glasses, treated with 10 µM retinoic acid (RA) alone for 6 days or treated with 5 µM nocodazole only for 1 h at 37°C, or treated with 10 µM RA for 6 days followed by 5 µM nocodazole treatment for 1 h at 37°C before they were fixed. We counted the cells with structural changes. Arrows (inset picture) indicate examples for cells with structural changes. We calculated the ratio of cells with structural changes to the total number of transfected cells, transfected with GFP-p42^{IP4} or GFP-only, which is displayed in the graph. Data was analyzed by an unpaired Student t-test, with ** p<0.01 considered to be significant. Results are from four independent experiments, in which four independent areas for each treatment were analyzed.

3.6 *In vitro experiments to verify the interaction of NRD and p42^{IP4}*

3.6.1 Pulldown experiments with recombinant NRD and p42^{IP4}

An interaction of NRD with p42^{IP4} could not be found using pulldown experiments with recombinant GST-p42^{IP4} together with recombinant human NRD (wt, ΔDAC, point mutants Cys C948A and HFLAH). We therefore assumed that the interaction between both proteins is weak. Alternatively, given the many interaction partners of both proteins we hypothesized that another protein may modulate the interaction.

3.6.2 Tubulin enhances the interaction of NRD1 with p42^{IP4}

To further investigate the interaction between NRD, p42^{IP4} and tubulin, we performed Far western blots. Far western blot is helpful to determine whether two proteins interact directly or whether a third protein mediates the physical interaction between both proteins (Wu et al., 2007).

For this purpose, we prepared Western Blot strips, containing 500 ng of recombinant p42^{IP4} and added recombinant NRD1 and polymerized tubulin to the blots, as described in materials and methods (see chapter 2.2.3.10). Firstly, to optimize the experimental conditions, we tried different concentrations of tubulin, ranging from 0.1 to 10 µg per reaction in a total volume of 1.25 ml. For normalizing the data, we set the binding of NRD to p42^{IP4} without addition of tubulin to 1 (Fig. 3.16 first bar chart in a, b and c).

Quantification of the blots showed that an amount of 0.1 µg of tubulin is sufficient to significantly increase the binding of hsNRD1 to p42^{IP4} (Fig. 3.16a). Furthermore, increasing the amount of tubulin in 10-fold steps shows that the relative binding of NRD to p42^{IP4} reaches a plateau level at 2.5 fold binding ratio, as compared to the blots without addition of tubulin. For the following experiments, we used the 10 µg tubulin per assay, because with this amount the detectable signal, as compared to background, was optimal both for visibility and signal strength (also Fig. 3.16a).

We were then interested to find out whether the interaction of NRD and p42^{IP4} is also enhanced, when tubulin is not polymerized prior to the incubation with NRD and application to p42^{IP4}. Quantification of the Far Western blots using nonpolymerized tubulin, shows that the addition of nonpolymerized tubulin does not significantly increase the relative binding of NRD1 to p42^{IP4} (Fig. 3.16b). The mean value was 1.5 ± 0.5 binding ratio which is not significant compared to the binding of NRD to p42^{IP4} without the addition of tubulin.

For polymerized tubulin on the contrary, the binding was clearly significantly enhanced with a mean value of 2.3 ± 0.4 binding ratio.
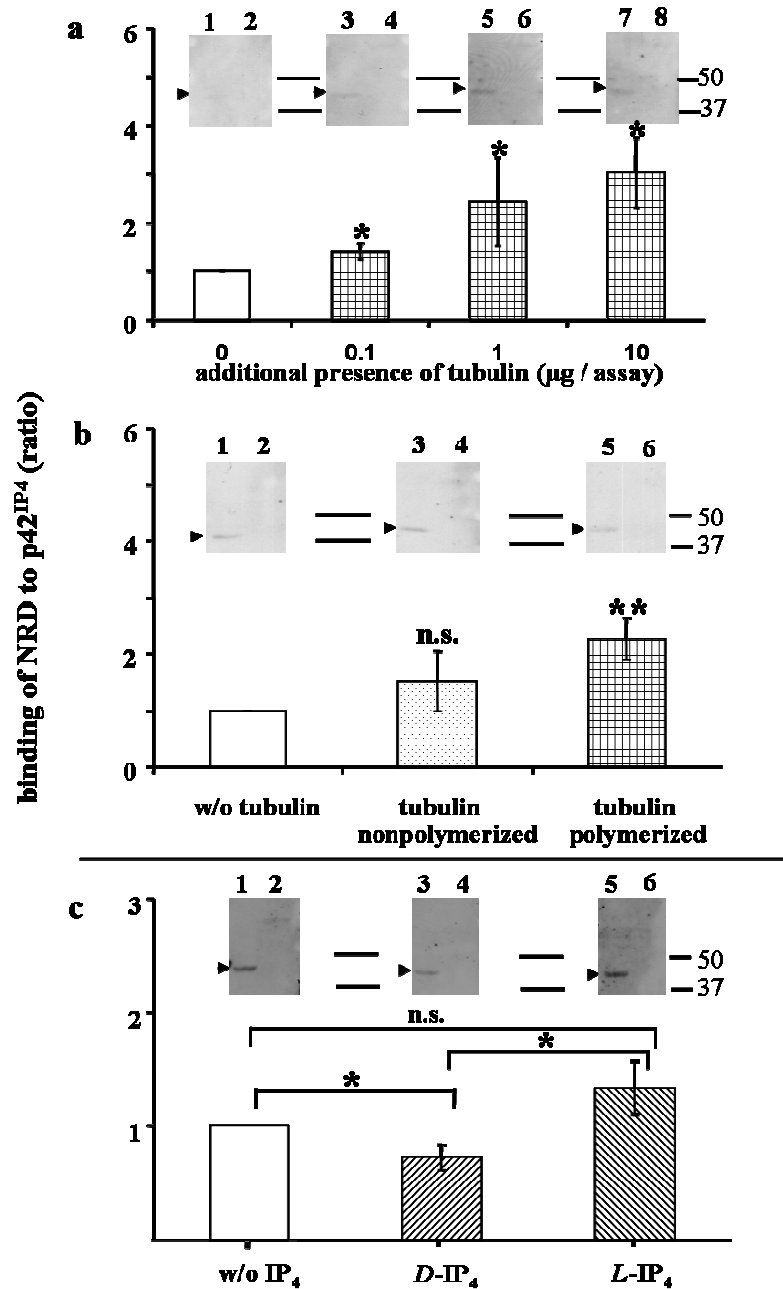
Fig. 3.16 Far-Western Blots to study the influence of tubulin on binding of NRD to p42^{IP4}.

For Western Blots we used 500 ng of recombinant p42^{IP4} protein (lanes 1, 3, 5, 7) or 500 ng of BSA (lanes 2, 4, 6, 8) for control. Lanes 1 and 2 are without addition of tubulin. The proteins were separated on a 10% SDS gel and blotted onto a nitrocellulose membrane. Far-Western Blots were done following a protocol described before (Wu et al., 2007) with modifications explained in Materials and Methods. (a) Influence of the concentration of polymerized tubulin on the binding of NRD to p42^{IP4}, testing 0.1, 1, and 10 µg tubulin per assay. The binding of NRD to p42^{IP4} without addition of tubulin corresponds to the ratio 1. (b) Influence of the polymerization status of tubulin on binding of NRD to p42^{IP4}. Experiments were performed as described in Materials and Methods, using 10 µg of non-polymerized or polymerized tubulin. The binding of NRD to p42^{IP4} without addition of tubulin corresponds to the ratio 1. (c) Influence of D-Ins(1,3,4,5)P$_4$ (lanes 3 and 4) and L-Ins(1,3,4,5)P$_4$ (lanes 5 and 6) on the binding of NRD to p42^{IP4} without the addition of tubulin. The binding of NRD to p42^{IP4} without the addition of D-Ins(1,3,4,5)P$_4$ or L-Ins(1,3,4,5)P$_4$ (lane 1) was used as control (ratio=1). We performed an unpaired Student-t-test with * p<0.05 and ** p<0.01 considered to be significant compared to control, with at least 4 (a), 6 (b) or 3 (c) independent experiments; n.s. not significant.

To prove that the binding of NRD to p42^{IP4} occurs with a functionally renatured of p42^{IP4} protein on the membrane, we performed Far-Western Blot experiments in the presence of both enantiomers of the soluble ligand of p42^{IP4} Ins(1,3,4,5)P$_4$.

D-Ins(1,3,4,5)P$_4$ is the effective ligand for p42^{IP4} whereas L-Ins(1,3,4,5)P$_4$ binds only weakly (Hanck et al., 1999). When incubated with p42^{IP4} and NRD, D-Ins(1,3,4,5)P$_4$ forces the dissociation of both proteins. However, the enantiomer L-Ins(1,3,4,5)P$_4$ is a very poor ligand for p42^{IP4} and has no influence on the interaction of NRD with p42^{IP4} (Stricker et al., 2006).

Therefore, the addition of the enantiomers to the membranes should result in a difference in the binding of NRD to p42^{IP4} if it is renatured. As shown in Fig. 3.16c, there is a significant difference between the binding of NRD to p42^{IP4} in the presence of either the D-Ins(1,3,4,5)P$_4$ or L-Ins(1,3,4,5)P$_4$. These results are consistent with protein binding experiments which were published before (Stricker et al., 2006). The binding of NRD to p42^{IP4} on the blots in the presence of the D-Ins(1,3,4,5)P$_4$ was decreased as compared to control conditions. As expected, in the presence of the low affinity ligand L-Ins(1,3,4,5)P$_4$, the binding of p42^{IP4} and NRD was not affected.

Moreover, the Far-Western Blot experiments presented in Fig. 3.16 show that the loss of interaction of NRD, p42^{IP4} and tubulin observed in SH-SY5Y-p42^{IP4} cells after nocodazole treatment has a biochemical basis.

3.6.3   Influence of NRD-mutants on binding to p42^{IP4}

Previous experiments from our group showed that p42^{IP4} can interact with NRD from rat brain lysate (Stricker et al., 2006). Moreover, interaction studies performed with p42^{IP4} and a recombinant DAC, from mouse or rat or human or combinations thereof, demonstrated that this domain of NRD is sufficient for interaction. Additionally it was confirmed that the interaction can be regulated via ligands of NRD and p42^{IP4} respectively (Stricker et al., 2006). As explained in detail in 3.3, p42^{IP4} can influence the catalytic activity of full length NRD. We were therefore interested, whether NRD-mutants, lacking important catalytic sites, have any differences in their binding properties with p42^{IP4}.

Furthermore, we wanted to verify, whether an addition of tubulin has the same effect on the binding of the mutants to p42^{IP4}, as on the wild type NRD. For this purpose, we

produced NRD mutants, as described in 3.1.1 and performed Far Western blot, without or with the addition of tubulin, as done before with NRD1.

Quantification of the blots (Fig. 3.17) showed that without the addition of tubulin wild type NRD1 and the NRD1-mutants show no differences in their interaction with $p42^{IP4}$. The catalytically inactive mutant of NRD, with a replacement of the glutamate in the HFLEH motif by an alanine, also showed increased binding to $p42^{IP4}$ in the presence of tubulin, comparable to wt NRD.

Interestingly, the interaction of $p42^{IP4}$ with the NRD-mutant C948A, where the proposed catalytically important cysteine was replaced with alanine, displayed no differences in binding to $p42^{IP4}$ irrespective of the presence or absence of tubulin.

The mutant of NRD, lacking the acidic domain (DAC) is able to bind $p42^{IP4}$. Addition of tubulin does not enhance the binding of NRD-ΔDAC to $p42^{IP4}$. This gives evidence that $p42^{IP4}$ binds not exclusively to the DAC and an interaction with NRD is possible even without this domain. Moreover, the DAC of NRD seems to be involved in the binding of tubulin during the interaction of NRD, tubulin, and $p42^{IP4}$. Additionally, the structure of NRD seems to be important for the selectivity of the potentiating effect of tubulin on the interaction of NRD, $p42^{IP4}$.
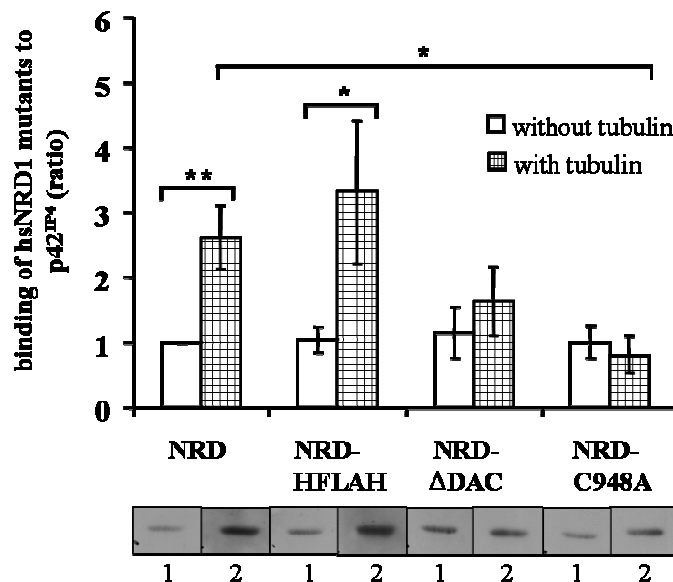
Fig. 3.17 Binding of NRD mutants to $p42^{IP4}$ in the absence or presence of tubulin. Far-Western Blots

To study the influence of tubulin on the binding of NRD mutants to $p42^{IP4}$ we produced wild type NRD and the NRD-mutants NRD-HFLAH, NRD-ΔDAC or NRD-C948A, as described in chapter 3.1 and performed Far-Western Blot, without or with the addition of polymerized tubulin as described in legend to Fig. 3.16. Blots in the lower panel show examples for the binding of NRD or NRD mutants to $p42^{IP4}$ without (1) and with (2) polymerized tubulin; the control lane (BSA, similar to Fig. 3.16) is not shown here. The binding of NRD to $p42^{IP4}$ without addition of tubulin was set as ratio 1. We performed an unpaired Student-t-test with * $p<0.05$ considered to be significant with at least 5 independent experiments.

3.6.4 Influence of p42^{IP4} on sAPPα-levels and Aβ-40 production in SH-SY5Y cells

It was shown that NRD can influence the production of sAPPα via TACE activation (Hiraoka et al., 2007). Moreover, treatment of SH-SY5Y cells with RA upregulates the release of sAPPα after 6 days (Holback et al., 2005). Therefore, we wanted to clarify whether the upregulation of NRD on day 6 in SH-SY5Y cells overexpressing p42^{IP4} (Fig. 3.11), results in an enhanced release of sAPPα into the culture medium. Such an increased release of sAPPα would prove an indirect influence of p42^{IP4} on the shedding of APP.

For detection of sAPPα release we used SH-SY5Y, SH-SY5Y-GFP and SH-SY5Y-p42^{IP4} cells, which were stimulated with 10 µM RA for 0, 3 or 6 days, to clarify whether the before mentioned upregulation of NRD on day 6 influences the release of sAPPα into the cell medium.

For detection of sAPPα we performed Western blots using the specific antibody 6E10. This antibody was shown to bind specifically to released sAPPα but can also detect membrane bound APP and Aβ. All experiments were carried out four times, each time in triplicate for both cell lysates and for the precipitated supernatant (the serum-free culture medium) from the respective culture.

Under our experimental conditions, neither in transfected SH-SY5Y nor in wt cells it was possible to get consistent results for sAPPα-release. Therefore, the data were not suitable for statistical evaluation and the Western blots of these of these experiments are not shown here.

The protein p42^{IP4} was found to be localized in AD-plaques and to interact with RanBPM, a protein influencing the APP-shedding via BACE1. Therefore, we investigated whether instead of promoting the APP cleavage via NRD and α-secretases p42^{IP4} influences the cleavage of APP via BACE1. For this, we investigated the effects of p42^{IP4} on the Aβ-40 release in SH-SY5Y cells, and SH-SY5Y cells transfected with p42^{IP4} or GFP-only. An Aβ-40 sandwich ELISA was used to measure the peptide released into the culture medium.

Incubation of the cells for 4 h and kept under serum-free conditions without RA-treatment and even increasing the incubation time to 18 h did not reveal any Aβ-40 release at all. Only after 6 days of serum-free incubation, we were able to detect a basal release of Aβ-40 into the culture media. Moreover, the difference in Aβ-40 release among the different cell types was not statistically significant (Fig. 3.18). There seems to be a tendency for the cells transfected with the GFP-tagged protein (p42^{IP4}-GFP and GFP-only) to have an increased Aβ-

40-release. Nevertheless, only the range of Aβ-40 release in GFP-only cells is wider than in GFP-p42^{IP4}.
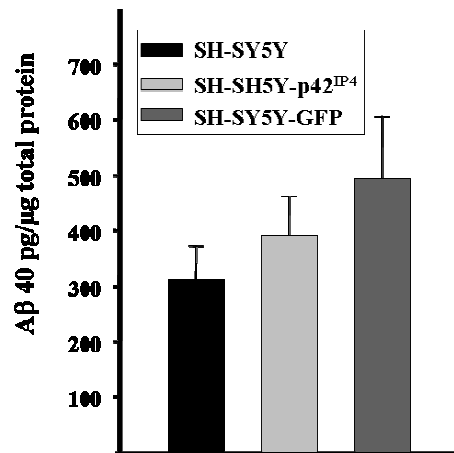
Fig. 3.18 Aβ-40-release from control and transfected SH-SY5Y cells.

For detection of released Aβ-40, SH-SH5Y cells, and SH-SH5Y-GFP cells, SH-SH5Y-p42^{IP4} cells were grown in serum-free media for 6 days without RA-treatment. The complete cell culture medium from each well was precipitated with trichloroacetic acid and dissolved in 50 µl of sample diluent of the Aβ40-ELISA-kit (hAmyloid β40 ELISA (HS), the GENETICS company, Schlieren Switzerland). The test was started immediately according to the manufacturer's instructions. Data presented here are from four independent experiments with each treatment performed in triplicate. We performed an unpaired Student-t-test with p<0.05 considered to be significant.

4 Discussion

The study presented here focused on the characterization of the interaction of p42^{IP4} with Nardilysin (NRD) on the molecular level, the modification of the interaction through a third interaction partner and the role of the protein-protein interaction for neurodegenerative and developmental processes and differentiation.

p42^{IP4} is a 42 kDa Arf-GAP protein, which is mainly expressed in neurons. Recently it was renamed ADAP1 for a consensus nomenclature (Kahn et al., 2008). It was demonstrated that p42^{IP4} interacts with a variety of proteins, which places this protein at an interesting position in various physiological processes in the cell, ranging from tissue regeneration, transport of vesicles to involvement in mitochondrial Ca^{2+} signaling. A clear functional role of p42^{IP4} has yet to be established. Therefore, the knowledge gained from investigations of individual interactions should help to define the functional role of p42^{IP4} in the cell.

It was published before that NRD and p42^{IP4} are involved in neurodegenerative diseases. p42^{IP4} was found to be colocalized in plaques of AD brains (Reiser and Bernstein, 2002). NRD was shown to be involved in myelination processes and axonal maturation (Ohno et al., 2009).

Moreover, it was demonstrated before that p42^{IP4} is able to modulate dendritic differentiation, to bind to actin and thereby modulate the neuronal actin cytoskeleton (Moore et al., 2007) (Thacker et al., 2004). Additionally, it was shown for p42^{IP4} as well as for NRD that they can bind to tubulin, albeit to different subunits (Galvita et al., 2009) (Ma et al., 2005). Previous investigations in our laboratory revealed that p42^{IP4} can interact with the domain of NRD, which is proposed to be important for regulation of the enzymatic activity (Stricker et al., 2006).

4.1 NRD does not cleave p42^{IP4}

NRD belongs to the inverzincin/M16-family of metalloendopeptidases (reviewed in (Hospital and Prat, 2004), a family with members that can act bifunctionally as a protease and through a non-enzymatic behavior.

We previously showed (Stricker et al., 2006) that the interaction of full length p42^{IP4} protein and the acidic domain (DAC) of NRD can be regulated by ligands of each of the interacting proteins. Therefore, we here investigated, whether the full-length metalloendopeptidase is able to cleave p42^{IP4}.

Discussion

```
(A)  1  MAKERRRAVL ELLQRPGNAR CADCGAPDPD WASYTLGVFI CLSCSGIHRN IPQVSKVKSV
    61  RLDAWEEAQV EFMASHGNDA ARARFESKVP SFYYRPTPSD CQLLREQWIR AKYERQEFIY
   121  PEKQEPYSAG YREGFLWKRG RDNGQFLSRK FVLTEREGAL KYFNRNDAKE PKAVMKIEHL
   181  NATFQPAKIG HPHGLQVTYL KDNSTRNIFI YHEDGKEIVD WFNALRAARF HYLQVAFPGA
   241  SDADLVPKLS RNYLKEGYME KTGPKQTEGF RKRWFTMDDR RLMYFKDPID AFARGEVFIG
   301  SKESGYTVLH GFPPSTQGHH WPHGITIVTP DRKFLFACET ESDQREWVAA FQKAVDRPML
   361  PQEYAVEAHF KHKP


(B)  1  MAKERRRAVL ELLQRPGNAR CADCGAPDPD WASYTLGVFI CLSCSGIHRN IPQVSKVKSV
    61  RLDAWEEAQV EFMASHGNDA ARARFESKVP SFYYRPTPSD CQLLREQWIR AKYERQEFIY
   121  PEKQEPYSAG YREGFLWKRG RDNGQFLSRK FVLTEREGAL KYFNRNDAKE PKAVMKIEHL
   181  NATFQPAKIG HPHGLQVTYL KDNSTRNIFI YHEDGKEIVD WFNALRAARF HYLQVAFPGA
   241  SDADLVPKLS RNYLKEGYME KTGPKQTEGF RKRWFTMDDR RLMYFKDPID AFARGEVFIG
   301  SKESGYTVLH GFPPSTQGHH WPHGITIVTP DRKFLFACET ESDQREWVAA FQKAVDRPML
   361  PQEYAVEAHF KHKP


(C)  1  MAKERRRAVL ELLQRPGNAR CADCGAPDPD WASYTLGVFI CLSCSGIHRN IPQVSKVKSV
    61  RLDAWEEAQV EFMASHGNDA ARARFESKVP SFYYRPTPSD CQLLREQWIR AKYERQEFIY
   121  PEKQEPYSAG YREGFLWKRG RDNGQFLSRK FVLTEREGAL KYFNRNDAKE PKAVMKIEHL
   181  NATFQPAKIG HPHGLQVTYL KDNSTRNIFI YHEDGKEIVD WFNALRAARF HYLQVAFPGA
   241  SDADLVPKLS RNYLKEGYME KTGPKQTEGF RKRWFTMDDR RLMYFKDPID AFARGEVFIG
   301  SKESGYTVLH GFPPSTQGHH WPHGITIVTP DRKFLFACET ESDQREWVAA FQKAVDRPML
   361  PQEYAVEAHF KHKP
```

Fig. 4.1 Putative cleavage sites for NRD in the p42[IP4] amino acid sequence.

Pairs of doublets of basic amino acids are indicated with (A) solely arginine residues (purple), (B) doublets of arginine and lysine residues (red), or arginine alone (purple). In (C) single arginine residues (green) are marked in addition to doublets as indicated in (A) and (B)

We could show that NRD does not act as a protease on p42[IP4] although the protein sequence of p42[IP4] contains several cleavage sites. As shown in Fig. 4.1 (A), p42[IP4] contains two doublets of Arg within the protein sequence.The first cleavage could be within the nuclear localization signal (MA**KERRR**AV) (Tanaka et al., 1999) and a second Arg-Arg site is at position 280-281. Cleavage at these sites would be clearly detectable with our cleavage assay, because it would result in a 30 kDa and a 10 kDa fragment of p42[IP4]. Furthermore, NRD was shown to cleave at pairs of basic amino acid residues, which do not solely contain Arg residues (Chesneau et al., 1994). These additional putative cleavage sites are marked in Fig 4.1 (B). Proteolysis at all of these sites would cause small peptides (14.3 kDa, 1.1 kDa, 13.2 kDa, 0.9 kDa, 5.5 kDa and 4.4 kDa) and result in a smear of bands, which we did not observe. Furthermore, experiments with a short time incubation (30 min) indicate that the total amount of full-length p42[IP4] does not change. Also long time cleavage assays (4 or 12 h) showed no reduced amount of p42[IP4].

Additionally, it is known that NRD is able to cleave at single basic amino acid residues (Chow et al., 2003), albeit with much lower efficiency. In Fig. 4.1 (C) the putative cleavages sites with single Arg residues are indicated (green). Single lysine residues are not shown in

Fig. 4.1 (C). Cleavage at those sites is not detectable with our methods. Further biochemical methods like mass spectrometry would be necessary to detect such small fragments.

In summary, we can most likely exclude cleavage of p42^{IP4} by NRD. Since NRD belongs to a family of metalloendopeptidases, which, besides their proteolytic activity, are able to act independently from that with other proteins, we were interested to find out, whether p42^{IP4} has the ability to influence the enzymatic activity of NRD.

4.2 p42^{IP4} enhances the enzymatic activity of NRD

Here, we could demonstrate that p42^{IP4} can enhance the enzymatic activity of the metalloendopeptidase 3 - 4 times. We measured the cleavage of a peptide derived from the bovine adrenal medulla peptide. This cleavage assay was performed *in vitro*, therefore it still has to be elucidated, whether this has functional relevance *in vivo*.

Moreover, experiments with NRD lacking the DAC, did not show an enhanced enzymatic activity after addition of p42^{IP4}. Therefore, we propose that the binding of p42^{IP4} to the DAC is important for the enzymatic activity of the metalloendopeptidase. We suggest that, depending on the part of the metalloendopeptidase where p42^{IP4} or ligands of NRD are bound, the physiological consequences may differ. We propose that the binding of p42^{IP4} to the DAC influences the enzymatic properties of NRD, whereas the binding to other parts of the metalloendopeptidase might be important for processes, which do not require the enzymatic activity of the metalloendopeptidase.

The first physiological substrate for NRD was reported recently (Kessler et al., 2011). It was demonstrated in that work that NRD is able to complement the proteasome activity, whereby it contributes to generation of Cytotoxic T lymphocyte epitopes of an Epstein-Barr virus protein. Additionally, NRD is able to enhance the shedding of HB-EGF (Nishi et al., 2006) and to influence the α-secretase activity of ADAM17 (Hiraoka et al., 2007). Moreover, NRD plays a role in the shedding of neuregulin (Ohno et al., 2009), a protein involved in myelination.

NRD was shown to cleave peptides such as somatostatin-28, dynorphin-A (Chesneau et al., 1994), α-neoendorphine (Csuhai et al., 1995), and miniglucagon (Fontes et al., 2005) *in vitro*. Recent studies (Bernstein et al., 2007) demonstrated that although NRD can cleave somatostatin *in vitro*, it does not colocalize with somatostatin-28. Nevertheless, besides the antigen processing activity of NRD (Kessler et al., 2011) other physiological relevant

substrates of NRD are still unknown. Moreover it was discussed that NRD to may have a role in neuropeptide metabolism (Seidah and Prat, 2002).

Whether or not p42^{IP4} can influence the catalytic activity of NRD in physiological environments remains to be elucidated.

4.3 Upregulation of NRD expression after stimulation with RA in SH-SY5Y cells not expressing p42^{IP4}

The expression of the proteins p42^{IP4} and NRD was shown to be regulated during development (Aggensteiner and Reiser, 2003) (Fumagalli et al., 1998). In addition to that, we could recently demonstrate that the metalloendopeptidase is expressed almost exclusively in neurons, with wide, but uneven distribution throughout the human brain (Bernstein et al., 2007). Moreover, a developmental regulation of the expression of NRD was found, together with a concomitant overlap between the expression of p42^{IP4} and NRD.

To elucidate the relationship of NRD and p42^{IP4} during differentiation, we first searched for a suitable cell culture model for further investigations.

Neuroblastoma cells are often used as an experimental model for neuronal differentiation and de-differentiation (reviewed in (Edsjo et al., 2007). Application of RA to neuroblastoma cells stops their proliferation and causes differentiation into a more neuronal cell type (Pahlman et al., 1984). Moreover, the vitamin A metabolite *all-trans* RA plays an important role in early embryonic development, the development of organs and organ systems, especially the nervous system. Therefore we decided to stimulate the neuroblastoma cell line SH-SY5Y with RA, to analyze changes in the expression of NRD and p42^{IP4} on both mRNA and protein level.

Although we were able to detect mRNA of both NRD and for p42^{IP4}, our investigations to verify the protein expression revealed that p42^{IP4} was not expressed in these neuroblastoma cells. In addition, stimulation with RA did not reveal the expression of the protein p42^{IP4}. Therefore, we used this cell line, overexpressing p42^{IP4} as GFP-fusion protein, as a model to elucidate the influence of p42^{IP4} on NRD expression.

We demonstrate here that stimulation of untransfected SH-SY5Y cells with 10 μM RA results in an upregulation of NRD protein levels, with a 6-fold rise after 15 days. It is known from the literature that NRD can be upregulated with RA in SK-N-BE(2) cells, another neuroblastoma cell line, albeit after 2 days of RA stimulation (Draoui et al., 1997). Although

it was discussed in that publication that NRD might contain RARE elements, which are responsible for the upregulation, promoter studies on NRD could not reveal such an element (Winter and Pierotti, 2000). For this reason we searched the cisRed (cis-regulatory) database (Robertson et al., 2006) for motifs, which could be responsible for the RA-induced upregulation of NRD. We found on human chromosome 1 (chr1: 52,117,180-52,117,191) a binding site for LXR-alpha_RXR-alpha, which we propose to be the cause for the upregulation. As already mentioned above, p42^{IP4} protein is not expressed in untreated SH-SY5Y cells and its expression was not induced after RA treatment. The latter finding was not surprising, because the search in the data base cisRed (Robertson et al., 2006) revealed neither RARE nor RXR elements in the p42^{IP4} gene.

The SH-SY5Y cell line was shown to consist of two phenotypes with a majority of neuroblast-like cells. Upon stimulation with RA, 25% of the cells grow extensions longer than 50 µm but at the same time the non-neuronal phenotype increases dramatically (Preis et al., 1988). Therefore, for all experiments using SH-SY5Y cells treated with 10 µM RA, it was necessary to avoid the non-neuronal phenotype, which rapidly overgrows the culture dish upon RA stimulation. We selected the neuronal cell type with trypsination. Moreover, it was difficult to choose the gene for normalization, because GAPDH and tubulin were upregulated in the time-course of the experiments. For actin it was published before that the ratio of actin expression relative to the total protein content was significantly increased in SH-SY5Y cells differentiated with RA (Asada et al., 1994). Therefore, in our analysis, all genes were normalized to the same gene under untreated (day 0) conditions.

4.4 Influence of p42^{IP4} on the upregulation of NRD in RA stimulated SH-SY5Y cells expressing p42^{IP4}

To clarify whether the concomitant expression of NRD and p42^{IP4} in brain and the developmental regulation of both proteins have a physiological role, the influence of p42^{IP4} on the expression of NRD in SH-SY5Y-p42 cells after stimulation with RA was investigated.

Interestingly, stable transfection of GFP-tagged-p42^{IP4} into SH-SY5Y cells and stimulation with RA for 3, 6, 9, 12, and 15 days shifts the increase in the expression of NRD to an earlier time point. NRD appears to be upregulated as early as day 6 in p42^{IP4}-GFP transfected SH-SY5Y cells, which represents a shift of 9 days compared to untransfected SH-SY5Y cells, where NRD is upregulated at day 15. Although the protein expression of NRD is decreased in p42^{IP4} - transfected SH-SY5Y cells at later time points (after day 6) treatment

Discussion
---

with 10 µM RA, similar results could be obtained with GFP-only transfected SH-SY5Y cells. Therefore, the upregulation after day 6 is not the result of overexpression of p42^{IP4} and most likely a result of the expression of the GFP-tag. For this reason, conclusions about the expression of NRD and the influence of p42^{IP4} can be made only until day 6 in GFP-p42^{IP4} transfected SH-SY5Y cells.

Nevertheless, the p42^{IP4}-dependent shift in the upregulation of NRD in SH-SY5Y-p42^{IP4} cells after stimulation with RA gives evidence that the developmental colocalization of both proteins has functional relevance (Bernstein et al., 2007). We propose that p42^{IP4} might directly influence the transcription of NRD, but further experiments, like chromosome immunoprecipitation need to be done to investigate this idea further.

It is known from the literature that p42^{IP4} can influence the transcription of certain genes. In a study to test the modulators of the activator protein-1 (AP1), using large scale genome functional profiling it was shown that p42^{IP4} is a putative modulator of AP-1 (Chanda et al., 2003). p42^{IP4} highly activates the AP-1 related reporters, the nuclear factor of activated T cells response elements (NFAT) and AP-1 (induced with PMA). Moreover, p42^{IP4} showed a lowered activation of the cAMP response element binding protein (CRE). Moreover, the transfection of siRNAs, coding for ERK pathway effectors like DGK1, MEKK1 and MEKK2, or directed against genes like MAP4K1 related to the JNK-pathway, extinguished the activity of p42^{IP4} on the AP-1 reporter (Chanda et al., 2003).

We could observe that independently of RA stimulation, cells stably transfected with p42^{IP4}-GFP showed a different behavior when treated with trypsin compared to SH-SY5Y-wt and GFP-only cells. p42^{IP4} - transfected cells detached much faster from their substrate compared to SH-SY5Y or SH-SY5Y-GFP cells. In this context it is interesting to note that p42^{IP4} can activate the AP-1 promoter (Chanda et al., 2003). This activation is noteworthy because p42^{IP4} can thereby moderate an oncogenic transformation of cells via the AP-1 signaling pathway, which includes also changes in cell adhesion and stimulates proliferation of cells (Chanda et al., 2003). The time course of the upregulation of NRD depends on the cell line investigated (15 days in SH-SY5Y cells, as shown here or after 2 or 3 days in SK-N-BE cells (Draoui et al., 1997)). It is interesting to note that RA can inhibit the transcription factor AP-1 (Schule et al., 1991). p42^{IP4} can activate the AP-1 pathway and therefore induces proliferation. We speculate that by transfection of p42^{IP4}, p42^{IP4} excerts its influence on the focal adhesion proteins (vinculin and paxillin) as published before (Thacker et al., 2004), which resulted in earlier detachment of the cells after trypsin treatment.

4.5 Influence of tubulin on the localization of NRD and p42^{IP4}

Using confocal microscopy, we found that NRD is localized in the cytosol and in the growing neurites of the stimulated SH-SY5Y. Furthermore, after 6 days of RA treatment, NRD appears to be localized within vesicular structures, which are even more visible after 9 days of RA treatment. We conclude that NRD is transported in developing neurites. Staining with p42^{IP4} antibodies showed no expression of this protein, neither in unstimulated nor in cells stimulated with RA.

SH-SY5Y cells, stably transfected with p42^{IP4}-GFP, showed the colocalization of NRD, p42^{IP4} and tubulin in the cytosol and at the plasma membrane. Treatment with nocodazole caused a redistribution of p42^{IP4} and tubulin, but did not change the colocalization of p42^{IP4} and tubulin, whereas the colocalization of all three proteins was visible only in vesicular structures. We hypothesize that this colocalization, which occurs only in vesicular structures, might have also a functional role in transport processes along microtubules.

The kinesin motor protein KIF13B, which interacts with p42^{IP4} (Venkateswarlu et al., 2005), was demonstrated to play a role in Schwann cell myelination, where it contributes to the cell membrane homeostasis, through transporting the myotubularin-related protein2 phospholipid phosphatase to places of myelination (Bolis et al., 2009).

Interestingly, it was reported that NRD regulates the myelination in the central and peripheral nervous system via enhancement of extracellular shedding of neuregulin (NRG1) by TACE (Ohno et al., 2009).

Recent investigations in our laboratory gave evidence that p42^{IP4} interacts with CNP from rat brain mitochondria (Galvita et al., 2009). Moreover, CNP is a microtubule - associated protein, which does not only polymerize tubulin but also links tubulin to the cell membrane (Bifulco et al., 2002). It was discussed that the localization of p42^{IP4} in the intermembrane space of mitochondria and the interaction with CNP influences the opening of the permeability transition pore (PTP) (Galvita et al., 2009). Although p42^{IP4} thereby contributes to drastic changes in the cellular Ca^{2+} levels, which happen to be disturbed in many neurodegenerative diseases (reviewed in (Celsi et al., 2009), the interaction of p42^{IP4} with CNP may also have other physiological consequences.

CNP was discussed to be a transporter for RNA along microtubules, due to its ability to bind simultaneously to tubulin and RNA (Gravel et al., 2009). Although the physiological role of CNP is unclear, it is thought to play a role in myelination. Interestingly, BACE -/- mice also diplay peripheral hypomyelination (Willem et al., 2006), which may be of

importance for the role of p42^{IP4} in neurodegenerative diseases via the interaction with RanBPM.

4.6 *Influence of tubulin on the interaction of NRD with p42^{IP4}*

Because it was not possible to provide evidence for an interaction of p42^{IP4} with NRD using pulldown experiments, we assumed that the rather weak interaction between both full-length proteins and possibly depends on other proteins, as most proteins exert their physiologic role in the interplay with other proteins.

Moreover, it was previously reported that NRD colocalizes with β-tubulin (Ma et al., 2005) and we recently reported an interaction of p42^{IP4} with α-tubulin (Galvita et al., 2009), which makes tubulin an ideal protein partner to support the interaction.

Nevertheless, one has to be careful when postulating a functional interaction with tubulin. Many proteins are known to interact with tubulin and an extensive list of proteins which co-sediment with microtubules from rat brain was published before (Sakamoto 2008).

Being among co-purified proteins does not necessarily mean that those proteins interact or maintain a functional relationship. Therefore, we were interested to find out, whether there is a simultaneous interaction of both proteins with tubulin. Moreover, we wanted to determine whether tubulin might have an impact on the interaction between p42^{IP4} and NRD and to reveal if changes in the tubulin-cytoskeleton affect the interaction of NRD and p42^{IP4}. For that, we examined the interaction between full length NRD, p42^{IP4} and tubulin in SH-SY5Y cells and *in vitro*.

Using Far Western Blot technique, we show *in vitro* that the interaction between p42^{IP4} and NRD can be enhanced by tubulin. It is critical for these kinds of experiments that the protein blotted on the membrane is properly refolded.

We assume that this must be the case in the experiments performed by us, because stereospecific ligands of p42^{IP4} – $_D$-IP$_4$ and $_L$-IP$_4$, clearly show a different behavior on the binding of NRD to p42^{IP4} on the membrane. We showed here that in Far Western Blots, $_D$-IP$_4$ diminishes the interaction of NRD and p42^{IP4}, which is similar to previously published results (Stricker et al., 2006). Compared to the data published before, the reduction was smaller but that difference might be explained by of the different binding capacities for p42^{IP4} of the DAC alone (used in (Stricker et al., 2006) and the full length NRD as used here.

Interestingly, the enhanced interaction between NRD and p42^{IP4} could not be observed, when tubulin was not polymerized. Polymerized tubulin may increase the probability for the

interaction of p42^{IP4} by bringing p42^{IP4} and NRD in close proximity. However, the functional consequences of an interaction between NRD, p42^{IP4} and tubulin and more specific the differences in the binding properties of NRD, p42^{IP4} and tubulin, depending on the polymerization status of tubulin are not clear.

Moreover, irrespective of the presence or absence of tubulin, NRD mutants, which have a substitution in a catalytic important amino acid residue (C948A), as discussed before in (Pierotti et al., 1994) and (Hospital and Prat, 2004) showed no differences in their binding to p42^{IP4}. Mutants that lack an entire domain (ΔDAC) showed a very small increase of NRD binding to p42^{IP4} in the presence of tubulin.

Therefore, we conclude that p42^{IP4} binds not exclusively to the DAC of NRD. Moreover, the different binding positions of p42^{IP4} to NRD might have consequences on the regulation by ligands of either NRD or p42^{IP4}. It was previously shown that the interaction of p42^{IP4} with the DAC alone can be regulated by ligands of NRD as well as of p42^{IP4} (Stricker et al. 2006). With the DAC, known to be important for the enzymatic activity of NRD, and the place for binding of NRD ligands, one could assume that the regulation by NRD ligands is important for processes, where NRD acts as an enzyme. With the here newly found interaction of p42^{IP4} with NRD lacking the DAC, ligands of NRD may not be important for the regulation of the binding of p42^{IP4} outside the DAC of NRD. This may influence processes in the cell, which do not require the enzymatic activity of NRD.

Tubulin does not influence the binding of the NRD-mutant ΔDAC to p42^{IP4} to the same extent like binding to the wild type NRD, which points towards a binding position of tubulin to NRD also in the DAC.

Moreover, while IP$_4$ forces a release of NRD (Stricker et al., 2006) and RanBPM (Haase et al., 2008) from p42^{IP4} the interaction with tubulin might be unaffected by IP$_4$. Therefore, the influence of tubulin on the interaction with the p42^{IP4} ligands requires further investigations.

We speculate that the interaction of NRD, p42^{IP4}, and tubulin might have some influence on transport processes, for example via the microtubule plus end directed KIF13B. p42^{IP4} itself interacts directly through its Arf-GAP domain with the stalk domain of the kinesin motor protein KIF13B (Venkateswarlu et al., 2005), which was found to be essential for the localization of p42^{IP4} to the leading edges of cells and for the Arf6-GAP activity of p42^{IP4} *in vivo*. Moreover through the binding of p42^{IP4} to the fork-head domain (FHA-domain) of KIF13B, PIP$_3$ vesicles can be connected to the motor protein and can be

Discussion

transported along microtubules to the end of the axon in neuronal cells (Horiguchi et al., 2006).

Previous reports suggested that p42^{IP4} can have dramatic effects on the actin cytoskeleton and can bind F-actin directly via its PtdIns(3,4,5)P$_3$-binding pleckstrin homology (PH) domain (Thacker et al., 2004).

Although many proteins are able to bind to either actin or tubulin, very few proteins can bind to both actin and tubulin simultaneously. The binding of actin and the modulated interaction of p42^{IP4} with NRD by tubulin may therefore place p42^{IP4} at such a crosslinker position between the actin and tubulin cytoskeleton. Functionally, p42^{IP4} might serve as an anchor between actin and microtubules during the transport of vesicles along microtubules.

A possible link between the actin- and the tubulin-network was discussed before (Halpain and Dehmelt, 2006), and those linker proteins also play a role in growth cone development (Dehmelt and Halpain, 2007). Besides their role in growth cone development, proteins that act as an actin-tubulin crosslinker are also important in the movement of growth cones, in regeneration processes, in wound healing and in virus infection of cells.

We recently discovered in a yeast-two-hybrid-screen with a human brain cDNA library and p42^{IP4} as bait that several p42^{IP4}-interacting clones represented peptides from the microtubule-associated proteins MAP1B and MAP1A (C.B. and G.R., unpublished results). Although this was not investigated further, evidence of this interaction *in vivo* would add to the understanding of p42^{IP4} and interaction with microtubules.

In this respect, it would be of great interest to know, whether p42^{IP4} is located in growth cones. One could expect p42^{IP4} to be co-localized with MAP1A/B alongside the axon with an interaction or colocalization with NRD. Additionally, it may also depend on the localization of p42^{IP4} in- or outside of mitochondria. As mentioned before, our group previously reported that p42^{IP4} shows mitochondrial localization. In growth cones mitochondria are expected to be localized to the central domain and transition zone of the growth cone (Geraldo and Gordon-Weeks, 2009).

Furthermore, investigations to identify the precise tubulin interacting domain of p42^{IP4} have to be performed. It is known from the actin-tubulin crosslinker neurofibromin that the mutation of the GAP-related domain impairs the binding of neurofibromin to microtubules (Xu and Gutmann, 1997) and that tubulin can even inhibit the Ras GAP activity of neurofibromin (Bollag et al., 1993). It would be interesting to investigate, whether p42^{IP4} displays analogous behavior, because it can bind to both actin and tubulin and work as GAP, albeit for Arf5 and Arf6.

Assuming that the GAP domain of p42^{IP4} is responsible for binding to both tubulin and NRD and with F-actin binding mostly to the PH2 domain of p42^{IP4} (Thacker et al., 2004), it will be interesting to investigate, whether mutations in the Arf-GAP domain of p42^{IP4} would diminish, if not even abolish the interaction with microtubules[‡].

Interestingly, neurofibromin is an actin tubulin crosslinker, which does not possess a tubulin binding domain, similar to MAPs (Li et al., 2001). Furthermore, during the development of telencephalic neurons, the expression of neurofibromin is regulated, so that depending on the developmental stage, a high coexpression with actin or with tubulin, even the colocalization was found to be dependent on the developmental stage (Li et al., 2001).

In dendritic spines p42^{IP4} might work as a linker as part of a transport complex, which localizes NRD to the postsynaptic membrane for shedding of substrates. Binding of PIP$_3$ or PIP$_2$ to p42^{IP4} may subsequentially fix NRD on the membrane. The binding of the p42^{IP4} ligand IP$_4$ to p42^{IP4} would force the release of NRD from the membrane into the cytosol. Additionally, p42^{IP4} might thereby regulate the shedding of substrates other than the adrenal medulla peptide (shown *in vitro* in this work) by NRD and thereby participate in neuropeptide metabolism.

To verify this hypothesis, it is important to elucidate the precise binding site of p42^{IP4} to NRD, but also to clarify the impact of NRD ligands.

It was published before that the PH2 domain of p42^{IP4} is the major binding place for actin and the PH1 domain has only a minor binding capacity, whereas the Arf-GAP domain is not important for the binding of actin (Thacker et al., 2004). Moreover, assuming that the PH2 domain binds to DAC, the question arises whether binding of p42^{IP4} ligands would influence the binding of p42^{IP4} to actin and thereby the potential crosslinking function of p42^{IP4} between actin and tubulin.

4.7 Influence of p42^{IP4} on sAPPα-levels and Aβ-40 production of APP

Another aim of this study was to investigate, whether p42^{IP4} has an impact on the shedding of the amyloid precursor protein (APP).

It is known that p42^{IP4} is localized in plaques of AD-patients, but the role of this protein in AD is still unknown (Reiser and Bernstein, 2002).

It was proposed before (Skovronsky et al., 2001) that the processing of APP is balanced between either amyloidogenic pathway, via BACE1 or non-amyloidogenic via α-secretases

---

[‡] Unpublished preliminary experiments with p42^{IP4} and a mutation in the Arf-GAP domain support this idea.

Discussion

(TACE for example). A shift towards APP processing via BACE results in increased levels of Aß, whereas preferential cleavage by α-secretases leads to the release of the neuroprotective sAPPα. A shift towards the amyloidogenic pathway may happen through inhibition of α-secretases or increased activation of BACE.

Several interaction partners of p42[IP4] were shown to be involved in processes connected to AD, albeit mostly not in a direct way. The PKC can activate directly (Diaz-Rodriguez et al., 2002) or indirectly the α-secretase, nucleolin is able to regulate the mRNA of APP (Zaidi and Malter, 1995) and RanBPM promotes the BACE1 induced cleavage of APP (Lakshmana et al., 2009).

For NRD it was previously reported that it can enhance the TNF-α-converting enzyme (TACE) – induced α-cleavage of APP which in turn leads to reduced production of the neurotoxic Aß (Hiraoka et al., 2007). Moreover, knockdown of the NRD protein expression leads to decreased α-secretase-activity and increased production of Aß.

Although p42[IP4] interacts with NRD and other proteins favoring the non-amyloidogenic pathway, it was found to be co-localized with Aß-plaques in AD-brains (Reiser and Bernstein, 2002). Moreover, RanBPM, another interaction partner of the neuronal protein p42[IP4] (Haase et al., 2008), was found to interact with BACE1 and to increase the release of Aß (Lakshmana et al., 2009).

Together with the enhancement of TACE – induced α-cleavage of APP via NRD (Hiraoka et al., 2007) and the decreased α-secretase-activity after knock-down of the NRD protein, sets p42[IP4] at an interesting position within the network of proteins involved in APP shedding. Our hypothesis was that p42[IP4] might have either a neuroprotective role via interaction with NRD, resulting in an increase of sAPPα release or a neurotoxic role via RanBPM and increased production of Aß. We firstly focused on the anti-amyloidogenic pathway, because our data on the influence of p42[IP4] on the expression of NRD let us expect an increase of sAPPα release via NRD and TACE. We investigated the sAPPα-secretion, via Western blot analysis. Although the overexpression of p42[IP4] in SH-SY5Y cells can influence the time-dependent upregulation of NRD after stimulation with 10 µM RA, this overexpression together with a concomitant treatment with RA has no clear effect on the shedding of APP via α-secretases. The reasons for the inconsistent detection of sAPPα are not obvious.

It might be that the sAPPα release was not influenced by p42[IP4], because the catalytically activity of NRD is not necessary for enhanced sAPPα production (Hiraoka et al.,

2007). The modulation of the enzymatic activity of NRD by p42^{IP4} may therefore have a different physiological function, which is not related to APP-shedding.

We can exclude that the inconsistent detectable levels of sAPPα are a result of technical problems with the antibody used for the experiments (6E10). We confirmed the functionality of this antibody with recombinant sAPPα (not shown).

Because of the difficulties in consistent sAPPα detection, we instead suspected that the influences of p42^{IP4} alone might shift the processing of APP towards the amyloidogenic pathway but are imbalanced through the effect of upregulation of NRD. We therefore avoided stimulation with RA for the experiments aiming to detect the release of Aβ40. An ELISA to detect the Aβ40-release revealed that the levels of this peptide remain at a basal level, even under serum-free condition of the cells for one week.

However, it is still a miracle, how p42^{IP4} ends up in the amyloid plaques of AD-brains. Although p42^{IP4} does not directly influence the α-secretase pathway via interaction with NRD, it also does not directly affect the β-secretase pathway. Most recent papers propose that the equilibrium between α-secretases and BACE1 might not be the critical point for developing AD, as it was assumed before (Jang et al., 2010). They discuss that the non-amyloidogenic p3 peptides, produced after α- secretase and γ-secretase cleavage, can form ion channels, which can permit Ca^{2+}-influx. The resulting high Ca^{2+} concentration is then the cause for disruption of neurites and finally leads to the death of neurons. It is possible that the localization of p42^{IP4} in mitochondria and the influence on the opening of the permeability transition pore contributes more to the localization of p42^{IP4} in plaques of AD-brains than its interaction with RanBPM or NRD.

In summary, although the physiological role of the interaction between p42^{IP4} and NRD is not yet clear, we propose that depending on the spatial and temporal localization of both proteins the interaction will translate into different physiological functions.

During development, p42^{IP4} may influence the protein expression of NRD and thereby allowing NRD to exert its enzymatic or non-enzymatic functions at an earlier time.

Additionally, our results may place p42^{IP4} at a linker position between the actin and the tubulin network. Through interaction of p42^{IP4} with adapter proteins of vesicles like KIF13B, p42^{IP4} may influence transport processes along microtubules, which also play a role in growth cone development.

In neurodegenerative diseases, p42^{IP4}, although found in amyloid plaques of AD brains, is not directly involved in the shedding of APP. p42^{IP4} instead may also participate in

neurodegenerative diseases linked to disturbances of myelination via an interplay with NRD and between NRD, BACE1, NRG1 and its interaction partners. Besides the putative role of $p42^{IP4}$ in neurodegenerative diseases, $p42^{IP4}$ may participate in neuropeptide metabolism, as it was shown in this work that $p42^{IP4}$ is not a substrate for NRD but can modulate the cleavage of a neuropeptide-derived substrate of NRD.

5   Abstract

The study presented here focused on the characterization of the interaction of the neuronal protein p42^{IP4} (centaurin α1; ADAP1) with the metalloendopeptidase nardilysin (NRD) and the modification of the interaction through tubulin.

NRD belongs to the inverzincin / M16 family of metalloendopeptidases, which have the ability to act as a protease and in a non-enzymatic way. We investigated, whether NRD acts as protease on p42^{IP4}. We could show here that recombinant, enzymatically active NRD does not cleave p42^{IP4}. Using a substrate of the metalloendopeptidase in an enzymatic assay revealed that the presence of p42^{IP4} enhances the enzymatic activity of NRD.

It has been published before that p42^{IP4} and NRD are developmentally regulated with a time-dependent overlap in their expression in developing human brain. To investigate this on cellular level, we used SH-SY5Y cells and differentiated them into a more neuronal phenotype with 10 µM retinoic acid (RA). Differentiation of these neuroblastoma cells by RA treatment resulted in an upregulation of NRD protein levels, with a 6-fold rise after 15 days. NRD expression was detectable in the neurites of RA-stimulated SH-SY5Y cells and NRD was localized in vesicular structures.

p42^{IP4} is not expressed in SH-SY5Y cells and an expression cannot be induced through stimulation with RA. We therefore produced SH-SY5Y cells, stably transfected with GFP-tagged-p42^{IP4} and used this cell system as a model to investigate whether a functional interaction exists between both proteins. Interestingly SH-SY5Y-p42^{IP4} cells showed an enhanced NRD protein expression already at an earlier time point after RA treatment. We propose that p42^{IP4} influences the transcription of NRD.

It is known from the literature that NRD can interact with β-tubulin and p42^{IP4} with α-tubulin. Therefore, we were interested to find out, whether tubulin can influence the interaction between NRD and p42^{IP4}. Using confocal microscopy, we observed a colocalization of NRD, p42^{IP4}, and tubulin in the cytosol and on the plasma membrane in the neuroblastoma cells SH-SY5Y, stably transfected with p42^{IP4}. To examine the importance of tubulin for the interaction of NRD with p42^{IP4} we treated these cells with nocodazole, a microtubule depolymerisation agent. Nocodazole did not affect colocalization of p42^{IP4} and tubulin, but caused a clear redistribution of the proteins in cells. A colocalization of p42^{IP4}, tubulin, and NRD was visible exclusively in multiple foci. We hypothesize that this colocalization, which occurs only in these foci, might have a functional role in transport processes along microtubules, via an interaction with other proteins. p42^{IP4} might help to transport NRD along microtubules via an interaction with KIF13B. To investigate the interaction between NRD, p42^{IP4}, and tubulin observed in the neuroblastoma cells, we performed Far-Western Blots to detect the protein-protein interactions directly. We could demonstrate that tubulin potentiates the interaction between NRD and functionally renatured p42^{IP4}. The enhancement depends on the polymerization of tubulin.

Moreover, the interaction between p42^{IP4}, NRD, and tubulin is very specific. We tested several mutants of NRD for their binding properties to tubulin and p42^{IP4}. NRD, with a mutation in the Zn^{2+}-binding motif (HFLAH->HFLEH) behaved like unmutated NRD. The mutation of a highly conserved cysteine residue in NRD to alanine abolished the potentiation by tubulin. The NRD mutant lacking the characteristic acidic domain (DAC) was able to bind p42^{IP4}, but addition of tubulin could not significantly potentiate the binding to p42^{IP4}. The interaction of p42^{IP4} with ΔDAC proves that p42^{IP4} also binds to NRD outside the DAC. The tubulin mediated enhancement of the interaction between p42^{IP4} and NRD, supports our concept of a novel role of p42^{IP4} as a linker between the actin and tubulin network in neural cells.

Furthermore, the interaction of both proteins is possibly important with regard to Alzheimer's disease (AD). The protein p42^{IP4} has been found to be colocalized with neuritic plaques in AD brains and to interact with RanBPM- a protein, which can activate the β-secretase (BACE1). Opposite to that, NRD has been shown to enhance the release of the neuroprotective sAPPα. We therefore studied whether p42^{IP4} affects the cleavage of APP. We could demonstrate here that overexpression of p42^{IP4} in SH-SY5Y cells has no effect on the shedding of APP, as both the release of the neuroprotective sAPPα and the release of Aβ40 remain on the basal level.

6 Zusammenfassung

In der hier präsentierten Arbeit wurde die Interaktion zwischen dem neuronalen Protein p42^{IP4} (centaurin α1; ADAP1) und der Metalloendopeptidase Nardilysin (NRD), sowie die Modifikation dieser Interaktion durch Tubulin untersucht.

NRD gehört zur Familie der Inverzinkin / M16 Metalloendopeptidasen. Einige Mitglieder dieser Familie haben die Fähigkeit, sowohl als Protease, wie auch auf nicht-enzymatische Weise ihre Wirkung zu entfalten. Es wurde hier als erstes untersucht, ob NRD als Protease auf p42^{IP4} wirken kann. Es konnte dabei gezeigt werden, dass rekombinantes, enzymatisch aktives NRD p42^{IP4} nicht schneidet. Durch den Einsatz eines Substrates der Metalloendopeptidase in einem enzymatischen Assay konnte gezeigt werden, dass unter Anwesenheit von p42^{IP4} die enzymatische Aktivität von NRD verstärkt wird.

Es ist aus Veröffentlichungen bekannt, dass p42^{IP4} und NRD entwicklungsbiologisch reguliert werden und die Expression beider Proteine während der Entwicklung des humanen Gehirns eine zeitliche Überlappung aufweist. Um dies auf zellulärer Ebene zu untersuchen, verwendeten wir hier die Neuroblastoma Zellen SH-SY5Y, um diese mit Hilfe von 10 µM Retinsäure (RA) in einen neuronaleren Phänotyp zu differenzieren. Die Differenzierung dieser Neuroblastomazellen mit Hilfe von RA hatte eine verstärkte Expression von NRD zur Folge, wobei nach 15 Tagen ein 6-facher Anstieg der NRD-Expression zu verzeichnen war. Die Expression von NRD ließ sich dabei in den Neuriten der mit RA stimulierten SH-SY5Y Zellen nachweisen und NRD konnte auch in vesikulären Strukturen beobachtet werden.

p42^{IP4} hingegen wird nicht in SH-SY5Y Zellen exprimiert und die Expression kann auch nicht durch Stimulation mit RA induziert werden. Deshalb wurden SH-SY5Y-p42^{IP4} Zellen hergestellt und als Modell genutzt, um zu untersuchen, inwiefern eine funktionelle Interaktion zwischen beiden Proteinen besteht. Interessanterweise zeigten SH-SY5Y Zellen, die stabil mit GFP-p42^{IP4} transfiziert wurden, zu früheren Zeitpunkten der RA Behandlung eine verstärkte Expression von NRD. Es wird deshalb vorgeschlagen, dass p42^{IP4} die Transkription von NRD beeinflusst.

Es ist aus der Literatur bekannt, dass NRD mit β-Tubulin und p42^{IP4} mit α-Tubulin interagiert. Aus diesem Grund wollten wir herauszufinden, ob Tubulin die Interaktion zwischen NRD und p42^{IP4} beeinflussen kann. Mittels Konfokalmikroskopie konnte in SH-SY5Y Neuroblastomazellen, die stabil mit p42^{IP4} transfiziert wurden, eine Kolokalisation von NRD, p42^{IP4} und Tubulin im Zytosol und an der Plasmamembran vorgefunden werden. Um die Bedeutung von Tubulin für die Interaktion von NRD mit p42^{IP4} genauer zu untersuchen, wurden diese Zellen mit Nocodazol behandelt, welches eine Substanz darstellt, die Mikrotubuli depolymerisieren kann. Nocodazol zeigte keine Beeinflussung der Kolokalisation von p42^{IP4} und Tubulin, verursachte aber eine eindeutige Umverteilung dieser Proteine in den Zellen, wobei eine Kolokalisation von p42^{IP4}, Tubulin und NRD ausschließlich in Multiplen Foci zu verzeichnen war. Wir vermuten, dass diese Kolokalisation im Zusammenspiel mit anderen

Zusammenfassung

Proteinen eine Rolle beim Transport entlang von Mikrotubuli spielen könnte. $p42^{IP4}$ könnte dabei via Interaktion mit KIF13B, eine Rolle beim Transport von NRD entlang der Mikrotubuli besitzen. Um die in den Neuroblastomazellen beobachtete Interaktion zwischen NRD, $p42^{IP4}$ und Tubulin zu untersuchen, wurden Far Western Blots durchgeführt. Die Protein-Protein Interaktion wurde dabei direkt auf dem Western Blot detektiert. Es konnte gezeigt werden, dass Tubulin die Interaktion zwischen NRD und dem zuvor auf der Membran funktionell renaturierten $p42^{IP4}$ verstärkt. Jedoch scheint diese Verstärkung vom Polymerisationsstatus des Tubulins abzuhängen.

Weiterhin scheint die Interaktion zwischen $p42^{IP4}$, NRD und Tubulin sehr spezifisch zu sein. Wir untersuchten verschiedene Mutanten von NRD hinsichtlich ihrer Bindungseigenschaften gegenüber Tubulin und $p42^{IP4}$. Die NRD-Mutante, die eine Mutation im Zn^{2+}-bindenden Motiv (HFLAH->HFLEH) besitzt, verhielt sich dabei wie nicht mutiertes NRD. Interessanterweise verursachte die Mutation eines in NRD hoch konservierten Cysteins zu Alanin eine Aufhebung der Potenzierung durch Tubulin. Die NRD-Mutante, der die charakteristische Saure Domäne (DAC) fehlt, war in der Lage $p42^{IP4}$ zu binden, aber die Zugabe von Tubulin konnte die Interaktion mit $p42^{IP4}$ nicht signifikant potenzieren. Die Interaktion von $p42^{IP4}$ mit der Deletionsmutante ΔDAC zeigt, dass $p42^{IP4}$ bei der Interaktion mit NRD auch außerhalb der DAC binden kann. Durch die von Tubulin vermittelte Verstärkung der Interaktion zwischen $p42^{IP4}$ und NRD schlagen wir für $p42^{IP4}$ eine neue Rolle als Linker zwischen dem Actin- und Tubulin-Zytoskelett in neuronalen Zellen vor.

Darüber hinaus ist die Interaktion beider Proteine möglicherweise im Hinblick auf die Alzheimer Erkrankung (AD) von Bedeutung. Das Protein $p42^{IP4}$ wurde in Gehirnen von AD Patienten vorgefunden, wobei es mit den AD-Plaques kolokalisiert. Weiterhin interagiert $p42^{IP4}$ mit RanBPM, einem Protein das die β-Sekretase (BACE1) aktivieren kann. Im Gegensatz dazu ist von NRD bekannt, dass es die Freisetzung des neuroprotektiven sAPPα verstärkt. Deshalb wurde untersucht, ob $p42^{IP4}$ einen Effekt auf die Spaltung von APP hat. Es konnte gezeigt werden, dass die Überexprimierung von $p42^{IP4}$ in SH-SY5Y Zellen keinen Einfluß auf die Prozessierung von APP hat. Sowohl die Freisetzung von neuroprotektivem sAPPα, wie auch die Freisetzung von Aβ40 bleiben auf einem basalen Spiegel.

7 References

Aggensteiner, M. and Reiser, G. (2003) Expression of the brain-specific membrane adapter protein p42IP4/centaurin alpha, a Ins(1,3,4,5)P4/PtdIns(3,4,5)P3 binding protein, in developing rat brain. *Brain Res Dev Brain Res*, **142**, 77-87.

Alzheimer, A., Stelzmann, R.A., Schnitzlein, H.N. and Murtagh, F.R. (1995) An English translation of Alzheimer's 1907 paper, "Uber eine eigenartige Erkankung der Hirnrinde". *Clin Anat*, **8**, 429-431.

Asada, H., Uyemura, K. and Shirao, T. (1994) Actin-binding protein, drebrin, accumulates in submembranous regions in parallel with neuronal differentiation. *J Neurosci Res*, **38**, 149-159.

Asai, M., Hattori, C., Szabo, B., Sasagawa, N., Maruyama, K., Tanuma, S. and Ishiura, S. (2003) Putative function of ADAM9, ADAM10, and ADAM17 as APP alpha-secretase. *Biochem Biophys Res Commun*, **301**, 231-235.

Beckman, M. and Iverfeldt, K. (1997) Increased gene expression of beta-amyloid precursor protein and its homologues APLP1 and APLP2 in human neuroblastoma cells in response to retinoic acid. *Neurosci Lett*, **221**, 73-76.

Bernstein, H.G., Stricker, R., Dobrowolny, H., Trubner, K., Bogerts, B. and Reiser, G. (2007) Histochemical evidence for wide expression of the metalloendopeptidase nardilysin in human brain neurons. *Neuroscience*, **146**, 1513-1523.

Bernstein, H.G., Stricker, R., Lendeckel, U., Bertram, I., Dobrowolny, H., Steiner, J., Bogerts, B. and Reiser, G. (2009) Reduced neuronal co-localisation of nardilysin and the putative alpha-secretases ADAM10 and ADAM17 in Alzheimer's disease and Down syndrome brains. *Age (Dordr)*, **31**, 11-25.

Biagiotti, T., D'Amico, M., Marzi, I., Di Gennaro, P., Arcangeli, A., Wanke, E. and Olivotto, M. (2006) Cell renewing in neuroblastoma: electrophysiological and immunocytochemical characterization of stem cells and derivatives. *Stem Cells*, **24**, 443-453.

Biedler, J.L., Helson, L. and Spengler, B.A. (1973) Morphology and growth, tumorigenicity, and cytogenetics of human neuroblastoma cells in continuous culture. *Cancer Res*, **33**, 2643-2652.

Biedler, J.L., Roffler-Tarlov, S., Schachner, M. and Freedman, L.S. (1978) Multiple neurotransmitter synthesis by human neuroblastoma cell lines and clones. *Cancer Res*, **38**, 3751-3757.

Bifulco, M., Laezza, C., Stingo, S. and Wolff, J. (2002) 2',3'-Cyclic nucleotide 3'-phosphodiesterase: a membrane-bound, microtubule-associated protein and membrane anchor for tubulin. *Proc Natl Acad Sci U S A*, **99**, 1807-1812.

Blader, I.J., Cope, M.J., Jackson, T.R., Profit, A.A., Greenwood, A.F., Drubin, D.G., Prestwich, G.D. and Theibert, A.B. (1999) GCS1, an Arf guanosine triphosphatase-activating protein in Saccharomyces cerevisiae, is required for normal actin cytoskeletal organization in vivo and stimulates actin polymerization in vitro. *Mol Biol Cell*, **10**, 581-596.

Bolis, A., Coviello, S., Visigalli, I., Taveggia, C., Bachi, A., Chishti, A.H., Hanada, T., Quattrini, A., Previtali, S.C., Biffi, A. and Bolino, A. (2009) Dlg1, Sec8, and Mtmr2 regulate membrane homeostasis in Schwann cell myelination. *J Neurosci*, **29**, 8858-8870.

Bollag, G., McCormick, F. and Clark, R. (1993) Characterization of full-length neurofibromin: tubulin inhibits Ras GAP activity. *Embo J*, **12**, 1923-1927.

References

Celsi, F., Pizzo, P., Brini, M., Leo, S., Fotino, C., Pinton, P. and Rizzuto, R. (2009) Mitochondria, calcium and cell death: a deadly triad in neurodegeneration. *Biochim Biophys Acta*, **1787**, 335-344.

Chanda, S.K., White, S., Orth, A.P., Reisdorph, R., Miraglia, L., Thomas, R.S., DeJesus, P., Mason, D.E., Huang, Q., Vega, R., Yu, D.H., Nelson, C.G., Smith, B.M., Terry, R., Linford, A.S., Yu, Y., Chirn, G.W., Song, C., Labow, M.A., Cohen, D., King, F.J., Peters, E.C., Schultz, P.G., Vogt, P.K., Hogenesch, J.B. and Caldwell, J.S. (2003) Genome-scale functional profiling of the mammalian AP-1 signaling pathway. *Proc Natl Acad Sci U S A*, **100**, 12153-12158.

Chesneau, V., Pierotti, A.R., Barre, N., Creminon, C., Tougard, C. and Cohen, P. (1994) Isolation and characterization of a dibasic selective metalloendopeptidase from rat testes that cleaves at the amino terminus of arginine residues. *J Biol Chem*, **269**, 2056-2061.

Chesneau, V., Prat, A., Segretain, D., Hospital, V., Dupaix, A., Foulon, T., Jegou, B. and Cohen, P. (1996) NRD convertase: a putative processing endoprotease associated with the axoneme and the manchette in late spermatids. *J Cell Sci*, **109 (Pt 11)**, 2737-2745.

Chow, K.M., Csuhai, E., Juliano, M.A., St Pyrek, J., Juliano, L. and Hersh, L.B. (2000) Studies on the subsite specificity of rat nardilysin (N-arginine dibasic convertase). *J Biol Chem*, **275**, 19545-19551.

Chow, K.M., Ma, Z., Cai, J., Pierce, W.M. and Hersh, L.B. (2005) Nardilysin facilitates complex formation between mitochondrial malate dehydrogenase and citrate synthase. *Biochim Biophys Acta*, **1723**, 292-301.

Chow, K.M., Oakley, O., Goodman, J., Ma, Z., Juliano, M.A., Juliano, L. and Hersh, L.B. (2003) Nardilysin cleaves peptides at monobasic sites. *Biochemistry*, **42**, 2239-2244.

Corpet, F. (1988) Multiple sequence alignment with hierarchical clustering. *Nucleic Acids Res*, **16**, 10881-10890.

Csuhai, E., Chen, G. and Hersh, L.B. (1998) Regulation of N-arginine dibasic convertase activity by amines: putative role of a novel acidic domain as an amine binding site. *Biochemistry*, **37**, 3787-3794.

Csuhai, E., Juliano, M.A., Juliano, L. and Hersh, L.B. (1999a) Kinetic analysis of spermine binding to NRD convertase. *Arch Biochem Biophys*, **362**, 291-300.

Csuhai, E., Juliano, M.A., Pyrek, J.S., Harms, A.C., Juliano, L. and Hersh, L.B. (1999b) New fluorogenic substrates for N-arginine dibasic convertase. *Anal Biochem*, **269**, 149-154.

Csuhai, E., Safavi, A. and Hersh, L.B. (1995) Purification and characterization of a secreted arginine-specific dibasic cleaving enzyme from EL-4 cells. *Biochemistry*, **34**, 12411-12419.

Dehmelt, L. and Halpain, S. (2007) Neurite outgrowth: a flick of the wrist. *Curr Biol*, **17**, R611-614.

Diaz-Rodriguez, E., Montero, J.C., Esparis-Ogando, A., Yuste, L. and Pandiella, A. (2002) Extracellular signal-regulated kinase phosphorylates tumor necrosis factor alpha-converting enzyme at threonine 735: a potential role in regulated shedding. *Mol Biol Cell*, **13**, 2031-2044.

Donaldson, J.G. (2003) Multiple roles for Arf6: sorting, structuring, and signaling at the plasma membrane. *J Biol Chem*, **278**, 41573-41576.

Draoui, M., Bellincampi, L., Hospital, V., Cadel, S., Foulon, T., Prat, A., Barre, N., Reichert, U., Melino, G. and Cohen, P. (1997) Expression and retinoid modulation of N-arginine dibasic convertase and an aminopeptidase-B in human neuroblastoma cell lines. *J Neurooncol*, **31**, 99-106.

Dubois, T., Howell, S., Zemlickova, E. and Aitken, A. (2002) Identification of casein kinase Ialpha interacting protein partners. *FEBS Lett*, **517**, 167-171.

References

Dubois, T., Kerai, P., Zemlickova, E., Howell, S., Jackson, T.R., Venkateswarlu, K., Cullen, P.J., Theibert, A.B., Larose, L., Roach, P.J. and Aitken, A. (2001) Casein kinase I associates with members of the centaurin-alpha family of phosphatidylinositol 3,4,5-trisphosphate-binding proteins. *J Biol Chem*, **276**, 18757-18764.

Dubois, T., Zemlickova, E., Howell, S. and Aitken, A. (2003) Centaurin-alpha 1 associates in vitro and in vivo with nucleolin. *Biochem Biophys Res Commun*, **301**, 502-508.

Edsjo, A., Holmquist, L. and Pahlman, S. (2007) Neuroblastoma as an experimental model for neuronal differentiation and hypoxia-induced tumor cell dedifferentiation. *Semin Cancer Biol*, **17**, 248-256.

Fontes, G., Lajoix, A.D., Bergeron, F., Cadel, S., Prat, A., Foulon, T., Gross, R., Dalle, S., Le-Nguyen, D., Tribillac, F. and Bataille, D. (2005) Miniglucagon (MG)-generating endopeptidase, which processes glucagon into MG, is composed of N-arginine dibasic convertase and aminopeptidase B. *Endocrinology*, **146**, 702-712.

Fumagalli, P., Accarino, M., Egeo, A., Scartezzini, P., Rappazzo, G., Pizzuti, A., Avvantaggiato, V., Simeone, A., Arrigo, G., Zuffardi, O., Ottolenghi, S. and Taramelli, R. (1998) Human NRD convertase: a highly conserved metalloendopeptidase expressed at specific sites during development and in adult tissues. *Genomics*, **47**, 238-245.

Galvita, A., Grachev, D., Azarashvili, T., Baburina, Y., Krestinina, O., Stricker, R. and Reiser, G. (2009) The brain-specific protein, p42 (ADAP 1) is localized in mitochondria and involved in regulation of mitochondrial Ca. *J Neurochem*.

Geraldo, S. and Gordon-Weeks, P.R. (2009) Cytoskeletal dynamics in growth-cone steering. *J Cell Sci*, **122**, 3595-3604.

Goodman, A.B. (2006) Retinoid receptors, transporters, and metabolizers as therapeutic targets in late onset Alzheimer disease. *J Cell Physiol*, **209**, 598-603.

Goodman, A.B. and Pardee, A.B. (2003) Evidence for defective retinoid transport and function in late onset Alzheimer's disease. *Proc Natl Acad Sci U S A*, **100**, 2901-2905.

Gravel, M., Robert, F., Kottis, V., Gallouzi, I.E., Pelletier, J. and Braun, P.E. (2009) 2',3'-Cyclic nucleotide 3'-phosphodiesterase: a novel RNA-binding protein that inhibits protein synthesis. *J Neurosci Res*, **87**, 1069-1079.

Gross, S.D. and Anderson, R.A. (1998) Casein kinase I: spatial organization and positioning of a multifunctional protein kinase family. *Cell Signal*, **10**, 699-711.

Haase, A., Nordmann, C., Sedehizade, F., Borrmann, C. and Reiser, G. (2008) RanBPM, a novel interaction partner of the brain-specific protein p42/centaurin alpha-1. *J Neurochem*, **105**, 2237-2248.

Haass. (2004) Take five--BACE and the gamma-secretase quartet conduct Alzheimer's amyloid beta-peptide generation. *Embo J*, **23**, 483-488.

Halpain, S. and Dehmelt, L. (2006) The MAP1 family of microtubule-associated proteins. *Genome Biol*, **7**, 224.

Hammonds-Odie, L.P., Jackson, T.R., Profit, A.A., Blader, I.J., Turck, C.W., Prestwich, G.D. and Theibert, A.B. (1996) Identification and cloning of centaurin-alpha. A novel phosphatidylinositol 3,4,5-trisphosphate-binding protein from rat brain. *J Biol Chem*, **271**, 18859-18868.

Hanck, T., Stricker, R., Krishna, U.M., Falck, J.R., Chang, Y.T., Chung, S.K. and Reiser, G. (1999) Recombinant p42^{IP4}, a brain-specific 42-kDa high-affinity Ins(1,3,4,5)P$_4$ receptor protein, specifically interacts with lipid membranes containing Ptd-Ins(3,4,5)P$_3$. *European Journal of Biochemistry*, **261**, 577-584.

Hanck, T., Stricker, R., Sedehizade, F. and Reiser, G. (2004) Identification of gene structure and subcellular localization of human centaurin alpha 2, and p42IP4, a family of two highly homologous, Ins 1,3,4,5-P4-/PtdIns 3,4,5-P3-binding, adapter proteins. *J Neurochem*, **88**, 326-336.

References

Harada, T., Matsuzaki, O., Hayashi, H., Sugano, S., Matsuda, A. and Nishida, E. (2003) AKRL1 and AKRL2 activate the JNK pathway. *Genes Cells*, **8**, 493-500.

Hardy, J. and Selkoe, D.J. (2002) The amyloid hypothesis of Alzheimer's disease: progress and problems on the road to therapeutics. *Science*, **297**, 353-356.

Hayashi, H., Matsuzaki, O., Muramatsu, S., Tsuchiya, Y., Harada, T., Suzuki, Y., Sugano, S., Matsuda, A. and Nishida, E. (2006) Centaurin-alpha1 is a phosphatidylinositol 3-kinase-dependent activator of ERK1/2 mitogen-activated protein kinases. *J Biol Chem*, **281**, 1332-1337.

Hiraoka, Y., Ohno, M., Yoshida, K., Okawa, K., Tomimoto, H., Kita, T. and Nishi, E. (2007) Enhancement of alpha-secretase cleavage of amyloid precursor protein by a metalloendopeptidase nardilysin. *J Neurochem*, **102**, 1595-1605.

Hiraoka, Y., Yoshida, K., Ohno, M., Matsuoka, T., Kita, T. and Nishi, E. (2008) Ectodomain shedding of TNF-alpha is enhanced by nardilysin via activation of ADAM proteases. *Biochem Biophys Res Commun*, **370**, 154-158.

Holback, S., Adlerz, L. and Iverfeldt, K. (2005) Increased processing of APLP2 and APP with concomitant formation of APP intracellular domains in BDNF and retinoic acid-differentiated human neuroblastoma cells. *J Neurochem*, **95**, 1059-1068.

Hooper, N.M. (1994) Families of zinc metalloproteases. *FEBS Lett*, **354**, 1-6.

Horiguchi, K., Hanada, T., Fukui, Y. and Chishti, A.H. (2006) Transport of PIP3 by GAKIN, a kinesin-3 family protein, regulates neuronal cell polarity. *J Cell Biol*, **174**, 425-436.

Hospital, V., Chesneau, V., Balogh, A., Joulie, C., Seidah, N.G., Cohen, P. and Prat, A. (2000) N-arginine dibasic convertase (nardilysin) isoforms are soluble dibasic-specific metalloendopeptidases that localize in the cytoplasm and at the cell surface. *Biochem J*, **349**, 587-597.

Hospital, V., Nishi, E., Klagsbrun, M., Cohen, P., Seidah, N.G. and Prat, A. (2002) The metalloendopeptidase nardilysin (NRDc) is potently inhibited by heparin-binding epidermal growth factor-like growth factor (HB-EGF). *Biochem J*, **367**, 229-238.

Hospital, V. and Prat, A. (2004) Nardilysin, a basic residues specific metallopeptidase that mediates cell migration and proliferation. *Protein Pept Lett*, **11**, 501-508.

Hospital, V., Prat, A., Joulie, C., Cherif, D., Day, R. and Cohen, P. (1997) Human and rat testis express two mRNA species encoding variants of NRD convertase, a metalloendopeptidase of the insulinase family. *Biochem J*, **327 (Pt 3)**, 773-779.

Hunzicker-Dunn, M., Gurevich, V.V., Casanova, J.E. and Mukherjee, S. (2002) ARF6: a newly appreciated player in G protein-coupled receptor desensitization. *FEBS Lett*, **521**, 3-8.

Ito, A. (1999) Mitochondrial processing peptidase: multiple-site recognition of precursor proteins. *Biochem Biophys Res Commun*, **265**, 611-616.

Jang, H., Arce, F.T., Ramachandran, S., Capone, R., Azimova, R., Kagan, B.L., Nussinov, R. and Lal, R. (2010) Truncated beta-amyloid peptide channels provide an alternative mechanism for Alzheimer's Disease and Down syndrome. *Proc Natl Acad Sci U S A*, **107**, 6538-6543.

Kahn, R.A., Bruford, E., Inoue, H., Logsdon, J.M., Jr., Nie, Z., Premont, R.T., Randazzo, P.A., Satake, M., Theibert, A.B., Zapp, M.L. and Cassel, D. (2008) Consensus nomenclature for the human ArfGAP domain-containing proteins. *J Cell Biol*, **182**, 1039-1044.

Kanamarlapudi, V. (2005) Centaurin-alpha1 and KIF13B kinesin motor protein interaction in ARF6 signalling. *Biochem Soc Trans*, **33**, 1279-1281.

Kang, J., Lemaire, H.G., Unterbeck, A., Salbaum, J.M., Masters, C.L., Grzeschik, K.H., Multhaup, G., Beyreuther, K. and Muller-Hill, B. (1987) The precursor of Alzheimer's disease amyloid A4 protein resembles a cell-surface receptor. *Nature*, **325**, 733-736.

References

Kessler, J.H., Khan, S., Seifert, U., Le Gall, S., Chow, K.M., Paschen, A., Bres-Vloemans, S.A., de Ru, A., van Montfoort, N., Franken, K.L., Benckhuijsen, W.E., Brooks, J.M., van Hall, T., Ray, K., Mulder, A., Doxiadis, II, van Swieten, P.F., Overkleeft, H.S., Prat, A., Tomkinson, B., Neefjes, J., Kloetzel, P.M., Rodgers, D.W., Hersh, L.B., Drijfhout, J.W., van Veelen, P.A., Ossendorp, F. and Melief, C.J. (2011) Antigen processing by nardilysin and thimet oligopeptidase generates cytotoxic T cell epitopes. *Nat Immunol*, **12**, 45-53.

Korovkina, V.P., Stamnes, S.J., Brainard, A.M. and England, S.K. (2009) Nardilysin convertase regulates the function of the maxi-K channel isoform mK44 in human myometrium. *Am J Physiol Cell Physiol*, **296**, C433-440.

Koryakina, A., Aeberhard, J., Kiefer, S., Hamburger, M. and Kuenzi, P. (2009) Regulation of secretases by all-trans-retinoic acid. *Febs J*, **276**, 2645-2655.

Kreutz, M.R., Bockers, T.M., Sabel, B.A., Hulser, E., Stricker, R. and Reiser, G. (1997a) Expression and subcellular localization of p42IP4/centaurin-alpha, a brain-specific, high-affinity receptor for inositol 1,3,4,5-tetrakisphosphate and phosphatidylinositol 3,4,5-trisphosphate in rat brain. *Eur J Neurosci*, **9**, 2110-2124.

Kreutz, M.R., Bockers, T.M., Sabel, B.A., Stricker, R., Hulser, E. and Reiser, G. (1997b) Localization of a 42-kDa inositol 1,3,4,5-tetrakisphosphate receptor protein in retina and change in expression after optic nerve injury. *Brain Res Mol Brain Res*, **45**, 283-293.

Laemmli, U.K. (1970) Cleavage of structural proteins during the assembly of the head of bacteriophage T4. *Nature*, **227**, 680-685.

Lakshmana, M.K., Yoon, I.S., Chen, E., Bianchi, E., Koo, E.H. and Kang, D.E. (2009) Novel role of RanBP9 in BACE1 processing of amyloid precursor protein and amyloid beta peptide generation. *J Biol Chem*, **284**, 11863-11872.

Lawrence, J., Mundell, S.J., Yun, H., Kelly, E. and Venkateswarlu, K. (2005) Centaurin-alpha 1, an ADP-ribosylation factor 6 GTPase activating protein, inhibits beta 2-adrenoceptor internalization. *Mol Pharmacol*, **67**, 1822-1828.

Li, C., Cheng, Y., Gutmann, D.A. and Mangoura, D. (2001) Differential localization of the neurofibromatosis 1 (NF1) gene product, neurofibromin, with the F-actin or microtubule cytoskeleton during differentiation of telencephalic neurons. *Brain Res Dev Brain Res*, **130**, 231-248.

Luckow, V.A. (1993) Baculovirus systems for the expression of human gene products. *Curr Opin Biotechnol*, **4**, 564-572.

Ma, Z., Chow, K.M., Csuhai, E. and Hersh, L.B. (2002) The use of proteolysis to study the structure of nardilysin. *Arch Biochem Biophys*, **401**, 198-204.

Ma, Z., Chow, K.M., Yao, J. and Hersh, L.B. (2004) Nuclear shuttling of the peptidase nardilysin. *Arch Biochem Biophys*, **422**, 153-160.

Ma, Z., Csuhai, E., Chow, K.M. and Hersh, L.B. (2001) Expression of the acidic stretch of nardilysin as a functional binding domain. *Biochemistry*, **40**, 9447-9452.

Ma, Z., Wang, X., Hockman, S., Snow, E.C. and Hersh, L.B. (2005) Subcellular localization of nardilysin during mouse oocyte maturation. *Arch Biochem Biophys*, **434**, 187-194.

Mattson, M.P. (2004) Pathways towards and away from Alzheimer's disease. *Nature*, **430**, 631-639.

Mingaud, F., Mormede, C., Etchamendy, N., Mons, N., Niedergang, B., Wietrzych, M., Pallet, V., Jaffard, R., Krezel, W., Higueret, P. and Marighetto, A. (2008) Retinoid hyposignaling contributes to aging-related decline in hippocampal function in short-term/working memory organization and long-term declarative memory encoding in mice. *J Neurosci*, **28**, 279-291.

References

Montero, J.C., Yuste, L., Diaz-Rodriguez, E., Esparis-Ogando, A. and Pandiella, A. (2000) Differential shedding of transmembrane neuregulin isoforms by the tumor necrosis factor-alpha-converting enzyme. *Mol Cell Neurosci*, **16**, 631-648.

Moore, C.D., Thacker, E.E., Larimore, J., Gaston, D., Underwood, A., Kearns, B., Patterson, S.I., Jackson, T., Chapleau, C., Pozzo-Miller, L. and Theibert, A. (2007) The neuronal Arf GAP centaurin alpha1 modulates dendritic differentiation. *J Cell Sci*, **120**, 2683-2693.

Niederreither, K. and Dolle, P. (2008) Retinoic acid in development: towards an integrated view. *Nat Rev Genet*, **9**, 541-553.

Nishi, E., Hiraoka, Y., Yoshida, K., Okawa, K. and Kita, T. (2006) Nardilysin enhances ectodomain shedding of heparin-binding epidermal growth factor-like growth factor through activation of tumor necrosis factor-alpha-converting enzyme. *J Biol Chem*, **281**, 31164-31172.

Nishi, E. and Klagsbrun, M. (2004) Heparin-binding epidermal growth factor-like growth factor (HB-EGF) is a mediator of multiple physiological and pathological pathways. *Growth Factors*, **22**, 253-260.

Nishi, E., Prat, A., Hospital, V., Elenius, K. and Klagsbrun, M. (2001) N-arginine dibasic convertase is a specific receptor for heparin-binding EGF-like growth factor that mediates cell migration. *Embo J*, **20**, 3342-3350.

Ohno, M., Hiraoka, Y., Matsuoka, T., Tomimoto, H., Takao, K., Miyakawa, T., Oshima, N., Kiyonari, H., Kimura, T., Kita, T. and Nishi, E. (2009) Nardilysin regulates axonal maturation and myelination in the central and peripheral nervous system. *Nat Neurosci*, **12**, 1506-1513.

Pahlman, S., Ruusala, A.I., Abrahamsson, L., Mattsson, M.E. and Esscher, T. (1984) Retinoic acid-induced differentiation of cultured human neuroblastoma cells: a comparison with phorbolester-induced differentiation. *Cell Differ*, **14**, 135-144.

Pierotti, A.R., Prat, A., Chesneau, V., Gaudoux, F., Leseney, A.M., Foulon, T. and Cohen, P. (1994) N-arginine dibasic convertase, a metalloendopeptidase as a prototype of a class of processing enzymes. *Proc Natl Acad Sci U S A*, **91**, 6078-6082.

Preis, P.N., Saya, H., Nadasdi, L., Hochhaus, G., Levin, V. and Sadee, W. (1988) Neuronal cell differentiation of human neuroblastoma cells by retinoic acid plus herbimycin A. *Cancer Res*, **48**, 6530-6534.

Reiser, G. and Bernstein, H.G. (2002) Neurons and plaques of Alzheimer's disease patients highly express the neuronal membrane docking protein p42IP4/centaurin alpha. *Neuroreport*, **13**, 2417-2419.

Reiser, G. and Bernstein, H.G. (2004) Altered expression of protein p42IP4/centaurin-alpha 1 in Alzheimer's disease brains and possible interaction of p42IP4 with nucleolin. *Neuroreport*, **15**, 147-148.

Reiser, G., Kunzelmann, U., Hulser, E., Stricker, R., Hoppe, J., Lottspeich, F. and Kalbacher, H. (1995) Peptide-specific antibodies indicate species heterogeneity of a 42 kDa high-affinity inositol 1,3,4,5-tetrakisphosphate receptor protein from brain. *Biochem Biophys Res Commun*, **214**, 20-27.

Robertson, G., Bilenky, M., Lin, K., He, A., Yuen, W., Dagpinar, M., Varhol, R., Teague, K., Griffith, O.L., Zhang, X., Pan, Y., Hassel, M., Sleumer, M.C., Pan, W., Pleasance, E.D., Chuang, M., Hao, H., Li, Y.Y., Robertson, N., Fjell, C., Li, B., Montgomery, S.B., Astakhova, T., Zhou, J., Sander, J., Siddiqui, A.S. and Jones, S.J. (2006) cisRED: a database system for genome-scale computational discovery of regulatory elements. *Nucleic Acids Res*, **34**, D68-73.

Rodgers, E.E. and Theibert, A.B. (2002) Functions of PI 3-kinase in development of the nervous system. *Int J Dev Neurosci*, **20**, 187-197.

References

Rojas-Cartagena, C., Ortiz-Pineda, P., Ramirez-Gomez, F., Suarez-Castillo, E.C., Matos-Cruz, V., Rodriguez, C., Ortiz-Zuazaga, H. and Garcia-Arraras, J.E. (2007) Distinct profiles of expressed sequence tags during intestinal regeneration in the sea cucumber Holothuria glaberrima. *Physiol Genomics*, **31**, 203-215.

Schule, R., Rangarajan, P., Yang, N., Kliewer, S., Ransone, L.J., Bolado, J., Verma, I.M. and Evans, R.M. (1991) Retinoic acid is a negative regulator of AP-1-responsive genes. *Proc Natl Acad Sci U S A*, **88**, 6092-6096.

Sedehizade, F., Hanck, T., Stricker, R., Horstmayer, A., Bernstein, H.G. and Reiser, G. (2002) Cellular expression and subcellular localization of the human Ins(1,3,4,5)P(4)-binding protein, p42(IP4), in human brain and in neuronal cells. *Brain Res Mol Brain Res*, **99**, 1-11.

Sedehizade, F., von Klot, C., Hanck, T. and Reiser, G. (2005) p42(IP4)/centaurin alpha1, a brain-specific PtdIns(3,4,5)P3/Ins(1,3,4,5)P4-binding protein: membrane trafficking induced by epidermal growth factor is inhibited by stimulation of phospholipase C-coupled thrombin receptor. *Neurochem Res*, **30**, 1319-1330.

Seidah, N.G. and Prat, A. (2002) Precursor convertases in the secretory pathway, cytosol and extracellular milieu. *Essays Biochem*, **38**, 79-94.

Selkoe, D.J. and Schenk, D. (2003) Alzheimer's disease: molecular understanding predicts amyloid-based therapeutics. *Annu Rev Pharmacol Toxicol*, **43**, 545-584.

Shelanski, M.L., Gaskin, F. and Cantor, C.R. (1973) Microtubule assembly in the absence of added nucleotides. *Proc Natl Acad Sci U S A*, **70**, 765-768.

Skovronsky, D.M., Fath, S., Lee, V.M. and Milla, M.E. (2001) Neuronal localization of the TNFalpha converting enzyme (TACE) in brain tissue and its correlation to amyloid plaques. *J Neurobiol*, **49**, 40-46.

Skovronsky, D.M., Moore, D.B., Milla, M.E., Doms, R.W. and Lee, V.M. (2000) Protein kinase C-dependent alpha-secretase competes with beta-secretase for cleavage of amyloid-beta precursor protein in the trans-golgi network. *J Biol Chem*, **275**, 2568-2575.

Spillantini, M.G., Bird, T.D. and Ghetti, B. (1998) Frontotemporal dementia and Parkinsonism linked to chromosome 17: a new group of tauopathies. *Brain Pathol*, **8**, 387-402.

Stricker, R., Adelt, S., Vogel, G. and Reiser, G. (1999) Translocation between membranes and cytosol of p42IP4, a specific inositol 1,3,4,5-tetrakisphosphate/phosphatidylinositol 3,4, 5-trisphosphate-receptor protein from brain, is induced by inositol 1,3,4,5-tetrakisphosphate and regulated by a membrane-associated 5-phosphatase. *Eur J Biochem*, **265**, 815-824.

Stricker, R., Chow, K.M., Walther, D., Hanck, T., Hersh, L.B. and Reiser, G. (2006) Interaction of the brain-specific protein p42IP4/centaurin-alpha1 with the peptidase nardilysin is regulated by the cognate ligands of p42IP4, PtdIns(3,4,5)P3 and Ins(1,3,4,5)P4, with stereospecificity. *J Neurochem*, **98**, 343-354.

Stricker, R., Hulser, E., Fischer, J., Jarchau, T., Walter, U., Lottspeich, F. and Reiser, G. (1997) cDNA cloning of porcine p42IP4, a membrane-associated and cytosolic 42 kDa inositol(1,3,4,5)tetrakisphosphate receptor from pig brain with similarly high affinity for phosphatidylinositol (3,4,5)P3. *FEBS Lett*, **405**, 229-236.

Stricker, R., Vandekerckhove, J., Krishna, M.U., Falck, J.R., Hanck, T. and Reiser, G. (2003) Oligomerization controls in tissue-specific manner ligand binding of native, affinity-purified p42(IP4)/centaurin alpha1 and cytohesins-proteins with high affinity for the messengers D-inositol 1,3,4,5-tetrakisphosphate/phosphatidylinositol 3,4,5-trisphosphate. *Biochim Biophys Acta*, **1651**, 102-115.

Tanaka, K., Horiguchi, K., Yoshida, T., Takeda, M., Fujisawa, H., Takeuchi, K., Umeda, M., Kato, S., Ihara, S., Nagata, S. and Fukui, Y. (1999) Evidence that a

References

phosphatidylinositol 3,4,5-trisphosphate-binding protein can function in nucleus. *J Biol Chem*, **274**, 3919-3922.

Tanaka, K., Imajoh-Ohmi, S., Sawada, T., Shirai, R., Hashimoto, Y., Iwasaki, S., Kaibuchi, K., Kanaho, Y., Shirai, T., Terada, Y., Kimura, K., Nagata, S. and Fukui, Y. (1997) A target of phosphatidylinositol 3,4,5-trisphosphate with a zinc finger motif similar to that of the ADP-ribosylation-factor GTPase-activating protein and two pleckstrin homology domains. *Eur J Biochem*, **245**, 512-519.

Thacker, E., Kearns, B., Chapman, C., Hammond, J., Howell, A. and Theibert, A. (2004) The arf6 GAP centaurin alpha-1 is a neuronal actin-binding protein which also functions via GAP-independent activity to regulate the actin cytoskeleton. *Eur J Cell Biol*, **83**, 541-554.

Tong, Y., Tempel, W., Wang, H., Yamada, K., Shen, L., Senisterra, G.A., Mackenzie, F., Chishti, A.H. and Park, H.W. (2010) Phosphorylation-independent dual-site binding of the FHA domain of KIF13 mediates phosphoinositide transport via centaurin {alpha}1. *Proc Natl Acad Sci U S A*, **107**, 20346-20351.

Venkateswarlu, K., Brandom, K.G. and Lawrence, J.L. (2004) Centaurin-alpha1 is an in vivo phosphatidylinositol 3,4,5-trisphosphate-dependent GTPase-activating protein for ARF6 that is involved in actin cytoskeleton organization. *J Biol Chem*, **279**, 6205-6208.

Venkateswarlu, K. and Cullen, P.J. (1999) Molecular cloning and functional characterization of a human homologue of centaurin-alpha. *Biochem Biophys Res Commun*, **262**, 237-244.

Venkateswarlu, K., Hanada, T. and Chishti, A.H. (2005) Centaurin-alpha1 interacts directly with kinesin motor protein KIF13B. *J Cell Sci*, **118**, 2471-2484.

Venkateswarlu, K., Oatey, P.B., Tavare, J.M., Jackson, T.R. and Cullen, P.J. (1999) Identification of centaurin-alpha1 as a potential in vivo phosphatidylinositol 3,4,5-trisphosphate-binding protein that is functionally homologous to the yeast ADP-ribosylation factor (ARF) GTPase-activating protein, Gcs1. *Biochem J*, **340 (Pt 2)**, 359-363.

Wang, H., Ma, J., Ruan, L. and Xu, X. (2009) Cloning of a centaurin-alpha1 like gene MjCent involved in WSSV infection from shrimp Marsupeneaus japonicus. *Fish Shellfish Immunol*, **26**, 279-284.

Willem, M., Garratt, A.N., Novak, B., Citron, M., Kaufmann, S., Rittger, A., DeStrooper, B., Saftig, P., Birchmeier, C. and Haass, C. (2006) Control of peripheral nerve myelination by the beta-secretase BACE1. *Science*, **314**, 664-666.

Winter, A.G. and Pierotti, A.R. (2000) Gene expression of the dibasic-pair cleaving enzyme NRD convertase (N-arginine dibasic convertase) is differentially regulated in the GH3 pituitary and Mat-Lu prostate cell lines. *Biochem J*, **351 Pt 3**, 755-764.

Wu, Y., Li, Q. and Chen, X.Z. (2007) Detecting protein-protein interactions by Far western blotting. *Nat Protoc*, **2**, 3278-3284.

Xu, H. and Gutmann, D.H. (1997) Mutations in the GAP-related domain impair the ability of neurofibromin to associate with microtubules. *Brain Res*, **759**, 149-152.

Zaidi, S.H. and Malter, J.S. (1995) Nucleolin and heterogeneous nuclear ribonucleoprotein C proteins specifically interact with the 3'-untranslated region of amyloid protein precursor mRNA. *J Biol Chem*, **270**, 17292-17298.

Zemlickova, E., Dubois, T., Kerai, P., Clokie, S., Cronshaw, A.D., Wakefield, R.I., Johannes, F.J. and Aitken, A. (2003) Centaurin-alpha(1) associates with and is phosphorylated by isoforms of protein kinase C. *Biochem Biophys Res Commun*, **307**, 459-465.

8 Abbreviations

aa	amino acids
AD	Alzheimer's disease
ADAP1	Arf-GAP with dual PH domain-containing protein 1
Aβ	amyloid ß-peptide
ADAM10	A disintegrin And Metalloproteinase 10
ADAM17	A Disintegrin And Metalloproteinase 17
APP	amyloid precursor protein
AP-1	activator protein 1
Arf	ADP-ribosylation factor
Arf-GAP	ADP-ribosylation factor- GTPase-Activating Protein
BACE	β-secretase
bp	base pairs
BSA	bovine serum albumin
C-terminal	carboxyl terminal
CNP	2', 3'-Cyclic-nucleotide 3'-phosphodiesterase
CNS	central nervous system
DMEM	Dulbecco's Modified Eagle's Medium
DMSO	dimethylsulfoxide
DNA	desoxyribonucleic acid
DNase	desoxyribonuclease
dNTPs	desoxyribonucleotides
DTT	dithiothreitol
DAC	Acidic Domain
ECL	enhanced chemiluminescence
EDTA	ethylene-diamine-tetra-acetic acid
EGF	Epidermal growth factor
ELISA	enzyme-linked immunosorbent assay
ERK	extracellular-signal-regulated kinase
EtOH	ethanol
EtBr	ethidium bromide
FCS	fetal calf serum
FSBB	fetal calf serum blocking buffer
GAP	GTPase-Activating Protein
GAPDH	glycerinaldehyde-3-phosphate-dehydrogenase
GEF	Guanine nucleotide exchange factor
GFP	green fluorescent protein
GPCR	G protein-coupled receptor
GSH	glutathione sepharose
GST	glutathione S-transferase
GTP	Guanosine-5'-triphosphate
HBSS	Hank's Buffered Salt Solution
HB-EGF	Heparin-binding EGF-like growth factor
HEK293	Human Embryonic Kidney 293 cells
HRP	Horseradish peroxidase
hsNRD1	homo sapiens NRD1
IPTG	Isopropylthio-β-galactoside
IP$_4$	Inositol-tetrakis-phosphate
kDa	kilo Dalton
MATra	Magnet Assisted Transfection
MAP	microtubule associated protein

Abbreviations

MAP kinase	Mitogen-activated protein kinase
MPP	mitochondrial processing peptidase
N-terminal	amino-terminal
NF1	neurofibromin 1
NRG1	neuregulin 1
OD	optical density
ON	overnight
PAGE	polyacrylamide gel electrophoresis
PBS	phosphate buffered saline
PCR	polymerase chain reaction
PER	ammonium peroxydisulfate
PFA	paraformaldehyde solution
PH	pleckstrin homology
PI3K	Phosphatidylinositol 3-kinase
PIP$_3$	Phosphatidylinositol (3,4,5)-trisphosphate
PIP$_2$	Phosphatidylinositol (3,4)-bisphosphate
PKC	protein kinase C
PS1	presenilin 1
PTP	permeability transition pore
RNA	ribonucleic acid
RNase	ribonuclease
RA	*all-trans* Retinoic Acid
RAR	retinoic acid nuclear receptors
RXR	retinoid X receptor
RARE	RA-responsive elements
RT	room temperature
RT-PCR	reverse transcriptase-polymerase chain reaction;
Sf9	Spodoptera frugiperda
SDS	sodium dodecylsulfate
siRNA	small interfering RNA
TACE	TNF-α-converting enzyme
TCA	Trichloroacetic acid;
TEMED	tetramethylethylenediamine
TNF-α	Tumor necrosis factor-α
wt	wild type

9   Appendix

Veröffentlichungen

Publikation von Ergebnissen der Doktorarbeit in:

(1) <u>Claudia Borrmann</u>, Rolf Stricker, Georg Reiser **Tubulin potentiates the interaction of the metalloendopeptidase nardilysin with the neuronal scaffold protein p42IP4/centaurin-α1** (**ADAP1**) *Cell and Tissue Res. [2011 Oct 5. [Epub ahead of print] PMID: 21972134*

(2) <u>Claudia Borrmann</u>, Rolf Stricker, Georg Reiser **Retinoic acid-induced upregulation of the metalloendopeptidase nardilysin is accelerated by co-expression of the brain-specific protein p42(IP4) (centaurin α1; ADAP1) in neuroblastoma cells.** *Neurochem Int. 2011 Jul 23. [Epub ahead of print] PMID: 21801775*

Publikation von Ergebnissen der Diplomarbeit in:

(3) Andrea Haase, Caroline Nordmann, Fariba Sedehizade, <u>Claudia Borrmann</u> and Georg Reiser **RanBPM, a novel interaction partner of the brain-specific protein p42(IP4)/centaurin alpha-1.** *J.Neurochem (2008)105, 2237; PMID: 18298663*

Selbständigkeitserklärung

Claudia Borrmann
Bördebogen 6
39126 Magdeburg

Erklärung

Hiermit erkläre ich, dass ich die von mir eingereichte Dissertation zum Thema

Interaction of the brain-specific Arf-GAP protein p42^{IP4} (centaurin α1, ADAP1) with the metalloendopeptidase nardilysin and modulation by tubulin

selbständig verfasst, nicht schon als Dissertation verwendet habe und die benutzten Hilfmittel und Quellen vollständig angegeben wurden.

Weiterhin erkläre ich, dass ich weder diese noch eine andere Arbeit zur Erlangung des akademischen Grades doctor rerum naturalium (Dr. rer. nat.) und anderen Einrichtungen eingereicht habe.

Magdeburg, 25. Oktober 2011

Claudia Borrmann